Mechanisms of Arterial Dilation in Exercise Hyperemia

Alexander Sutherland Keller

Kennett Square, Pennsylvania

B.S., Duke University, 2012

A Dissertation presented to the Graduate Faculty of the University of Virginia
in Candidacy for the Degree of Doctor of Philosophy

Department of Pharmacology

University of Virginia
May, 2019

_____

_____

_____

_____

_____

ABSTRACT

Matching oxygen supply to consumption across different tissues is a critical function of the vasculature. The remarkably wide range of metabolic demand between resting and active skeletal muscle renders control of blood flow to skeletal muscle tissues especially important and challenging. Mechanisms of exercise hyperemia are believed to be multifaceted and redundant, reflecting both the complexity of this response as well as its importance. We explored two candidate mechanisms of exercise hyperemia, examining ATP release from red blood cells and hemoglobin alpha in the endothelium of resistance arteries.

We first studied the participation of Pannexin 1 in a red blood cell pathway reported to link hypoxia to elevated cyclic AMP and finally ATP release via Pannexin 1 to promote vasodilatory signaling in the endothelium. Our findings contradict previous claims that these components participate in the same signaling pathway. Furthermore, our work highlights a number of methodological considerations that we present as best practices for future *in vitro* work studying ATP release from red blood cells. Finally, we report exercise data that suggests more broadly a lack of significant role for Pannexin 1 in exercise performance.

Subsequently, we hypothesized a novel role for endothelial hemoglobin alpha as a nitrite reductase during hypoxia. This mechanism has received significant attention in red blood cell hemoglobin, but has not previously been examined in the endothelium. Creating

novel genetic models of *Hba1* deletion, we demonstrated a reduction in exercise performance upon deletion of endothelial *Hba1* in mice. These effects appear to be independent of the endothelial Hbα-eNOS interaction previously reported by our laboratory. Preliminary myography data shows impaired dilation of EC Hba1$^{\Delta/\Delta}$ skeletal muscle resistance arteries in response to hypoxia. We identify further experiments planned to clarify the mechanism underlying these results. Taken together, our findings point to a novel role for endothelial hemoglobin alpha as a critical regulator of skeletal muscle blood flow during exercise.

TABLE OF CONTENTS

LIST OF FIGURES

CHAPTER 3

CHAPTER 4

LIST OF ABBREVIATIONS

8Br-cAMP	8-bromo cyclic adenosine monophosphate
A°	Angstrom
ΔAbs	Differential absorbance
AC	Adenylate cyclase
ADP	Adenosine diphosphate
AMP	Adenosine monophosphate
ANOVA	Analysis of variance test
ATP	Adenosine triphosphate
A/V	Arterio-venous
BSA	Bovine serum albumin
Ca^{2+}	Calcium
cAMP	Cyclic adenosine monophosphate
CBC	Complete blood count
CBX	Carbenoxolone
CD (#)	Cluster of differentiation (#)
CFTR	Cystic fibrosis transmembrane conductance regulator
CO	Carbon monoxide

CO_2	Carbon dioxide
CRISPR	Clustered regularly interspaced short palindromic repeats
CT	Carboxyl terminus
Cx43	Connexin 43
DAB	3,3’-diaminobenzidine
DAF-FM	4-Amino-5-methylamino-2’,7’-difluorofluorescein diacetate
DAPI	4’6-diamidino-2-phenylindole
deoxyHb	Deoxygenated hemoglobin
DMSO	Dimethyl sulfoxide
EC	Endothelial cell
EDTA	Ethylenediaminetetraacetic acid
EGTA	Ethylene glycol-bis(β-aminoethyl ether)-N,N,N’,N’-tetraacetic acid
EL1	First extracellular loop
EL2	Second extracellular loop
eNOS	Endothelial nitric oxide synthase
ENTPDase	ectonucleotidase 5’-triphosphohydrolase
Flp	Flippase

FRT	Flippase recognition target
Hb	Hemoglobin
Hbα	Hemoglobin alpha
Hbβ	Hemoglobin beta
HBSS	Hanks' buffered salt solution
hct	Hematocrit
HR	Heart rate
HUVEC	Human umbilical vein endothelial cell
IBMX	3-isobutyl-1-methylxanthine
IEL	Internal elastic lamina
IgG	Immunoglobulin G
iNOS	Inducible nitric oxide synthase
K^+	Potassium
KCl	Potassium chloride
KGlu	Potassium gluconate
K-H	Krebs-Henseleit (buffer)
L-NAME	L-N(G)-Nitroarginine methyl ester
L-NMMA	L-N(G)-monomethyl arginine

MAP	Mean arterial pressure
MEJ	Myoendothelial junction
μM	Micromolar
mM	Millimolar
mmHg	Millimeters of mercury
Na^+	Sodium
NE	Norepinephrine
Neo	Neomycin cassette
nNOS	Neuronal nitric oxide synthase
NO	Nitric oxide
NOS	Nitric oxide synthase
NT	Amino terminus
O_2	Oxygen
oxyHb	Oxygenated hemoglobin
Panx1	Pannexin 1
PCR	Polymerase chain reaction
PE	Phenylephrine
PKA	Protein kinase A

PLA	Proximity ligation assay
pO_2	Partial pressure of oxygen
pS	Picosiemens
RBC	Red blood cell
RIPA	Radioimmunoprecipitation assay (buffer)
RT	Room temperature
SDS-PAGE	Sodium dodecyl sulfate polyacrylamide gel electrophoresis
siRNA	Small interfering ribonucleic acid
SMC	Smooth muscle cell
SNO-Hb	S-nitrosylated hemoglobin
TBS	Tris-buffered saline
TBS-T	Tris-buffered saline plus Tween 20
TDA	Thoracodorsal artery
UPLC	Ultra-performance liquid chromatography
UTP	Uridine triphosphate
VDAC	Voltage dependent anion channel
VSMC	Vascular smooth muscle cell
WT	Wild type

DEDICATION

This dissertation is dedicated to the many people who have helped me to this point. To my family, for their love and support over the past three decades, and for ensuring that I was equipped with the resources needed to succeed at every stage. To my father, Doug, for inspiring my interest in biomedical science through his work in toxicology. To my mother, Patsy, for teaching me to read carefully and write clearly – impactful science depends on effective communication. To my brother, Duncan, for being my number one fan (the feeling is mutual). To my wife Cate, for her willingness to move to Charlottesville to support my academic aspirations, and for the selfless love she has shown me through more forms of support during this process than I have room to list here. Her baking deserves its own mention, and frequently fuels the entire lab. To my mother-in-law, Carol, my father-in-law, Craig, and my sister-in-law, Emily, for being tireless cheerleaders of my efforts. To all of my extended family and friends, who have encouraged me from afar and asked for the past five years when I will be graduating.

To both Duke and UVA, for the endless academic opportunities they have offered me. To Heather Stapleton, my undergraduate mentor, who gave me my start in science and has provided invaluable mentorship, and to everyone in her lab at Duke. To everyone at HESI who allowed me explore diverse areas of applied biomedical science and find my path towards graduate research. To my teammates on Duke Roadrunners and friends on Duke T&F/XC, for helping me explore just how far the limits of the human body can be pushed, and in the process helping to inspire in me a fascination with endurance athletics.

To my doctoral mentor, Brant Isakson, for asking the hard questions, enthusiastically pursuing bold experiments, and constantly challenging me to step outside my scientific comfort zone. To everyone in the Isakson lab, for sharing ideas, advice, reagents, and support in many other forms along the way. To all of my collaborators in this research – I am lucky to have had the chance to work with such a knowledgeable, talented group of scientists and colleagues. To my dissertation committee, for providing thoughtful insight on my research from a variety of perspectives I might not otherwise have considered. To all of my other professors in the Department of Pharmacology, the Robert M. Berne Cardiovascular Research Center, and beyond, for creating an inspiring environment of scientific and academic rigor.

To my friends, for helping me make the most of my time in Charlottesville outside of the laboratory. To Shenandoah National Park, the Blue Ridge mountains, the Rivanna Trail, and the beautiful Virginia countryside, for keeping me sane during stressful periods through the healing power of the great outdoors.

To the reader. I hope my research is of use to yours.

CHAPTER 1: GENERAL INTRODUCTION

Among the most fundamental physiologic processes is the ability of the cardiovascular system to regulate blood supply in order to match oxygen (O_2) delivery to cellular metabolic demand across all tissues. Maintenance of this delicate balance requires not only regulation of total cardiac output, but also careful distribution of blood flow across the peripheral vasculature in proportion to the varying metabolic needs of diverse tissues. Such precise distribution of blood flow, in turn, demands highly coordinated integration of myriad signal inputs to achieve precise and distinct responses across multiple types of vascular beds.

Controlling the greatest blood pressure drop in the vasculature, resistance arteries in particular regulate the perfusion of downstream arteriolar networks, constricting or dilating to allow greater or lesser blood flow down certain branches in comparison to others.[1] Reduction of arteriolar resistance is a particularly important means of facilitating increased blood flow: in accordance with Poiseuille's law, the drop in pressure during laminar flow over a given length of vessel is inversely correlated with the fourth power of vessel diameter.[2] In the context of metabolically active skeletal muscle during exercise, reduced arterial and arteriolar resistance is particularly critical to ensure adequate O_2 supply via functional hyperemia.[3]

This general introduction summarizes the existing body of research on control of exercise hyperemia, discussing especially the mechanisms underlying nitric oxide (NO)-based vasodilatory signaling. Two reported mechanisms of NO production come into particular focus: the purinergic pathway by which deoxygenated RBCs release adenosine

triphosphate (ATP) to induce NO production by eNOS in the vascular endothelium; and the redox-based production of NO from nitrite by deoxygenated hemoglobin (deoxyHb).

1.1 Exercise hyperemia and hypoxic regulation of blood flow

The remarkably wide range of metabolic demand between resting and active skeletal muscle renders control of blood flow to skeletal muscle tissues especially important and challenging; thus, the microcirculation of skeletal muscle has long been a system of particular interest in efforts to understand mechanisms blood flow regulation.[3] In accordance with Fick's principle[4] stipulating conservation of mass, the total oxygen extraction rate from the blood flowing through muscle tissue – calculated as the product of vascular conductance through muscle tissue and the O_2 arterio-venous (A/V) gradient in that same muscle – must equal the total mitochondrial oxygen consumption rate of the muscle tissue. Because the metabolic capacity of skeletal muscle to consume oxygen is so great, intense activity in as little as one-third of overall muscle mass can create oxygen demand equal to that provided by maximum cardiac output in a sedentary adult human.[5] The cardiovascular system may therefore be pushed to its limit during intense exercise.

As the theoretical upper bound of the A/V gradient for O_2 is limited to the total amount of O_2 carried by a given volume of arterial blood, extreme increases in oxygen extraction by highly metabolic tissues such as exercising skeletal muscle cannot be satisfied by increased O_2 extraction from a constant supply of blood. Greater blood flow to metabolically active skeletal muscle is thus required to meet its O_2 demand. Additional

perfusion of active skeletal muscle is achieved both though increased cardiac output, as well as the proportional redistribution of blood flow away from less active tissues and towards active muscles.[4] Indeed, blood flow to active skeletal muscle can increase by two to three orders of magnitude[4-6] during heavy exercise, even while total cardiac output only increases by up to half an order of magnitude.[4]

Differential vascular resistance is leveraged to divert increased blood flow only where it is needed during exercise, while tightly regulating blood flow to tissues that display unchanged or reduced metabolic demand. Simultaneously constricting arteries upstream of non-exercise-related tissues while dilating arteries upstream of active skeletal muscle and other exercise-related organs pushes an overwhelming majority of blood to the muscle tissues where metabolic demand is highest.[3] Increased perfusion of this magnitude requires not only dilation of arterioles, but the larger resistance arteries that feed the arteriolar and capillary networks throughout active muscles: an order of magnitude or greater of increase in blood flow must be provided not on the scale of individual muscle fibers, but that of entire muscles. To achieve this task, a high degree of integration across arterial networks facilitates the coordinated spread of ascending vasodilation. Mechanisms including flow-mediated dilation and EC-EC, EC-smooth muscle cell (EC-SMC), and SMC-SMC electrical conduction allow the propagation of vasodilation to vessels upstream of the initial signal.[3]

1.1.1 Mechanisms of hyperemia in exercise

To facilitate intricate control of skeletal muscle perfusion, mechanisms of vasomotor control must be both spatially and temporally precise. An array of vasomotor control mechanisms have been considered as potential explanations of the hyperemic response, including hormonal, neural, physical, metabolic, endothelial, and smooth muscle mechanisms.[7] Exercise-induced vasodilation appears to result from the integration of multiple synergistic and redundant mechanisms;[8, 9] however, a few of the above are not believed to play a role. Global circulation of hormonal factors renders them a poor candidate for spatiotemporally precise blood flow regulation. Regulation by the nervous system allows for temporal and local precision; however, while blood flow to resting skeletal muscle is regulated in part by sympathetic vasoconstriction, it appears that autonomic control does not play an important role in increasing blood flow to exercising muscle. Indeed, Corcondilas *et al.* demonstrated in 1964 that increased blood flow following a single forearm contraction was similar in healthy and sympathectomized arms,[10] while Donald *et al.* demonstrated in 1970 that, canine blood flow was equal in normal and sympathectomized limbs during exercise.[11]

To the contrary, the sympathetic nervous system plays a conflicting but equally important role during intense exercise. By limiting blood flow to less metabolically active tissues, and even somewhat to active skeletal muscle,[12] sympathetic vasoconstriction prevents total peripheral resistance from dropping beyond the minimum needed to maintain adequate arterial pressure under maximal cardiac output.[5] Marshall *et al.* demonstrated this principle in 1961 in orthostatic hypotension patients, who suffer from a loss of autonomic

nervous function, as well as a thoracolumbar sympathectomy patient. In the absence of compensatory sympathetic constriction, blood pressure regulation failed during mild supine leg exercise and radial arterial pressure fell by ~40%.[13]

In the context of central mechanisms acting to restrict overall vasodilation during exercise, achieving precise dilation upstream of metabolically active skeletal muscle is believed to rely on more local mechanisms, including the physical effects of contracting muscle, metabolic signals, or the local release of vasodilatory substances. A consensus has emerged that the overall response is highly integrated, comprising a variety of initial signals and downstream messengers to mediate vasodilation with temporal and locational precision, as well as a remarkable level of redundancy.[3, 7-9]

Increased blood flow to metabolically active skeletal muscle typically progresses in biphasic fashion following onset of exercise. A rapid initial increase in blood flow to active muscle is followed by a slower, more sustained second phase of vasodilation and hyperemia. In humans and other mammals, the fast response is initiated within a second, or a few seconds at most.[7] Testing human subjects who performed single isometric forearm contractions at a range of intensities, Tschakovsky *et al.* demonstrated a direct, linear relationship between voluntary contraction intensity and forearm blood flow within the first cardiac cycle, in the absence of HR or mean arterial pressure effects.[14]

As various mechanisms of vasomotor control require different time scales for operation, not all are candidates for the rapid response. Most proposed mechanisms response require too long a time course to account for the rapid initial phase of increase in blood flow. For example, metabolites released from contracting muscle would be unlikely

to diffuse to adjacent vessels quickly enough to facilitate the rapid response.[15] The appropriate mechanism(s) must be able to integrate a signal of skeletal muscle activity into a near-immediate response within less than a second.[16, 17] Thus, a longstanding argument is that mechanical action of muscle contraction drives the rapid response by physically drawing blood from arteries into veins,[18] although the extent of its contribution is contentious.[19-21]

Acetylcholine spillover to the vasculature from nearby motor nerves in skeletal muscle has also been considered as a contributor to the rapid hyperemic response, but does not appear to make a significant contribution to hyperemia in humans.[22] Somewhat more likely to play a role in the rapid response is transient hyperpolarization of vascular smooth muscle in response to extracellular potassium released by skeletal muscle contractions, as potassium (K^+) concentrations in the interstitium and plasma have been shown to rise within seconds following initial muscle contraction.[23, 24] Armstrong *et al.* found that pharmacologic inhibition of voltage-dependent K^+ channels, the Na^+ K^+ ATPase, or inward rectifying K^+ channels each reduced the magnitude of the rapid phase of vasodilation by half to two-thirds.[25] However, it is critical to note that these experimental treatments may affect not only the release of K^+ from skeletal muscle, but also the function of vascular smooth muscle. Thus, it is unclear if Armstrong and colleagues in fact inhibited a potassium-based signal from skeletal muscle to smooth muscle, or if they instead blocked the ability of smooth muscle to respond to other vasodilatory inputs. It is also notable that in an inverse experimental setup, hyperkalemia via intra-arterial KCl infusion had no effect on sustained hyperemia in steady-state conditions.[26] Any hyperemic role for K^+ would most

likely be limited to the rapid initial phase of vasodilation, as excess K^+ is quickly cleared and periarteriolar K^+ concentrations return to baseline within a few minutes during sustained skeletal muscle contraction.[27]

Looking beyond the persistent questions surrounding the rapid phase of hyperemia, a slower secondary phase opens for consideration a wide variety of chemical mediators known from traditional vasodilatory signaling pathways, including NO, purines, and prostaglandins. It is critical to note here that while multiple candidate pathways have received substantial inquiry, study of chemical dilators in exercise hyperemia is fundamentally complicated by redundancy across mechanisms. Although demonstrating the existence of each particular pathway may be experimentally simple, it is far more difficult to measure precisely the extent of any one contribution in a highly redundant system. This challenge is experimentally illustrated by the less than synergistic combination of four inhibitors to blunt multiple vasodilatory pathways, achieving only 80% inhibition of the hyperemic response to a single forearm contraction in contrast to 50-60% inhibition following separate blockade of the individual components.[4]

1.1.2 Hypoxic Regulation of Blood Flow in Exercise

As discussed previously, the elevated rate of O_2 consumption by metabolically active skeletal muscle is central to the requirement of increased blood flow to that tissue. As the vasculature delivers O_2 to active skeletal muscle, muscle O_2 consumption may also be considered from the perspective of the blood: increased skeletal muscle activity results in

reduced blood pO_2.[9] Hypoxia has accordingly received keen attention as a primary signal of elevated skeletal muscle metabolic demand,[28] and has been studied in the context of numerous downstream signaling mechanisms to translate reduced O_2 into vasodilation.

Perhaps because (1) capillaries are viewed as the hub of gas and nutrient exchange between blood and tissues, and (2) increased oxygen extraction during exercise is typically reported in terms of elevated A/V gradient, it may be incorrectly assumed that capillaries and veins become hypoxic during exercise while the oxygenation of arteries is unaffected. However, the arterial oxygenation reported in A/V gradient measurements is typically taken from large conduit arteries, where blood is fresh from the heart and near its maximum oxygenation. In contrast, resistance arteries and arterioles are in fact a location of significant O_2 diffusion into surrounding muscle tissues.[29] As O_2 extraction increases dramatically during exercise, cells in both the blood and the vascular wall of resistance arteries and arterioles most likely see much lower pO2 values during engagement of local skeletal muscle than at rest. The smooth muscle and endothelium of resistance arteries – as well as blood cells passing through – are therefore ideally situated to integrate hypoxia into signaling pathways in order to initiate a local vasodilatory response.

Chemical messengers believed to lie downstream of hypoxia have been studied extensively in the context of hypoxia-induced vasodilation, both at rest and during exercise.[30] NO has emerged as a signal of particular interest in this context,[31] believed to mediate heterocellular communication potentially originating from multiple upstream hypoxia-sensing mechanisms. ATP (along with its derivatives adenosine diphosphate (ADP), adenosine monophosphate (AMP), and adenosine) has also been highlighted as an

important messenger of hypoxia. RBCs are believed to serve as potential O_2 sensors and signal in response to hypoxia via the release of ATP into the vascular lumen, signaling to the endothelium in order to regulate vascular tone.[32] The proposed RBC-dependent pathway has been studied at some length by Sprague and Ellsworth and is elaborated by them in detail.[33]

The Isakson laboratory has extensive experience in studying the roles of ATP,[34-37] NO,[38-41] and the proteins that regulate them as important heterocellular signals in the resistance vasculature. Thus, our laboratory is uniquely positioned to explore these purported signaling links between hypoxia and hyperemia. The following sections will provide further background about the vascular roles of NO, eNOS, and hemoglobin α (Hbα) (1.2), as well as ATP and Panx1 (1.3).

1.2 Nitric Oxide signaling in the vasculature

The 1998 Nobel Prize in Physiology or Medicine recognized the critical signaling role of NO in the cardiovascular and nervous systems, highlighting research by Drs. Furchgott, Ignarro, and Murad.[42] Vascular NO is most notable for its function as an endothelium-derived relaxing factor,[43-46] but the diatomic gas also plays important cardiovascular roles in regulating platelet aggregation,[47, 48] cardiac contractility,[49] and vascular SMC proliferation,[50, 51] among a broad array of other effects via S-nitrosylation.[52]

In the vascular wall, NO regulates both O_2 consumption and supply, competing with O_2 binding to cytochrome c oxidase (mitochondrial Complex IV) to restrict mitochondrial O_2 demand[53] while promoting relaxation of smooth muscle[54, 55] to regulate vascular

resistance.[56] The latter function is achieved via activation of soluble guanylyl cyclase[57] to generate the second messenger cGMP and activate protein kinase G,[58] in turn activating K^+ channels and reducing intracellular calcium (Ca^{2+}) levels[59, 60] to inhibit the activation of myosin light chain kinase and prevent its phosphorylation of smooth muscle myosin light chain,[61] thereby inhibiting smooth muscle contraction. Through this pathway, NO is one of the principal mechanisms by which the endothelium regulates the contraction state of vascular smooth muscle.[62]

1.2.1 eNOS production of NO in the endothelium

NO is enzymatically produced by the nitric oxide synthase family of proteins, which consists of neuronal NOS (nNOS, NOS1), inducible NOS (iNOS, NOS2), and endothelial NOS (eNOS, NOS3). Each homodimeric isozyme converts L-arginine into NO and L-citrulline via a redox reaction, releasing NO as a signaling molecule.[63] All three NOS isoforms contribute to NO production in the vasculature. Expressed in nitrergic nerves innervating vascular smooth muscle, nNOS provides a source of NO in opposition to sympathetic inputs, and in addition plays a role in central nervous system regulation of blood pressure.[64] While iNOS is not typically expressed until induced by cytokines or other activating signals, once activated – most notably in macrophages as a cytotoxic agent – iNOS is constitutively active and produces large amounts of NO.[65] Expressed in arteries during inflammation, iNOS may contribute to vascular dysfunction.[66]

The classic vascular NOS isozyme is eNOS, so named for its canonical expression in endothelial cells (ECs), although it is also expressed in cardiac myocytes[67] and other cell

types.[68] The importance of eNOS as a source of NO in the vasculature is underlined by the fact that $eNOS^{-/-}$ mice are hypertensive, exhibiting elevated blood pressure 20 mmHg above $eNOS^{+/+}$ controls.[69, 70] eNOS is believed to play a particularly important role in mid- to large-sized arteries,[71, 72] where the proportional contribution of NO to vasodilatory signaling is greatest.[73, 74]

In the vascular endothelium, eNOS localizes to caveolae, signaling microdomains on the plasma membrane of ECs, with caveolin-1 acting as an important negative allosteric regulator of eNOS activity by impeding the interaction between eNOS and Ca^{2+}/calmodulin.[75] The production of NO by eNOS is activated by multiple upstream pathways,[76, 77] serving as a hub for vasodilatory signaling in the vascular endothelium. Many of these pathways facilitate eNOS activation by modulation of its complicated system of post-translational modifications:[78] for example, bradykinin stimulation promotes eNOS activation via both dephosphorylation of T495[79] and phosphorylation of S1177.[77] Conversely, eNOS is also regulated by upstream vasoconstrictive signaling: angiotensin II induces the phosphorylation of Y657 to attenuate eNOS production of NO.[80]

While the extent to which enzymatic NO production influences skeletal muscle hyperemia during exercise remains uncertain, use of NOS inhibitors has demonstrated a role for NOS-derived NO in this setting.[81] Endothelial shear stress is an important activator of eNOS,[82-84] particularly in the context of blood flow regulation during exercise,[85] although its exact contribution to the latter remains unclear.[86] NOS-derived NO is further believed to play a vasodilatory role in the context of hypoxia, both at rest[87] and during

exercise,[31] although its relative contribution similarly remains unknown in the context of other redundant vasodilatory mechanisms.[88]

1.2.2 Role of eNOS in red blood cells?

Until recently, red blood cells (RBCs) have been viewed predominantly as a site of NO consumption, due to the large propensity of hemoglobin to scavenge NO.[89-92] In that light, the possibility of NO production in RBCs was considered unlikely.[93] However, the reality may be more complex than previously assumed. NO consumption rates in RBCs are two orders of magnitude lower than cell-free hemoglobin,[92] likely due in part to decreased interactions between RBC-bound hemoglobin and NO in the lumen.[94, 95] Potential barriers to NO scavenging by hemoglobin in RBCs include an RBC-free zone at the periphery of the vessel lumen[90, 91] and the RBC plasma membrane, which inhibits NO diffusion into the circulating cell.[89]

The presence of NOS in RBCs has also been reported by multiple groups with varying details. Circa 2000, studies reported that both eNOS and iNOS are present in RBCs,[96, 97] though Kang *et al*. reported that RBC NOS isoforms were not catalytically active.[97] Furthermore, both groups hypothesized that if functional NOS were expressed on RBCs, the observed ability of RBC hemoglobin to scavenge NO from its surroundings would be compromised by competitive binding of locally-produced NO.[96, 97] More recent evidence has been presented to suggest that RBCs universally express a catalytically active eNOS on the inner leaflet of the plasma membrane and in the cytoplasm.[93, 98] RBC eNOS may

play an important role in both routine and diseased vascular function, as its activity and impairment were found to correlate, respectively, with flow-mediated vessel dilation and endothelial dysfunction.[98] Additional research suggests that RBC eNOS contributes to circulating nitrite levels, which may play a role in blood pressure regulation.[99]

Though the claim is subject to some controversy, RBCs may be an important source of NO in the microvasculature. Under normoxic conditions, more NO may be produced in RBCs than any other cellular compartment,[98] and NO production by RBC eNOS could have multiple physiological functions. One hypothesis is that RBC eNOS can create an ‘‘NO shield’’ against scavenging by RBCs, preventing interruption of intracellular signaling.[98] Furthermore, shear stress in hypoxic conditions has been indicated to activate RBC eNOS,[100] which in turn could play an important role in the regulation of RBC deformability to ensure adequate perfusion and oxygen distribution.[101] This proposed function in particular suggests the potential for importance of NO from RBC eNOS in regulation of vascular flow. Finally, a broader RBC endocrine—or ‘‘erythrocrine’’—function has recently been proposed in which RBCs provide systemic NO regulation throughout the vasculature.[102] Thus, an emerging perspective is that much of the NO interacting with RBCs may be produced locally, and that RBCs provide an important transport function involved in localizing NO signaling.

A major remaining question is to what extent RBCs represent an *in vivo* sink for vascular NO, and how this role is altered among different physiological regions and pathological states (e.g., across a range of blood oxidation levels or other variations in

blood chemistry). Even when considered simply as a sink for NO, the role of RBCs in this context could be more dynamic than initially assumed if RBC eNOS provides a local shielding effect against NO scavenging. The variable extent of an RBC eNOS shielding effect could conceivably modulate the impact of NO release from other sources, such as eNOS in the endothelium, by allowing a given RBC to scavenge less or more NO from its surroundings. The possibility of this phenomenon is relevant to the study of NO regulation of local myogenic tone and inflammation. Additionally, the ability of RBCs to influence the speciation of nitrogen oxide metabolites could define the potential of these cells as major signaling players in the vasculature. The ability of RBCs to scavenge and release NO in various settings suggests that they may be capable of activating or inhibiting NO signaling pathways in response to changes in blood chemistry across the vascular tree. Because of the key role of RBCs in the microcirculation, this potentially important site of NO generation requires further investigation in the contexts of vasodilation and inflammation.

* Section 1.2.2 is adapted from a review section written by the author and published in Shu *et al.* (2015, Cell. Mol. Life Sci.).[103]

1.2.3 Hemoglobin Alpha in the vasculature

Hbα is best known for its role alongside hemoglobin β (Hbβ) in the α,α,β,β hemoglobin tetramers responsible for O_2 transport.[40] Existing in roughly equimolar ratios in adult human RBCs, Hbα and Hbβ account for the overwhelming majority of total RBC protein

copy number[104] and mass. Tetrameric Hb carries O_2 molecules via heme-coordinated iron held within a porphyrin complex,[105] loading O_2 in the oxygen-rich pulmonary vasculature and transporting it throughout the systemic vasculature to release into metabolically active tissues around the body. The affinity of Hb-carried heme for O_2[106] is tightly regulated, allowing for precise control of O_2 delivery.[107] Besides O_2, Hb binds an array of similar blood-borne gases including carbon dioxide (CO_2),[108] carbon monoxide (CO),[109] and NO.[95, 110] These additional interactions are important both for their effects on the ability of Hb to bind O_2,[109] as well as for their regulation of separate signaling processes in the vasculature.[95]

Beyond the Hb expressed in RBCs, in 2012 the Isakson laboratory reported novel Hbα expression in the ECs of human and murine resistance arteries.[38] In the vascular wall, Hbα is enriched in myoendothelial junctions (MEJs), specialized cellular projections through the internal elastic lamina (IEL) that allow ECs and SMCs to communicate directly with one another.[111, 112] Localization to the MEJ allows endothelial Hbα to functionally couple with eNOS,[39] regulating the bioavailability of eNOS-derived NO to adjacent smooth muscle. In its Fe^{2+} oxidation state, Hbα scavenges NO,[113] limiting its diffusion and bioactivation.[38] The localization of Hbα to the MEJ is intrinsic to this function: while the absolute abundance of endothelial Hbα may be less than that of Hb in RBCs, its proximity to eNOS in the MEJ likely allows endothelial Hbα to play a proportionally greater role in regulating NO bioavailability to SMCs.[40]

Endothelial Hbα regulation of NO is critical for the normal constriction of resistance arteries: when thoracodorsal arteries (TDAs) were treated with Hbα siRNA[38] or the Hbα

mimetic peptide HbαX[39] to prevent the Hbα-eNOS interaction, constriction was severely impeded in response to phenylephrine (PE) stimulation. NO regulation by Hbα plays a significant role in blood pressure regulation as well, with HbαX-treated mice displaying significant reductions in systolic, diastolic, and mean arterial pressure as compared to scrambled peptide-treated controls.[39] Together, the Isakson laboratory's findings identify Hbα as a key regulator of NO signaling, peripheral resistance, and vessel diameter in the resistance vasculature.

1.2.4 NO production from nitrite

A growing field of research has evolved surrounding the complicated interactions between Hb and NO.[114] While oxygenated heme rapidly oxidizes NO to nitrate,[113, 114] enabling functions such as the previously discussed role of endothelial Hbα, deoxygenated heme is also capable of facilitating the reduction of nitrite to NO. Possessing extremely high O_2 affinities, the prosthetic heme groups of neuroglobin (p_{50} = 7.5 mmHg), myoglobin (p_{50} = 3 mmHg), and cytoglobin (p_{50} = 1 mmHg) predominantly reside in an oxygenated state.[114] In contrast, Hb (p_{50} = 26 mmHg) is functionally optimized to load O_2 in the pulmonary circulation and unload O_2 in the systemic circulation during each transit through the cardiovascular system.[107] Thus, while other heme-carrying globins are capable of reducing nitrite to NO, particularly in severely hypoxic conditions,[115, 116] Hb has received the greatest attention as a physiological nitrite reductase.[117-119]

A competing hypothesis to explain NO creation and clearance by Hb involves the S-nitrosylation of Hb in allosteric cooperation with O_2 uptake and release, allowing Hb to deliver NO to sites of low pO_2. However, numerous shortcomings of the SNO-Hb hypothesis have been identified,[119] making it appear increasingly unlikely as a primary explanation for Hb regulation of NO levels. In contrast, the role of nitrite as a source of NO has been demonstrated from numerous angles of supporting evidence. The discovery in 2000 by Gladwin *et al.* of a significant A/V gradient for plasma nitrite[120] is particularly notable in that it demonstrates the loss of nitrite from plasma during transit from the arterial to venous circulation. Furthermore, the same study demonstrated that nitrite consumption between the arterial and venous circulation increased during exercise and pharmacological NOS inhibition. These findings supported an emerging narrative: as metabolically active skeletal muscle extracts a greater amount of O_2 from the blood, an elevated proportion of deoxyHb exerts increasing influence as a nitrate reductase.

A subsequent study in 2003 by Cosby, Gladwin, *et al.* demonstrated the ability to experimentally manipulate blood flow at rest and in exercise via nitrite-derived NO production. First establishing that the infusion of nitrite into the forearm via the brachial artery significantly elevated forearm blood flow from baseline, they then repeated the same experiment while treating both groups with the NOS inhibitor L-NMMA, finding a persistent increase in forearm blood flow in response to nitrite infusion in both cases. Most importantly, infusion of both nitrite and L-NMMA led to a considerable elevation in blood flow to the exercising forearm as compared to that in an exercising, L-NMMA-treated control lacking nitrite infusion.[117] The latter result demonstrates the particular relevance of

nitrite to the exercise-induced hyperemic response, as inhibition of NOS enzymes removes their potential for NO contribution. Meanwhile, *in vitro* experiments compared production of NO from nitrite and RBCs at a range of oxygen tensions, establishing deoxyHb nitrite reductase activity and NO production as a potential mechanism for the results collected *in vivo*.[117] Taken together, these findings demonstrate the role of nitrite-derived NO in exercise hyperemia, independent from the contributions of NOS enzymes.

Maher *et al.* built upon the findings of Cosby *et al.* in a study published four years later in 2007, employing an elegant series of dose-response experiments in a similar experimental setup.[121] Maher *et al.* first demonstrated that intrabrachial nitrite infusion increased forearm blood flow under normoxic conditions only at supraphysiologic concentrations an order of magnitude or more above those shown by Cosby *et al*. Reverting then to a lower nitrite infusion rate of 314 nmol/L/min, similar to the near-physiologic concentrations Cosby *et al.* tested, Maher *et al.* found that nitrite infusion resulted in elevated forearm blood flow in hypoxic, but not normoxic, conditions. Hypothesizing that nitrite would play an even greater dilatory role in veins due to their lower pO_2 levels, they demonstrated increased venodilation in direct response to nitrite infusion, raising further questions about the impacts of nitrite on central blood volume and cardiac preload. These findings underscore the importance of oxygen tension to nitrite's vasodilatory function, highlighting hypoxia as the critical driving force behind elevated nitrite-derived NO production during exercise.

Additional discussion has explored the relationship between the oxygen saturation threshold for Hb-facilitated nitrite reduction and the oxygen tensions reached in arteries of

various calibers, both at rest and during exercise.[118, 122] While other globins such as myoglobin may contribute substantial nitrite reductase activity at lower oxygen tensions in the range of single digit mmHg,[115, 118] it appears evident that the (likely prominent) nitrite reductase role of Hb may peak around its 26 mmHg p_{50} point for O_2 saturation, at which Hb conformational state and deoxyHb availability combine to create a maximal rate of nitrite reduction to NO. Therefore, the vascular location of NO generation from nitrite is influenced by the extent of O_2 extraction from the blood, shifting upstream into the arteriolar network as the metabolic demand of tissue increases.[122]

The evolving understanding that nitrite can be recycled to NO necessitates a paradigm shift in the NO cycle.[123] With plasma concentrations on the order of tens of μM,[124] nitrate constitutes the overwhelming majority of total NO-related compounds in the blood; however, humans lack the ability to activate nitrate without assistance from commensal bacteria to reduce it to nitrite[125, 126] (reviewed at length by Lundberg *et al.*[127]). Circulating at hundred-nM to near-μM levels[124] and readily converted to NO by multiple, abundant human proteins, nitrite is thus recognized as an influential storage pool of NO in the blood.[117] While the half-life of NO is on the order of a millisecond, nitrite can circulate for multiple minutes,[124] surviving multiple laps of the cardiovascular system. Thus, NO may be released in any blood or tissue location where circumstances support the reduction of circulating nitrite.

1.3 Purines and Panx1 in the vasculature

Adenosine and related purinergic nucleotides have been understood as powerful signaling molecules in cardiovascular physiology for nearly a century.[128] Adenosine is not only known as an important regulatory signal in multiple cardiac capacities,[129] but was also explored in an ischemic context in the cerebral vasculature as early as the 1970s, including notable work by Robert M. Berne at the University of Virginia.[130, 131] A robust field of research has evolved surrounding the numerous and complex roles of both physiological and pathophysiological vascular purinergic signaling,[132] too extensive to review here in full. The Isakson laboratory has made recent contributions to the understanding of vascular purinergic signaling, including a particular focus on vascular roles and regulation of the novel ATP release channel Panx1.[34, 133-137]

1.3.1 *Purinergic signaling in the regulation of vascular tone*

The functions of ATP in regulating vascular tone are dependent on multiple variables, including the adjacent cells, the purinergic receptors present, and the presence of ectonucleotidases. The latter regulate the proportional availability of different purinergic compounds to carry out different signaling roles, while purinergic receptor expression profiles help determine how these signals are transduced into downstream cellular signaling pathways. A helpful schematic of the major families of purinergic receptors and ectonucleotidases is available in the first figure of an extensive 2014 review by Burnstock and Ralevic.[132] ATP may be hydrolyzed to varying degrees by ectonucleotidase 5'-

triphosphohydrolases (ENTPDases) such as CD39 to form ADP and AMP (as well as ADP to AMP, and similarly with uridine triphosphate (UTP)). AMP is hydrolyzed to adenosine by ecto-5'-nucleotidase (CD73). ATP and ADP act on ionotropic P2X and metabotropic P2Y receptors, while adenosine acts on metabotropic $A_1/A_{2A}/A_{2B}/A_3$ receptors. Extensive tables detailing the expression the of these receptors in SMCs and ECs of various vessels and species, as well as their effects on vasoconstriction and vasodilation in these contexts, are also available in Burnstock and Ralevic's review.[132]

Sympathetic innervation of vascular smooth muscle imparts a critical influence on vascular tone in the context of broad cardiovascular regulation by the autonomic nervous system.[138] In addition to releasing norepinephrine (NE) to activate adrenergic receptors on SMCs, sympathetic nerve terminals have been shown to achieve synergistic influence through the function of ATP as a cotransmitter[139, 140] to activate purinergic receptors on SMCs such as the $P2X_1$ channel[141] and enhance rapid constriction. The relative contributions of NE and ATP to sympathetic transmission appear to vary by vascular bed.[142-145] The Isakson laboratory recently demonstrated that α1D-adrenergic stimulation of smooth muscle in thoracodorsal resistance arteries also leads to Panx1-dependent ATP release by SMC, and that this autocrine/paracrine signaling is necessary for both α1 adrenergic receptor-dependent vasoconstriction and sympathetic regulation of blood pressure.[34, 134, 137]

In contrast to the effects of ATP as a vasoconstrictor on SMCs, in the endothelium purines predominantly act to stimulate vasodilation via EC-dependent dilation pathways.[146-148] Thus, a balance between the influence of ATP and related purines on

smooth muscle and endothelium defines the overall influence of purinergic signaling on vascular tone. Increased shear stress stimulates ATP release from ECs,[149-152] which is believed to occur via a vesicular mechanism.[153] Luminal ATP acts in autocrine/paracrine fashion on endothelial P2Y receptors, stimulating an increase in intracellular Ca^{2+} and downstream vasodilatory signals including prostacyclin and NO.[154] In comparison to P2Y receptors, ionotropic P2X receptors are less well-studied in the vascular endothelium, but they may also play a more complicated role in this context.[155] ATP-induced ATP release has been demonstrated in human umbilical vein ECs (HUVECs),[156] suggesting the possibility of positive feedback loops in vascular endothelial purinergic signaling.

RBCs have also been reported to release ATP in response to hypoxic conditions, reduced pH,[32] and mechanical deformation, representing an additional source of vasodilatory ATP signaling to the endothelium in conditions related to exercise hyperemia. Hypoxic ATP release from RBCs has been reported in humans[157] as well as in other mammals including hamsters[32] and rats[158] (the latter demonstrating both ATP release and dilation of *ex vivo* cerebral arterioles). Based largely on work from the Ellsworth and Sprague laboratories, an elaborate pathway has been proposed[33] in which $G\alpha_i$[159] or $G\alpha_s$[160] activation leads, perhaps via β subunit activity,[161] to adenylyl cyclase activation and generation of cyclic AMP (cAMP),[160, 162] resulting in PKA activation[162] and ultimately ATP release via Panx1,[163] with possible but loosely defined involvement of the cystic fibrosis transmembrane conductance regulator (CFTR).[164] However, this purported pathway rests upon a tenuous link between hypoxia and mechanical deformation, established by treatment of RBCs with diamide (tetramethylazodicarboxamide, an

oxidizing agent used to induce disulfide bonds) to reduce RBC deformability and inhibit hypoxia-induced ATP release.[165] While Panx1-dependent ATP release from RBCs has been demonstrated as a result of both hypoxia[163] and high potassium, hypo-osmotic buffer,[166] other steps in the reported pathway such as cAMP have been demonstrated instead as a result of mechanical[162] or pharmacologic[160, 162] stimulation, leaving overall mechanistic connectivity uncertain. The role of Panx1 in ATP release from RBCs is explored experimentally in Chapter 3.

1.3.2 *Panx1 properties and channel function*

Pannexin 1 (Panx1), first discovered in the early 2000s,[167, 168] is one of three proteins in the pannexin family, related to invertebrate innexins and less closely to the gap junction-forming connexin proteins.[167] While pannexins were named based on the wide phylogenetic range in which they are found,[167] Panx1 is also fairly ubiquitous in its expression across an array of mammalian tissues (reviewed at length by Bond and Naus in 2014[169]). In the vasculature, Panx1 is expressed in resistance artery, arteriole, and venule SMCs, as well as in ECs in a wide variety of vessels,[170, 171] and in RBCs.[163] Established early on as an ATP release channel,[172] Panx1 is involved in a variety of vascular purinergic signaling pathways, including in sympathetic vasoconstriction[34, 134, 137] and regulation of cerebral myogenic tone,[136] as well as endothelial regulation of inflammation.[136, 173]

Structurally, Panx1 consists of intracellular N- and C-termini, two extracellular loops, one intracellular loop, and four transmembrane domains. Panx1 hexamerizes to form large-

pore channels, which in contrast to connexins, are not known to form cell-cell gap junctions.[171] Though noted for their permeability to ATP,[172] Panx1 channels exhibit low ion selectivity and thus offer a broad, if transitory, window from the cytoplasm to the extracellular space.[166, 174] A discrepancy exists regarding Panx1 channel conductance,[175] which was originally reported at ~450–500 pS[166, 172, 176] but more recently has been reported on the order of 70–75 pS.[177-179] Panx1 channels are reported to be outwardly rectifying[172] with a pore size estimated at 17–21 A° (1 A° = 0.1 nm)[180] (although the structure is not yet resolved) suggesting that Panx1 channels may have the potential to undermine the selective permeability of the cell membrane.[174] This large permeability is likely why Panx1 channels predominantly remain closed at physiologic voltages[172] and undergo extensive post-translational modification (see "Post-translational modification of pannexins" section in Good *et al.*[181]).

Panx1 channels open to varying extents in response to multiple stimuli.[37, 169] However, the cytoplasmic C-terminus of Panx1 is critical to the maintenance of the channel-closed state and may inhibit the Panx1 channel via a "ball-and-chain" mechanism, similar to that observed in other ion channels, whereby the C-terminus may enter the pore from the cytoplasmic side.[182, 183] The well-described caspase cleavage of the C-terminus between amino acids 376 and 379[182, 184] renders Panx1 channels constitutively truncated and permanently active.[184] Among channels with similarly hypothesized ball-and-chain mechanisms, Panx1 is the first known to undergo cleavage of the C-terminus as a method to permanently remove this channel inhibition mechanism.[182]

Potentially important in the vasculature (e.g. in conduction pathways), a positive feedback loop of ATP-induced ATP release has been hypothesized, stemming from Panx1 channel release of ATP in response to mechanical stress.[185] Subsequent ATP activation of P2Y receptors on the same and/or adjacent cells could initiate a signaling cascade that releases intracellular Ca^{2+}, opening further Panx1 channels to propagate an extracellular ATP signal alongside an intracellular wave of Ca^{2+} and inositol triphosphate.[185] This possibility is reliant on Panx1 channels being sensitive to intracellular Ca^{2+}, a concept for which there appears to be common knowledge but sparse physiological evidence.

Additionally, ATP-induced ATP release is also thought to be mediated through Panx1 channels and P2X receptors (which have been found to co-localize) whereby Panx1 channels open in response to ATP-gated $P2X_7$ receptor activation.[186-188] This positive feedback loop of ATP-induced ATP release may in turn be negatively regulated by extracellular ATP. Substituted cysteine accessibility data suggest that the first transmembrane domain and first extracellular loop (EL1) line the Panx1 channel pore.[189] At high extracellular concentrations, ATP is believed to inhibit Panx1 by interacting with arginine 75 on EL1, perhaps providing a steric obstruction at the extracellular end of the pore to block ATP passage through the open channel.[174] This mechanism could have critical importance in providing negative regulation to the purinergic receptor-activated positive feedback loop of ATP-induced Panx1 ATP release.[190] However, outside of evidence provided from non-vascular cell culture, it is currently not clear how this observation might relate to the intact vasculature.

Other important mechanisms controlling pannexin channel activation include membrane depolarization, decreased circulating oxygen levels, and mechanical stimulation. Although there are reports of Panx1 channels being responsive to mechanical stimulation such as cell swelling or stretching, it remains an active area of investigation whether this mechanism occurs *in vivo*.[172, 188, 191] Reduced blood pO_2 levels have also been shown to open Panx1 channels on RBCs, releasing ATP to induce upstream vasodilation.[163] In addition, a key regulator in maintaining blood pO2 levels, the carotid body, also releases ATP through Panx1 channels on type II cells, potentially further amplifying activation of the afferent nerves.[192] However, the impact of oxygen content on ECs or vascular smooth muscle cells (VSMCs) Panx1 channel activation is unknown. Lastly, membrane depolarization methods via the activation of TRPM5 channels, the addition of extracellular KCl, or the application of a depolarizing voltage step have all been shown to activate Panx1 channels *in vitro*.[193-195] However, KCl-induced vasoconstriction in isolated arteries was found to be independent of Panx1 channel activity, indicating that the mechanisms for Panx1 channel activation are likely either cell type-specific or altered *in vitro*.[34]

Of note, the stimuli suggested to activate Panx1 channels (mechanical stimulation,[172, 188, 191] increasing extracellular potassium concentration,[195] rise in intracellular Ca^{2+},[185] membrane depolarization,[193] increased intracellular redox potential,[196] S-nitrosylation,[133] and oxygen deprivation[163, 192]) could all be physiologically relevant to vascular physiology/pathophysiology. Hence, caution should be taken in experimental designs intended to study the role of Panx1 in the vascular wall. Vessel tension, K^+ and Ca^{2+} concentrations, and oxygen tension should be maintained as near as possible to *in vivo*

conditions. Control over these parameters is critical to accurately assess the role of Panx1 in the vasculature.

* Section 1.3.2 is adapted from a review section written by the author and published in Good *et al.* (2015, Biochem. Soc. Trans.)

CHAPTER 2: MATERIALS AND METHODS

2.1. Materials and Methods for Chapter 3:

Materials

Rabbit polyclonal antibodies against the second extracellular loop (EL2) and carboxy-terminus (CT) of Panx1 were a generous gift from Silvia Penuela and Dale Laird (University of Western Ontario, Lon- don, Canada). Rabbit monoclonal antibody against the amino-terminus (NT) of Panx1 was purchased from Thermo Fisher (no. 487900). Spectrin mouse monoclonal antibody was purchased from Sigma Aldrich (no. S3396). Connexin 43 (Cx43) rabbit polyclonal antibody was purchased from Sigma Aldrich (no. C6219).

Human Subjects

Human blood samples were acquired from healthy male and female volunteers between 20 and 30 years old in concordance with the study protocol approved by the ethics committee of the Heinrich-Heine University. All subjects gave written informed consent in accordance with the declaration of Helsinki. *Human experiments were performed by colleagues at HHU Dusseldorf.*

Animals

Mice were handled according to approved animal protocols at the University of Virginia. $Panx1^{-/-}$ (24) and WT control (C57Bl/6 background) mice of both sexes aged between 9 and 14 weeks were used for this study.

Forced Exercise Capacity Test

In accordance with established methods (18), mice were acclimatized to the treadmill for three consecutive days before the experimental day. Acclimatization consisted of 10 min of treadmill running at 0% incline and speed of 13 m/min each day. On the day of testing, the treadmill was set to 5% incline. Running speed was set at 13 m/min for 30 min and increased by 2.7 m/min every 30 min (maximum of 27 m/min) until perceived exhaustion, as determined by refusal to run despite encouragement for 20 s. Blood lactate was measured immediately before and following the acute exercise test to verify exhaustion.

Voluntary Exercise Capacity

As published previously (18), mice were randomly selected and housed individually in cages with running wheels. Mice were allowed free access to the running wheel, food, and water. Sedentary mice were kept in communal cages. Daily running distance was recorded via computer monitoring for 14 days.

Blood Collection and Separation of RBCs

Human whole blood was collected into heparin-coated tubes and RBCs were immediately centrifuged for 10 min, at 800 *g* and 4°C (Hettich, Rotina 38R, 2140 rpm). Plasma and buffy coat were aspirated. The RBC pellets were washed three times with Hanks' buffered salt solution (HBSS) containing calcium and 0.5% bovine serum albumin (BSA) by centrifugation at 300 *g* for 10 min at 4°C. Washed RBCs were re-suspended to

20% hematocrit (hct) in HBSS containing 0.5% BSA and used for experiments. *Human RBC experiments were performed by colleagues at HHU Dusseldorf.*

To collect mouse blood, mice were anesthetized and exsanguinated via cardiac puncture with syringes coated with EDTA (no. E5134, Sigma-Aldrich) before use to prevent coagulation. Whole blood was centrifuged for 5 min, at 500 *g* and room temperature (RT) (Fisher, accuSpin Micro 17, 2300 rpm), after which plasma and buffy coat were removed by aspiration. The remaining RBC pellet was washed three times in a modified Krebs- Henseleit (K-H) buffer (1.2 mM KH_2PO_4, 5.0 mM KCl, 1.2 mM $MgSO_4$, 1.6 mM $CaCl_2$, 118 mM NaCl, 24.8 mM $NaHCO_3$, 10 mM glucose) and centrifuged for 5 min at 500 *g* between each wash. Washed RBCs were resuspended to 5% hct in K-H buffer and used for experiments.

Detection and Localization of Panx1 on RBC Membrane by Immunostaining

For detection of Panx1 by immunohistochemistry, mouse afferent arteriole kidney sections were fixed in 4% paraformaldehyde, treated with Histoclear (Sigma Aldrich), progressive ethanol washes, and H_2O_2, then incubated with primary antibodies (Panx1 NT, Cx43, IgG control, or no primary) overnight at 4°C, and subsequently biotin-conjugated anti-rabbit IgG secondary antibody then 3,3'-diaminobenzidine (DAB) solution, and finally hematoxylin and eosin staining before mounting. DAB-stained kidney slides were imaged using a Nikon Eclipse TS100 microscope at x20 objective. *This experiment was performed by Leon DeLalio.*

For detection of Panx1 by immunofluorescence, washed RBCs were blocked (PBS + 10% fish skin gelatin, 0.25% Triton X-100, 0.5% BSA, 10% donkey serum) and incubated with primary antibodies (Panx1 EL2 and CT) while rocking overnight at 4°C, and AlexaFluor donkey anti-rabbit secondary antibodies while rocking for 2 hours at RT. RBCs were then mounted onto slides via Cytospin for 5 min at 1,000 *g*, mounting medium was added, and a coverslip was applied. Slides were imaged using an Olympus IX81/FV1000 confocal microscope at x20 objective.

Western Blot Analysis of Panx1 Expression in RBCs

Washed RBCs were lysed in 10 times their volume of hypotonic RBC lysis buffer with two changes of buffer (three washes total), and RBC ghost membranes were collected by centrifuging for 5 min at 3,000 *g*. RBC ghosts were added to RIPA buffer (50 mM Tris·HCl, 150 mM NaCl, 5 mM EDTA, 0.5% Triton X-100, 1% sodium deoxycholate, 20 mM NaF, 1 mM NaVO4, pH 7.4, supplemented with 10 µl/ml each of protease inhibitor cocktail PI and phosphatase inhibitor cocktails P2 and P3), mixed with Laemmli buffer and subjected to SDS-PAGE on a 4 –12% Bis-Tris Midi gel (no. WG1401BX10, Invitrogen) followed by transfer to nitrocellulose membrane. Blots were blocked in TBS-T (0.2% Tween in TBS (50 mM Tris, 150 mM NaCl, pH 7.53)) containing 3% BSA and incubated overnight with primary antibodies at 4°C, followed by fluorescently tagged secondary antibodies (goat anti-mouse and goat anti-rabbit; LICOR) for 1 h at RT. Both primary and secondary antibody incubations took place in 5% BSA in TBS-T. Blots were imaged via fluorescence using a LICOR Odyssey imaging system.

Extraction and Measurement of Intracellular cAMP

For extraction of intracellular nucleotides, cells were lysed and protein precipitated by addition of an ice-cold solution of 20% acetonitrile, 40% methanol, and 40% water to the RBC pellet, followed by incubation at 60°C for 10 min. Samples were then cooled on ice and centrifuged at 3,000 *g* for 30 min at 4°C to remove cellular debris. The supernatant was removed and kept separately while cell pellets were washed with the extraction solution and centrifuged again as described above. The supernatants of both extraction steps were combined and taken to dryness in a Speedvac system. Purines were separated by reversed-phase liquid chromatography (Waters UPLC BEH C18 column, 1.7 μm beads; 2.1 x 150 mm; Milford, MA) and assayed using a triple quadrupole mass spectrometer (TSQ Quantum-Ultra; ThermoFisher Scientific, San Jose, CA) operating in the selected reaction monitoring mode with a heated electrospray ionization source essentially as described (15). The mobile phase consisted of a linear gradient of 1% acetic acid in water (pH 3; mobile phase A) and 100% methanol (mobile phase B). The mobile phase flow rate was 300 μl/min and was delivered with a Waters Acquity ultra-performance liquid chromatographic system. The gradient (A/B) was as follows: from 0 to 2 min, 99.6%/0.4%; from 2 to 3 min, to 98.0%/2.0%; from 3 to 4 min, to 85.0%/15.0%; from 4 to 6.5 min, to 99.6%/0.4%. Instrument settings were as follows: sample tray temperature, 10°C; column temperature, 50°C; ion spray voltage, 4.0 kV; ion transfer tube temperature, 350°C; source vaporization temperature, 320°C; Q2 CID gas, argon at 1.5 mTorr; sheath gas, nitrogen at 60 psi; auxiliary gas, nitrogen at 35 psi; Q1/Q3 width, 0.7/0.7 units full-width half-

maximum; scan width, 0.6 units; scan time, 0.01 s. *Intracellular cAMP measurements were performed by colleagues at HHU Dusseldorf and the University of Pittsburgh.*

Protocols for Induction of ATP Release:

Hypotonic potassium gluconate stimulation

Washed mouse RBCs were resuspended in potassium gluconate (KGlu) solution (150 mM KGlu in H_2O) containing 300 μM ARL 67156 trisodium (ARL) (no. 1283, Tocris) at 1% hct and incubated for 30 min at RT. Afterwards, samples were diluted with an equal volume of either 150 mM KGlu solution or H_2O and incubated at RT for 5 min at RT.

Stimulation with 8Br-cAMP

Washed RBCs were resuspended in K-H buffer at 10% hct and mixed with an equal volume of K-H buffer containing either 200 μM carbenoxolone (CBX) (no. 154930, MP Biomedicals) or vehicle to reach 5% hct and a final concentration of CBX of 100 μM. RBCs were incubated at RT for 120 min. 8-Bromo cyclic adenosine monophosphate (8Br-cAMP) (100 μM) or vehicle was added and samples were incubated for 30 min at RT before analysis. A 50 μl sample was removed for ATP analysis without centrifugation.

Induction of intracellular cAMP production

Washed human RBCs were diluted to 20% hct in 0.5% BSA HBSS. Samples were pretreated with the phosphodiesterase inhibitor 3-isobutyl-1-methylxanthine (IBMX) or left untreated as a control for 10 min at 37°C with gentle shaking, and then treated for 10 min at 37°C with isoproterenol, forskolin, vehicle control of dimethyl sulfoxide (DMSO), or left untreated for control, as indicated. RBCs were pelleted by centrifugation (10 min at

300 *g* at RT). ATP in the supernatant was assessed as described below in *Measurement of ATP in the cell supernatant*. Intracellular nucleotides were extracted from RBC pellets and cAMP was assessed by liquid chromatography mass spectrometry as described above in *Extraction and Measurement of Intracellular cAMP*. *These experiments were performed by colleagues at HHU Dusseldorf.*

Measurement of intracellular ATP

Washed RBCs at 5% hct in K-H buffer were lysed in 10x volume of H_2O, then vortexed at top speed for 10 s and sonicated 10 x 1 s to ensure thorough lysis. An aliquot of this lysed suspension was diluted 10x in K-H buffer for analysis as described below in *Measurement of ATP in the cell supernatant*.

Measurement of ATP in the cell supernatant

Extracellular ATP release was measured using a luciferin-luciferase assay as described previously (35, 36) by mixing equal parts crude firefly tail extract (10 mg/ml in diH_2O, no. FLE250, Sigma Aldrich) and D-luciferin (0.5 mg/ml in diH_2O, no. L9504, Sigma Aldrich). Alternately, a luciferase assay kit (ATP Bioluminescence Assay Kit HS II (Roche) or ATP Determination Kit (no. A22066, Invitrogen)) was also used as indicated in the figure legends. For mouse experiments, 50 µl of each sample was transferred into a well of a 96-well plate (no. 12565501, Fisher), 50 µl of luciferase assay mixture (Roche) was automatically injected into each sample and the resulting luminescence was measured in a FLUOstar Omega plate reader (BMG Labtech). For human experiments, 200 µl of luciferase assay mixture (Invitrogen) was injected into 20 µl sample. A freshly prepared

dilution curve of ATP standard in the experimental buffer was run alongside each set of experimental samples. ATP levels in the supernatant were normalized to total protein concentration in the RBC suspension, which was taken as a measure of cell concentration. Total protein was assessed by BCA assay (kit no. 23227, Pierce) for mouse experiments or by Lowry assay (kit no. 5000116, Bio-Rad) for human experiments. *Experiments using human blood were performed by colleagues at HHU Dusseldorf.*

Evaluation of Hemolysis

Following removal of an aliquot for extracellular ATP analysis, samples were centrifuged for 5 min at 500 *g* at RT to pellet RBCs. A 50 µl aliquot of the supernatant of each sample was transferred into a well of a 96-well plate. A broad-spectrum absorbance reading was collected from each sample. Cell-free Hb was measured by absorbance at 570 nm, which corresponds to an isosbestic point of oxyhemoglobin (oxyHb) and deoxyHb spectra near a local peak absorbance of each species. Net absorbance (ΔAbs) was calculated by subtracting out a background absorbance measurement at 700 nm.

Statistics

Data are expressed as means ± SEM. ATP release and intracellular cAMP data were compared by one-way analysis of variance test (ANOVA) with multiple comparisons using Tukey's test. A significance cutoff of $P < 0.05$ was imposed. Shapiro-Wilks tests were performed to confirm normality of data.

* Section 2.1 is adapted from an original research article (Keller *et al.*, 2017, A.J.P. Cell. Physiol.) written by the author.[197]

*2.2. **Materials and Methods for Chapter 4:***

Animals

Mice were handled according to approved animal protocols at the University of Virginia. Mice featuring global deletion of *Hba1* ("Hba1$^{-/-}$") were used as described by us.[198] *Hba1$^{fl/fl}$* mice were bred and validated as described in Figure 1, in partnership with Ingenious Targeting Laboratory. *Hba1$^{fl/fl}$* mice were crossed with the Cdh5-Cre/ERT2 line to yield a model of tamoxifen-inducible, endothelial-cell-specific *Hba1* deletion ("EC Hba1"). EC Hba1 mice and Cre^{-} controls received 10 days of tamoxifen injections (100 µl at 10 µg/ml) starting at 6 weeks of age. Hba1$^{\Delta 36\text{-}39/wt}$ mice were created via CRISPR/Cas9, deleting four amino acids from the conserved region of *Hba1*-derived Hbα that binds to eNOS.[39] All mice used were on a C57Bl/6 background, of both sexes.

Confocal microscopy for globin expression, proximity ligation assay, and capillary density

Ex vivo TDAs were embedded in paraffin, sectioned, stained for Hbα expression (Abcam, ab102758) or proximity ligation assay (Duolink kit, Sigma), and imaged on an Olympus FLUOVIEW FV1000 confocal laser scanning microscope. *PLA experiments were contributed by TC Steven Keller IV*.

Hindlimb muscles were removed, flash-frozen in OCT medium, sectioned, stained for CD31 expression (Abcam, ab56299), and imaged via confocal microscopy. Images were processed using ImageJ and regions staining positive for CD31 were manually counted to calculate capillary density.

Acute endurance test

Mice aged 10-13 weeks were acclimatized to the treadmill in accordance with established methods.[199] On the day of testing, treadmill was set to 5% incline at 13 m/min (0.5 miles per hour) for 30 min, and increased by 2.7 m/min (0.1 miles per hour) every 30 minutes (to a maximum of 27 m/min (1.0 miles per hour)) until mice reached exhaustion, defined by a refusal to run when induced by 20 strokes on the tail with a wire brush. Blood lactate was measured immediately before and after the test via tail snip and lactate measurement using a Lactate Scout handheld instrument.

Mitochondria Content

Following euthanization, hindlimb muscles were dissected from mice and flash-frozen in liquid nitrogen. Muscle tissue was digested in RIPA buffer (50 mM Tris·HCl, 150 mM NaCl, 5 mM EDTA, 0.5% Triton X-100, 1% sodium deoxycholate, 20 mM NaF, 1 mM NaVO4, pH 7.4, supplemented with 10 µl/ml of protease inhibitor cocktail PI) and physically processed by dounce homogenization and sonication to extract protein, separating excess tissue by micro-centrifugation. Protein concentration was assessed by BCA assay, and equal amounts of protein from each sample were mixed with Laemmli buffer and loaded into a 4 –12% Bis-Tris Midi gel (no. WG1401BX10, Invitrogen) for SDS-PAGE followed by transfer to nitrocellulose membrane. Total protein content of blots was determined using REVERT total protein stain (LICOR). Blots were blocked in TBS-T (0.2% Tween in TBS (50 mM Tris, 150 mM NaCl, pH 7.53)) containing 3% BSA and

incubated overnight with antibody for VDAC (Cell Signaling Technologies, #4661) at 4°C, followed by fluorescently tagged secondary antibodies (goat anti-rabbit; LICOR) for 1 h at RT. Both primary and secondary antibody incubations took place in 5% BSA in TBS-T. Blots were imaged via fluorescence using a LICOR Odyssey imaging system and protein measurements were normalized to the total protein content of each sample as measured by total protein stain.

Pressure Myography

Freshly isolated TDAs were placed into ice-cold Krebs-HEPES solution containing (in ml) NaCl 118.4 KCl 4.7, $MgSO_4$ 1.2, $NaHCO_3$ 4, KH_2PO_4 1.2, $CaCl_2$ 2, HEPES 10, and Glucose 6. The vessels were then mounted in a pressure arteriograph (Danish MyoTechnology) with the lumen filled with Krebs-HEPES solution. The vessels were pressurized to 80 mmHg and heated to 37˚C. Between experiments, bath solution was washed out for 10 minutes with fresh Krebs-HEPES buffer, after which a new Krebs-HEPES solution was added and allowed to re-equilibrate. All vessels were tested for endothelial function before (NaS_2O_4 experiments) or after (PE curve experiments) use by assessing dilatory response to 1μM NS309. PE Preconstriction was determined by addition of PE at the doses indicated, waiting until a stable plateau of internal diameter before continuing to the next stimulation condition. Following conclusion of experimental stimulations, maximal constriction of vessels was determined using a stimulation of 30mM KCl, and finally vessels were washed with a Ca^{2+}-free Krebs-HEPES solution supplemented with 1mM EGTA and 10μM sodium nitroprusside to determine maximal passive diameter. Constriction to PE was calculated as: ((passive

diameter – active diameter) / passive diameter) * 100. Dilation to NaS_2O_4 was calculated as ((diameter after NaS_2O_4 stimulation – diameter before NaS_2O_4 stimulation) / (passive diameter – diameter before NaS_2O_4 stimulation) * 100. *Preliminary data for PE constriction curves was contributed by Henry Askew Page.*

Statistics

Data expressed as mean +/- SEM. Comparison difference between groups was performed by student's t-test, confirming normality via Shapiro-Wilk test. * = $p<0.05$; ** = $p<0.01$; *** = $p<0.001$; **** = $p<0.0001$.

CHAPTER 3. POSSIBLE ROLES FOR ATP RELEASE FROM RBCs EXCLUDE THE cAMP-MEDIATED PANX1 PATHWAY

3.1 Abstract

RBC-derived ATP has been proposed as an integral component in the regulation of oxygen supply to skeletal muscle. In *ex vivo* settings, RBCs have been shown to release ATP in response to a number of stimuli, including stimulation of adrenergic receptors. Further evidence suggested that ATP release from RBCs was dependent on activation of adenylate cyclase (AC)/cAMP-dependent pathways and involved the pannexin 1 (Panx1) channel. Here we show that RBCs express Panx1 and confirm its absence in Panx1 knockout ($Panx1^{-/-}$) RBCs. However, $Panx1^{-/-}$ mice lack any decrease in exercise performance, challenging the assumptions that Panx1 plays an essential role in increased blood perfusion to exercising skeletal muscle and therefore in ATP release from RBCs. We therefore tested the role of Panx1 in ATP release from RBCs *ex vivo* in RBC suspensions. We found that stimulation with hypotonic potassium gluconate buffer resulted in a significant increase in ATP in the supernatant, but this was highly correlated with RBC lysis. Next, we treated RBCs with a stable cAMP analog, which did not induce ATP release from WT or $Panx1^{-/-}$ mice. Similarly, multiple pharmacological treatments activating AC in RBCs increased intracellular cAMP levels (as measured via mass spectrometry) but did not induce ATP release. The data presented here question the importance of Panx1 for exercise performance and dispute the general assumption that ATP release from RBCs via Panx1 is regulated via cAMP.

3.2 Introduction

Roles for extracellular nucleotides in vasodilatory signaling pathways have long been established.[200, 201] ATP has been recognized as an important autocrine/paracrine regulator of cell signaling and function involving P2X (ionotropic) and P2Y (metabotropic) receptors, causing changes in membrane permeability (Na^+, Ca^{2+}) and potential.[200, 201] A well-established hypothesis is that RBC-derived ATP release into the lumen of small blood vessels is an integral component in balancing supply of oxygen to skeletal muscle.[32, 158, 202] The discoveries in the mid-1990s that hypoxia[32] and mechanical deformation[203] each caused ATP release from RBCs inspired an array of follow-up studies to understand the mechanism(s) underlying these phenomena, including studies proposing mechanisms of mechanosensation and mechanotransduction in RBCs.[204-206] As summarized recently,[33] the reported pathway proposes that Hb desaturation signals via $G\alpha_i$ (and not $G\alpha_s$) to activate adenylyl cyclase (AC) and produce cyclic adenosine monophosphate (cAMP), which activates protein kinase A (PKA) to stimulate ATP release through pannexin 1 (Panx1) in a CFTR-dependent mechanism. Indeed, RBCs were shown to express Panx1 on their surface, and Panx1 was proposed to be the main channel regulating ATP release from RBCs in response to high extracellular K^+ and hypotonic stress.[166] Panx1 was also identified as the likely route of hypoxia-driven ATP release from RBCs, as assessed by inhibiting the latter with three pharmacological inhibitors of Panx1.[163] Because of the well-known off-target effects of Panx1 inhibitors, the experiments were confirmed using RBCs from $Panx1^{-/-}$ mice.[207] However, in contrast to the studies implicating CFTR[164] and cAMP[162] in ATP release from RBCs, Panx1-dependent ATP release was not initially tested

downstream of mechanical stimulation, so the connectivity between these elements of the reported pathway is unclear.[162] More recently, the hypothesized connection between mechanical stimulation of RBCs and Panx1-dependent ATP release was explored with a single nonspecific inhibitor of Panx1.[208] Moreover, adding to the general confusion in the field, an independent group could not confirm the presence of Panx1 on mouse RBCs,[209] and hemolysis was proposed recently as the main factor responsible for ATP release from RBCs.[210]

In this work, the expression and membrane localization of Panx1 was analyzed on mouse RBCs, while the role of cAMP signaling on ATP release was studied in RBCs from $Panx1^{-/-}$ mice, WT mice, and humans. The data presented here confirm the presence of Panx1 on the RBC membrane; however, they do not confirm the general assumption that ATP release from RBCs via Panx1 is regulated by cAMP. A critical discussion on the pitfalls encountered in assessment of ATP release from RBCs via Panx1 is provided.

3.3 Results

Mouse RBCs Express Panx1

To examine the role of Panx1 in ATP release from RBCs, we first sought to confirm that RBCs express Panx1, as this protein has been separately reported to be either present[166] or absent[209] on the membrane of mouse RBCs. Using three antibodies targeting epitopes on the NH_2 terminus (NT), second extracellular loop (EL2), and COOH terminus (CT) of mouse Panx1 (Fig. 1A), we examined Panx1 expression on RBCs via Western blotting,

immunofluorescence, and immunohistochemistry. Comparison of RBC ghost lysates via Western blotting with anti-Panx1 CT and anti-Panx1 EL2 antibodies confirmed expression of Panx1 in RBCs of WT, but not Panx1$^{-/-}$ mice (Fig. 1B). Confocal immunofluorescence microscopy of RBCs using anti-Panx1 CT and anti-Panx1 EL2 antibodies (Fig. 1C) further clarified localization of Panx1 to the plasma membrane of RBCs. We additionally analyzed the presence of Panx1 in situ on RBCs trapped in the blood vessels of nonperfused mouse kidney sections by DAB staining (Fig. 1D). Using the anti-Panx1 NT antibody, we detected DAB staining on the surface of RBCs; however, we detected no DAB staining using Cx43 antibody, an IgG control, or a secondary antibody-only control. While plasma membrane localization might be expected given the absence of intracellular organelles in RBCs, its confirmation nevertheless provides for the reported participation of Panx1 in the purported release of intracellular ATP across the plasma membrane into the extracellular environment. No expression of Cx43 was detected via Western blotting in WT or Panx1$^{-/-}$ RBCs (Fig. 1B) or DAB staining in WT RBCs (Fig. 1D), ruling out Cx43 hemichannels as possible alternative ATP release channels in this setting.

FIGURE 1. MOUSE RBCs EXPRESS PANNEXIN 1 (PANX1)

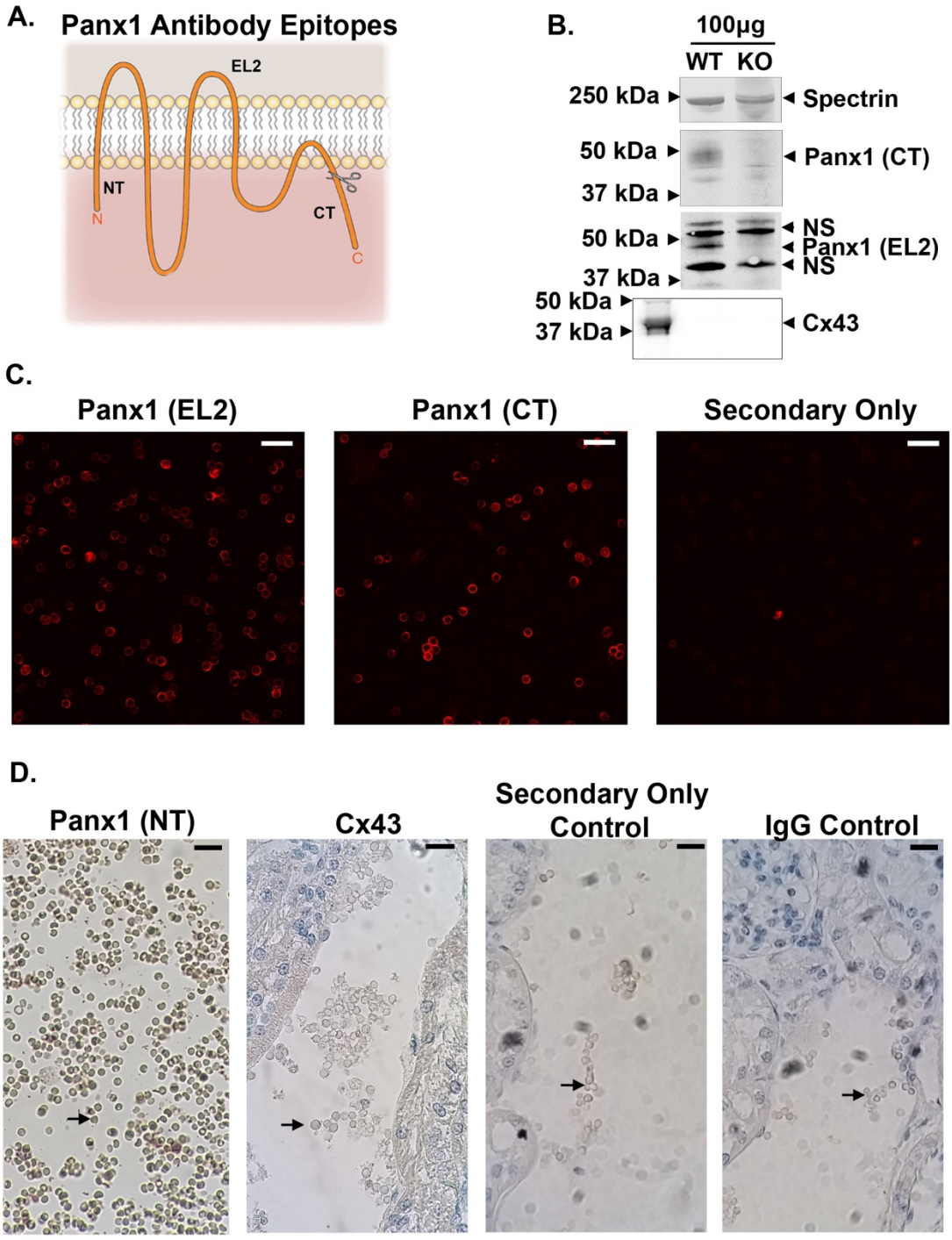

Figure 1. Mouse RBCs express pannexin 1 (Panx1).

A: Topological schematic of Panx1 indicates the location of the epitopes targeted by the three antibodies used. Scissors indicate caspase cleavage site on COOH terminus. **B**: Analysis of protein content in RBC ghosts via Western blotting with carboxy-terminus (CT) and second extracellular loop (EL2) antibodies shows Panx1 expression in WT but not $Panx1^{-/-}$ (KO) RBCs. No connexin 43 (Cx43) expression was detected. Far-left Cx43 band is 20 μg mouse lung lysate, used as a positive control. NS, nonspecific bands. **C**: Confocal immunofluorescence micros- copy of RBCs using CT and EL2 antibodies shows expression of Panx1 in RBCs. Scale bar, 20 μm. **D**: 3,3'-diaminobenzidine (DAB) staining of RBCs trapped in afferent arteriole kidney tissue slices using amino- terminus (NT) antibody confirms Panx1 expression on both endothelium and RBCs, stained dark brown. Arrows denote RBCs. No DAB staining was detected when sections were probed with Cx43 antibody, IgG antibody, or secondary antibody only. Scale bar, 20 μm.

Genetic Deletion of Panx1 Does Not Impair Exercise Capacity in Mice

Panx1 in RBCs has been previously described as a necessary component of Hb deoxygenation-induced ATP release from RBCs,[163] a process believed to be particularly important for the regulation of blood perfusion in skeletal muscle;[202] however, this role for Panx1 has only been tested in vitro. To examine the role of Panx1 in an exercise setting *in vivo*, we subjected $Panx1^{-/-}$ and control mice to an acute forced exercise capacity test.[199] $Panx1^{-/-}$ mice exhibited no reduction in endurance capacity compared with control mice (Fig. 2A), and both groups showed the same level of exertion via blood lactate measurements (Fig. 2B). $Panx1^{-/-}$ and control groups exhibited similar body weight (Fig. 2C). There were no effects seen due to sex (Fig. 2D) or age (Fig. 2E) of the mice. When individually housed in cages with a wheel available, $Panx1^{-/-}$ also showed no significant difference from control mice in total distance run over the course of 2 weeks (Fig. 2F) or at daily time points (Fig. 2G).

FIGURE 2. GENETIC DELETION OF PANX1 DOES NOT IMPAIR EXERCISE CAPACITY IN MICE.

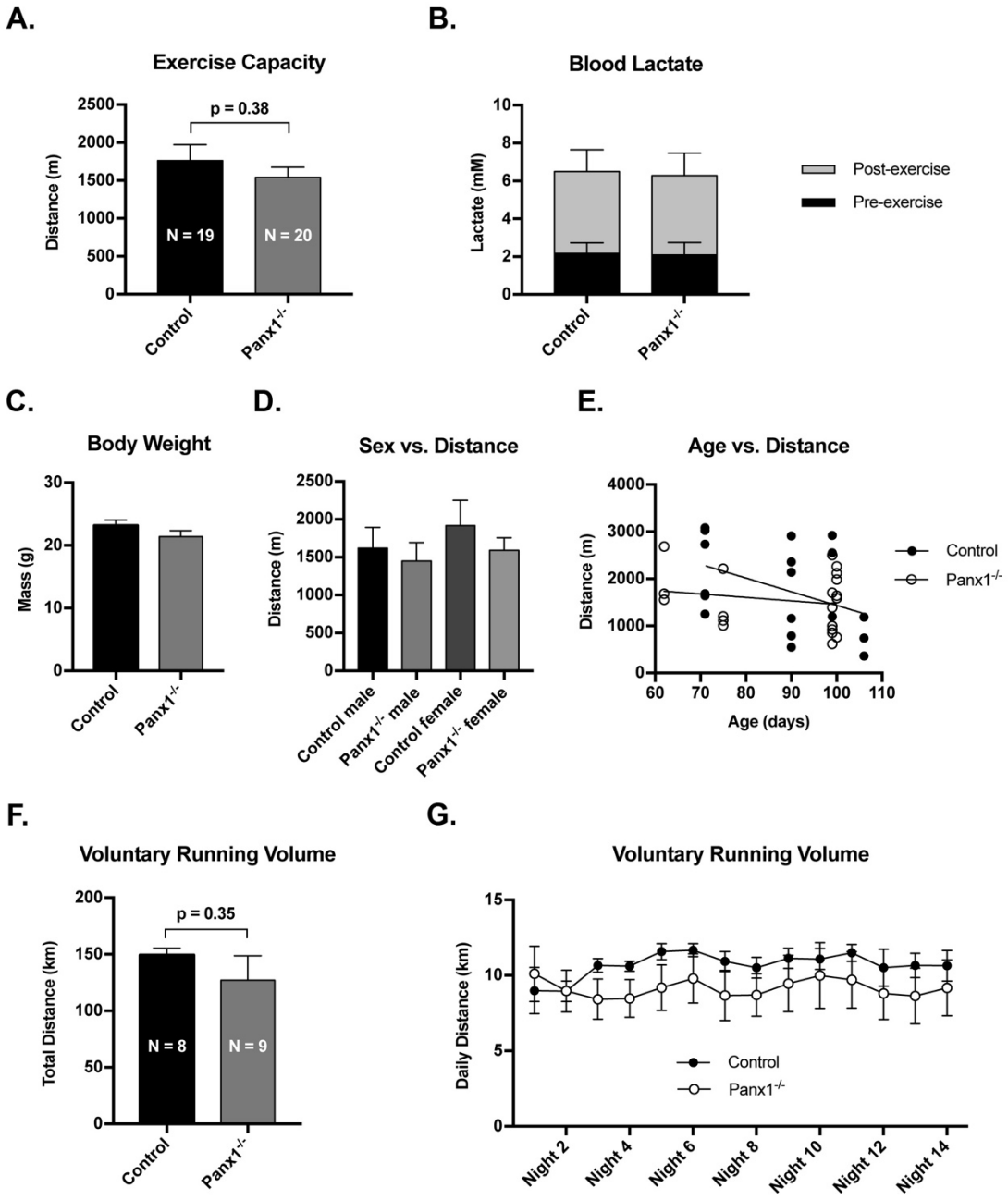

Figure 2. Genetic deletion of Panx1 does not impair exercise capacity in mice. A: $Panx1^{-/-}$ and Cre^{-} $Panx1^{fl/fl}$ control mice subjected to forced acute exercise via incremental treadmill test showed no significant difference in exercise capacity. $N = 20$ ($Panx1^{-/-}$) and $N = 19$ (control). **B:** Blood lactate measurements before and after exercise show equal exertion during treadmill test. **C-E:** Comparisons of mass (**C**), sex (**D**), and age (**E**) across all mice tested. **F:** $Panx1^{-/-}$ and Cre^{-} $Panx1^{fl/fl}$ mice housed individually in cages with running wheels showed no difference in voluntary running activity over a 2-wk period. $N = 9$ ($Panx1^{-/-}$) and $N = 8$ (control). **G:** Daily running data from **F**.

Background Concentration of ATP in the Supernatant and the Luciferin-Luciferase Assay

Because of the variety of experimental setups used previously in measuring ATP release from RBCs, we first carefully optimized the experimental conditions and tested a few notable variables to identify possible sources of variation in ATP measurements. To minimize extracellular ATP concentrations and increase precision of measurement, after isolating and washing RBCs we measured changes in extracellular ATP concentration with time in the experimental preparation, as determined immediately after washing and after different time intervals of incubation at RT on the bench top, up to 120 min.

We observed a time-dependent decrease in extracellular ATP concentration (Fig. 3A). As the extracellular concentration of ATP decreases with time, choice of incubation time influences the level of extracellular ATP encountered in the supernatant of control cells. Minimization of extracellular ATP in control cells enables more precise measurement of experimentally induced ATP release. Notably, while we observed a slight decrease in intracellular ATP content after 120 min incubation, RBCs did not experience significant rundown of ATP gradient (Fig. 3B). Furthermore, mouse and human RBCs exhibited similar background levels of extracellular ATP following isolation and washing (Fig. 3C). To further optimize the assay, we also compared a commercially available luciferase assay kit to a crude mixture of raw luciferin and luciferase, as was utilized earlier in the literature. While crude enzymatic preparation exhibited a stronger signal than the kit assay, both assays showed linear responses across the range of ATP concentrations being tested (data not shown). Additionally, we tested the impact of the commonly used ecto-ATPase inhibitor ARL 67156 trisodium (ARL) on the luciferase assay. While previous research has

shown that RBCs possess only minor ecto-ATPase activity,[211] ARL is a common component of extracellular ATP assays. As a structural analog of ATP, ARL could conceivably interfere with the luciferase assay. Across the range of ATP concentrations encountered in our experiments, ARL had no adverse effect on the ability of the luciferase assay to detect ATP vs. the assay in its absence (Fig. 3D). However, based on the slow timescale of extracellular ATP degradation in the absence of ARL in the sample preparation observed in Fig. 3A, and the previously reported low ecto-ATPase activity of ~28 fmol x $(10^6$ cells min$)^{-1}$ on human RBCs,[211] we deemed use of ARL unnecessary in our experiments.

FIGURE 3. METHODOLOGICAL CONSIDERATIONS FOR MEASURING ATP RELEASE FROM RBCs IN VITRO

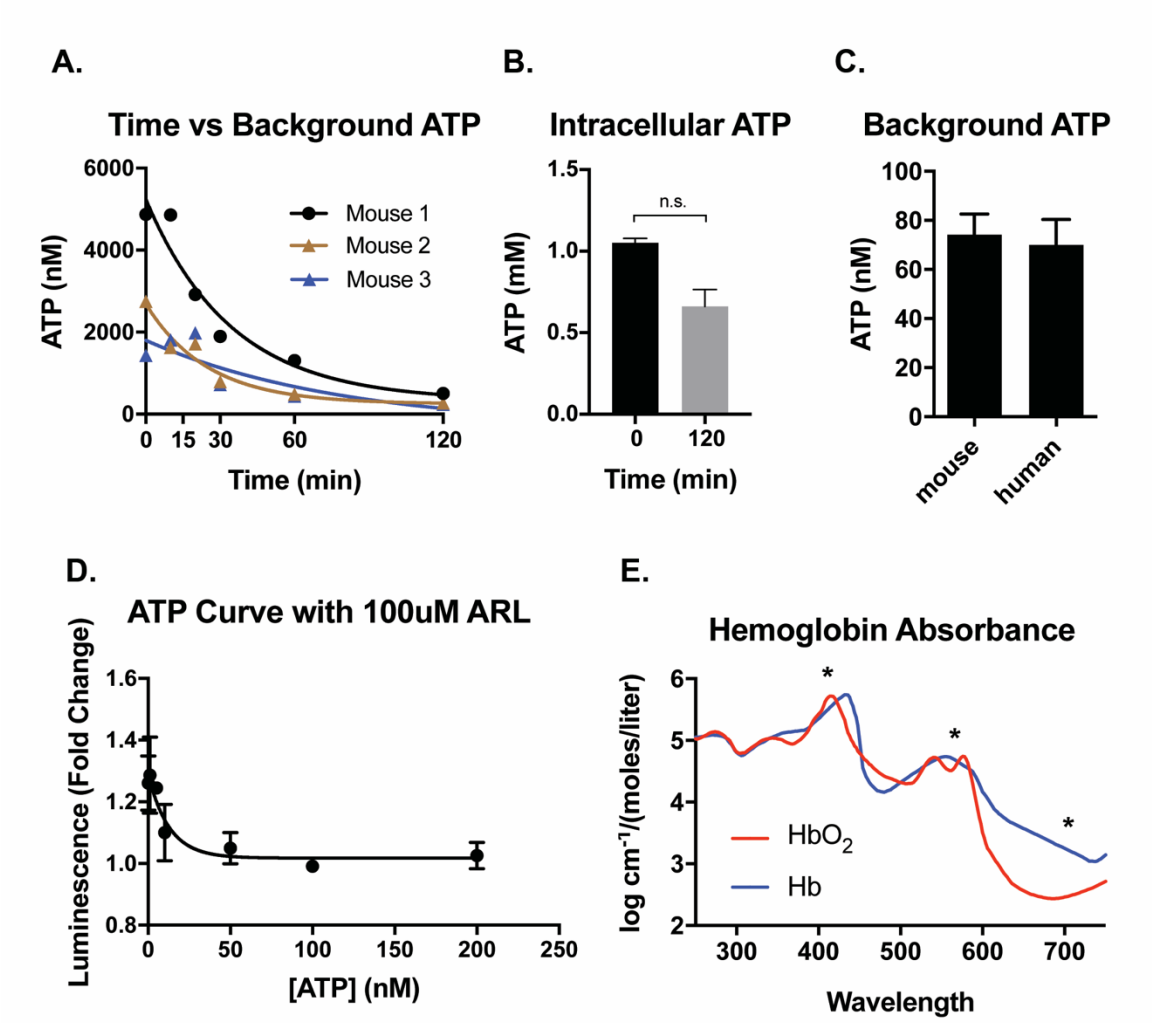

Figure 3. Methodological considerations for measuring ATP release from RBCs in vitro.

A: Decay of extracellular ATP in washed mouse RBC samples at room temperature. N = 3. R^2 = 0.93 (*mouse 1*), 0.94 (*mouse 2*), 0.68 (*mouse 3*). **B:** Intracellular ATP concentration in mouse RBCs at start and end of timeframe in **A**. **C:** Background ATP content in samples of mouse (N = 4) and human (N = 7) RBCs at 25% hct, using luciferase assay built from scratch. **D:** Effects of ARL 67156 trisodium (ARL) on luciferase assay built from scratch, independent of RBCs. **E:** Optical absorbance curves for oxyhemoglobin (HbO_2) and hemoglobin (Hb). Asterisks indicate absorbance peak at 405 nm, isosbestic point at 570 nm, and background measurement at 700 nm.

Stimulation of ATP Release by Hypotonic Potassium Gluconate Solution Causes Hemolysis of Mouse RBCs

The first examination of Panx1-dependent ATP release in mouse RBCs took place under stimulation with high-potassium solution or hypo-osmotic stress,[166] or by treatment with hypotonic KGlu solution.[207] Substitution of KGlu in place of physiologic extracellular ions complicates the experimental study of Panx1 channels in RBCs. Since the physiologic concentration gradients of K^+, Na^{2+}, Ca^{2+}, and Cl^- are reversed, and since gluconate is not a rapidly permeant anion like Cl^-, a KGlu-based buffer would be expected to cause perturbations in ionic influx and efflux,[212] altered pH balance,[213] and cell volume.[214, 215] When we exposed RBCs from WT mice to KGlu as previously done to activate Panx1-mediated ATP release,[207] we indeed observed an approximately 10-fold increase in extracellular ATP (Fig. 4A); however, we also observed a large increase in RBC lysis (Fig. 4B). To determine whether increases in ATP release were due to hemolysis of RBCs as observed with other treatments/conditions (including substitution of NaCl with KCl in the supernatant),[210] we examined the presence of Hb in the supernatant of the RBCs treated with KGlu by UV-visible spectrophotometry by analyzing the absorbance of oxyHb at 570 nm minus the background assessed at 700 nm. In Fig. 3E the absorption spectrum of oxyHb and deoxyHb is depicted, where the highest absorbance peak at 405 nm, the isosbestic point at 570 nm and the background reading at 700 nm are marked with asterisks. Following treatment of mouse RBCs with hypotonic KGlu solution, we found that hemolysis and extracellular ATP levels were highly correlated across all samples with $r^2 = 0.98$ (Fig. 4C),

indicating that the overwhelming source of extracellular ATP in our experiment was lytic release of cellular contents, not mechanistically controlled ATP release.

FIGURE 4. HYPOTONIC STIMULATION OF MOUSE RBCs IN VITRO FAILS TO STIMULATE CONTROLLED ATP RELEASE

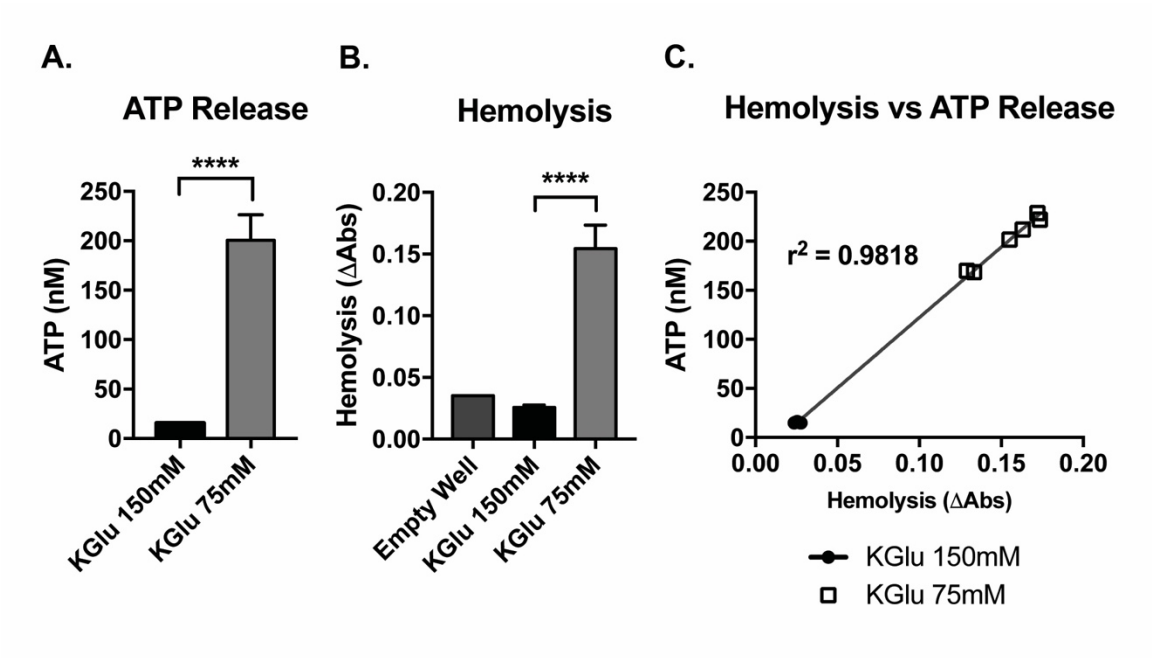

Figure 4. Hypotonic stimulation of mouse RBCs in vitro fails to stimulate controlled ATP release.

A: Extracellular ATP concentration resulting from in vitro stimulation of RBCs with hypotonic, high-K^+ buffer or isotonic, high-K^+ buffer, measured via Roche luciferase assay kit. **B:** Hb absorbance readings from the supernatant of the samples in **A** as a measurement of cell- free Hb attributable to RBC lysis. **C:** X–Y plot of hemolysis against ATP release from **A** and **B**. R^2 values indicate the extent to which changes extracellular ATP are attributable to hemolysis. ****$P < 0.0001$.

Treatment with 8Br-cAMP Fails to Stimulate Controlled ATP Release from Mouse RBCs

Given the currently understood pathway of Panx1-dependent RBC ATP release lying downstream of cAMP-dependent PKA activation,[33] we next examined pharmacologic stimulation of mouse RBCs with an active cAMP analog, 8Br-cAMP, similar to the conditions used in early examination of the reported pathway.[162] Our experimental setup included both WT and Panx1$^{-/-}$ RBCs, as well as the Panx1 inhibitor CBX, seeking to connect these upstream steps to the more recent identification of Panx1 as the conduit of subsequent ATP release.[163] We hypothesized that stimulation of WT RBCs with 8Br-cAMP should induce ATP release that could be inhibited by genetic deletion or pharmacologic inhibition of the Panx1 channel. However, we observed no change in extracellular ATP concentration across all conditions with similar hemolysis levels (Fig. 5C). Applying the hemolysis calculation described in Fig. 3E, we report the influence of hemolysis on our ATP release measurements in Fig. 5, A and B. Including all raw data points from the original data set, we found no changes in extracellular ATP across stimulation conditions (Fig. 5A); however, we observed a range of hemolysis measurements and a clear correlation between elevated hemolysis and higher extracellular ATP readings (Fig. 5B). Based on the clustering of data, we imposed a cutoff of ΔAbs = 0.15, excluding ATP release data for all samples with hemolysis measurements exceeding the cutoff. While in this experiment our finding of no significant change in extracellular ATP concentrations across stimulation conditions remained unchanged (Fig. 5C), the r^2 value showing the relationship between hemolysis and extracellular ATP was reduced from

0.67 to 0.03, indicating that our corrected ATP data are fully independent of the influence of hemolysis (Fig. 5D).

FIGURE 5. PHARMACOLOGIC STIMULATION OF MOUSE RBCs IN VITRO FAILS TO STIMULATE CONTROLLED ATP RELEASE

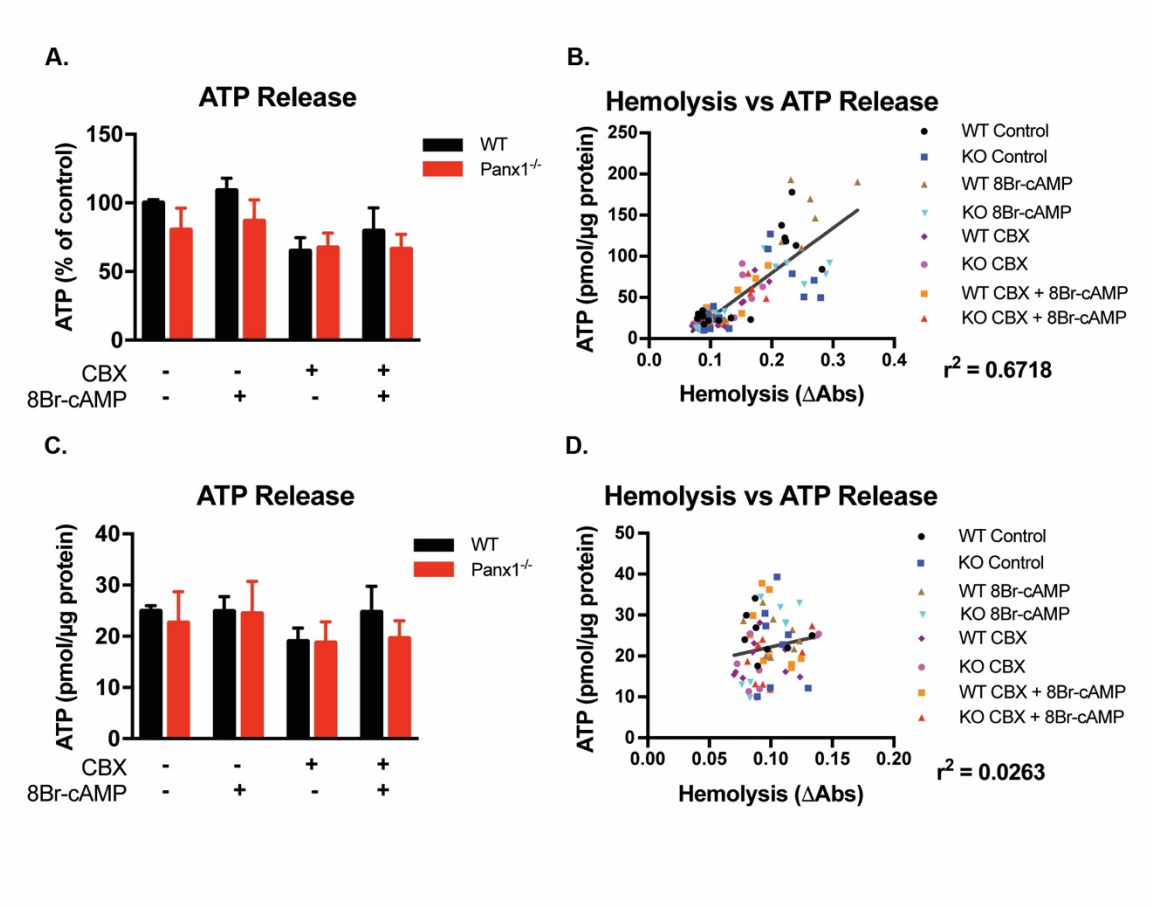

Figure 5. Pharmacologic stimulation of mouse RBCs in vitro fails to stimulate controlled ATP release.

A: Extracellular ATP concentration resulting from in vitro stimulation of WT and Panx1$^{-/-}$ RBCs with the active cyclic AMP analog 8-bromo cyclic adenosine monophosphate (8Br-cAMP), with or without pretreatment with the Panx1 inhibitor CBX, using luciferase assay built from scratch. N = 5, n = 15. **B:** X–Y plot of hemolysis against ATP release from the experiment in **A**. **C:** Replotting of data in A after removing data points in which hemolysis exceeded a cutoff of change in optical density of 0.15. N = 3, n = 9. **D:** X–Y plot of hemolysis against ATP release from the experiment in **C**. R^2 values indicate the extent to which changes in extracellular ATP are attributable to hemolysis.

Pharmacologic Stimulation of Intracellular cAMP Production Does Not Induce ATP Release from Human RBCs

Having failed to identify ATP release from mouse RBCs *in vitro* following stimulation with an active cAMP analog, we next turned to human RBCs, in which the bulk of trailblazing experiments was performed.[162, 163] Exposure of RBCs to a variety of pharmacologic agents including the combination of β-adrenergic agonist isoproterenol + the nonspecific phosphodiesterase inhibitor IBMX (though neither alone), the AC activator forskolin, and the combination of forskolin + IBMX, all increased intracellular cAMP levels significantly (Fig. 6A). Based on a recent report that PDE5 inhibition contributes to ATP release through a parallel cAMP-dependent pathway (4), we also tested sildenafil as a stimulation condition, but we saw no resulting increase in intracellular cAMP. While forskolin, forskolin + IBMX, and isoproterenol + IBMX elevated cAMP, none of the conditions tested resulted in an increase in extracellular ATP (Fig. 6B). In this experiment, we observed a weak relationship ($r^2 = 0.3295$) between hemolysis and extracellular ATP (Fig. 5C); however, since the amount of hemolysis observed was minimal and no difference in extracellular ATP was observed between conditions, hemolysis-driven ATP release does not appear to have affected these results meaningfully. Taken together, these data show that increases in intracellular cAMP by modulation of its synthesis or breakdown did not increase ATP release from human RBCs.

FIGURE 6. PHARMACOLOGIC STIMUALTION OF HUMAN RBCs IN VITRO STIMULATES A RISE IN INTRACELLULAR cAMP BUT FAILS TO STIMULATE CONTROLLED ATP RELEASE

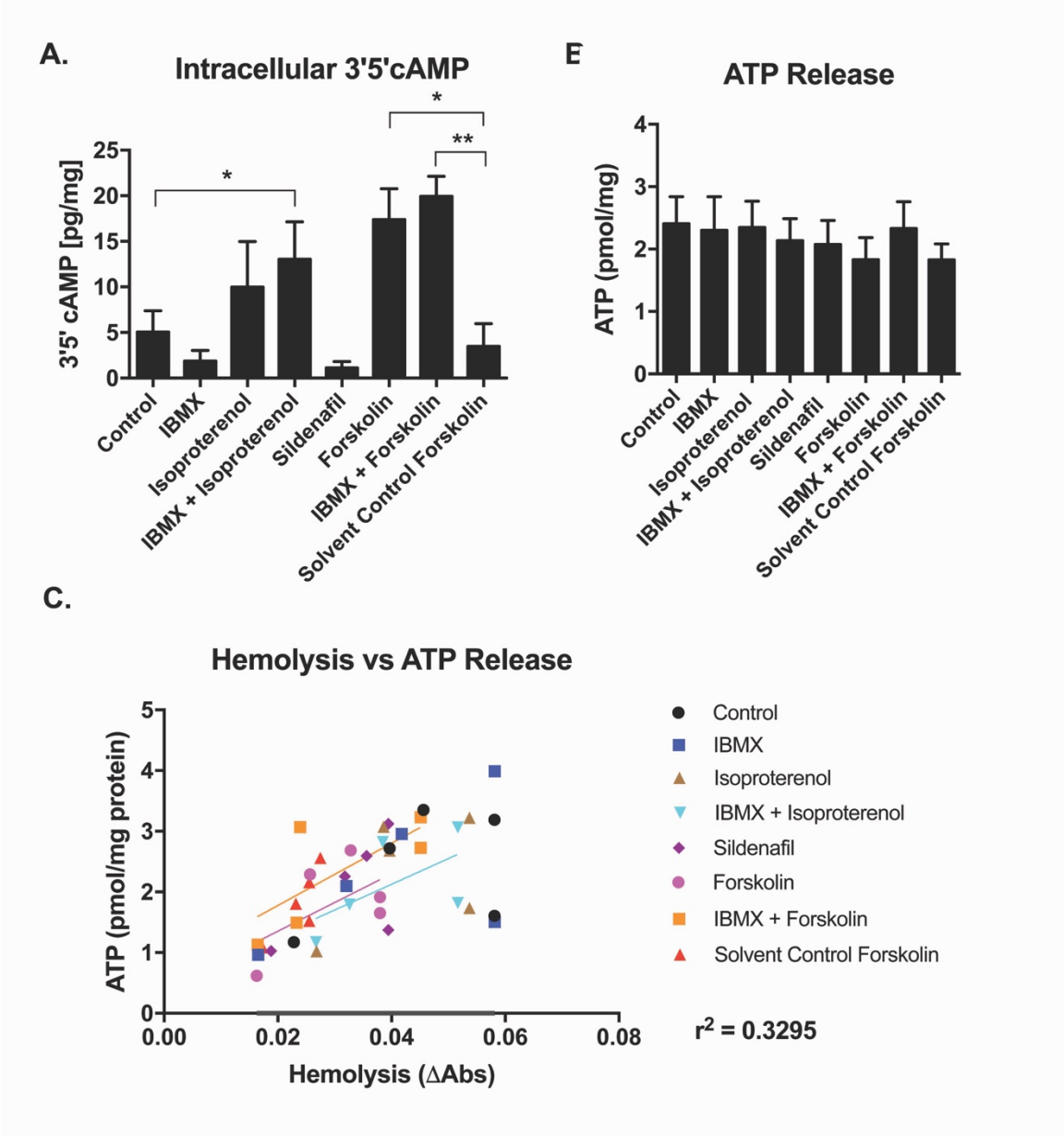

Figure 6. Pharmacologic stimulation of human RBCs in vitro stimulates a rise in intracellular cAMP but fails to stimulate controlled ATP release.

A: 3',5'-cAMP concentrations measured by mass spectrometry following in vitro stimulation of RBCs with pharmacologic activators. **B:** Extracellular ATP concentrations resulting from the experiment in **A**, using Invitrogen luciferase assay kit. **C:** X–Y plot of hemolysis against ATP release from the experiment in **B**. R^2 value indicates the extent to which changes in extracellular ATP are attributable to hemolysis. *$P < 0.05$, **$P < 0.01$.

3.4 Discussion

Are cAMP-Dependent Signaling and Panx1 in RBCs Part of the Same Pathway?

Panx1 was proposed to be the main channel responsible for ATP efflux from RBCs;[163, 166, 207] however, its presence on RBCs could not be confirmed by others.[209] We here show that RBCs express Panx1 and lack Cx43, as assessed by Western blot analysis, immunofluorescence, and immunohistochemistry. However, we found that the combination of high-potassium solution and hypo-osmotic stress, a treatment used previously to assess the functional role of Panx1 in RBCs[207] induced hemolysis-derived ATP release (as also shown by others[210]) instead of regulated ATP release.

According to the current paradigm,[33, 216] a single signaling pathway leading from RBC deoxygenation to ATP release involves activation of AC to produce cAMP,[162] culminating in Panx1 activation.[33, 162, 163] In contrast, we found that treatment of RBCs with a cAMP analog did not induce ATP release from either WT or Panx1$^{-/-}$ RBCs. Moreover, untreated extracellular ATP concentrations were similar between WT and Panx1$^{-/-}$ RBCs, and between untreated and CBX-treated WT RBCs. Our findings suggest that Panx1 is not responsible either for controlled ATP release in response to cAMP stimulation, nor for any controlled ATP release that may contribute to the baseline ATP levels in our experimental setup. To the best of our knowledge, no direct evidence exists to support the participation of PKA in this pathway. Along with the lack of response to cAMP assessed here, it therefore appears unlikely to us that cAMP and Panx1 are in fact closely connected within the same pathway.

These findings also call into question the role of CFTR, which was proposed to participate in the ATP release pathway downstream of RBC deformation.[164] Unfortunately, the study examining CFTR involvement relied upon nonspecific drugs,[207, 217-221] and no rescue experiments were performed to validate specificity. Furthermore, it is difficult to speculate on the molecular mechanism underpinning the proposed interaction of CFTR and Panx1, leaving unclear how exactly CFTR might be expected to participate in the proposed pathway.

Taken together, multiple questions remain about the relationships among these various signaling elements (AC, cAMP, PKA, CFTR, Panx1) and whether they all lie in a single pathway connecting hypoxia/RBC deformation to ATP release from RBCs. Future studies must integrate these components to identify whether physiological stimuli drive ATP release from RBCs by activation of one pathway, or multiple pathways, and which signaling components do or do not interact.

Role of Panx1 in Exercise

Because of its dramatic increase in blood flow during exercise,[6] skeletal muscle is recognized as an ideal context for study of luminal ATP release as a vasodilatory modulator.[32, 202, 222] However, the role of Panx1 in hypoxia-induced ATP release from RBCs, a process believed to be particularly important for the regulation of blood perfusion in skeletal muscle, has not previously been studied in this physiologic context. Based on the previously reported role of Panx1 in gating ATP release from RBCs in response to increased Hb deoxygenation, we hypothesized that $Panx1^{-/-}$ mice would exhibit reduced endurance capacity as a result of inadequate blood perfusion to active skeletal muscle.

However, Panx1$^{-/-}$ and control mice performed similarly in both acute and chronic tests of endurance capacity. The lack of any decrease in exercise performance following genetic deletion of Panx1 challenges the assumption that Panx1 regulates in- creased blood perfusion to exercising skeletal muscle. This result could indicate either that Panx1 does not play an essential role in this pathway of ATP release from RBCs, or that the pathway in question does not make a significant contribution to muscle performance during exercise. Additional investigation into the effects of Panx1 deletion on blood flow in exercising skeletal muscle, measuring changes in blood flow as an end point, will help to elaborate on this finding.

Hemolysis or ATP Release from RBCs?

Among the main issues concerning the assessment of ATP release from RBCs are well-known methodological aspects underlying the ex vivo measurement of ATP release from RBCs, including: RBC concentration and integrity, incubation buffer, incubation time (to match pathways in question), as well as protocol of ATP measurement and purity of luciferase preparation.

Loss of RBC membrane integrity (hemolysis) is one of the main confounding factors concerning assessment of ATP release from RBCs and has been a recent topic of significant debate in the field[210, 223, 224] concerning reproducibility issues. Controlled versus lytic sources of ATP release can be distinguished by assessing cell-free Hb concentration in the supernatant of samples. While early papers in the field reference hemolysis readings at a variety of wavelengths,[162] the 405 nm oxyHb absorbance peak (marked with asterisk in Fig. 3E) appears to be the most popular and current measurement.[163] However, since the

absorbance of oxyHb is ~30% higher than that of deoxyHb at the 405 nm wavelength, this measurement may be affected by the oxygenation status of a sample. Alternatively, the presence of Hb in the supernatant of cells can be assessed by measuring absorbance at 570 nm, where an isosbestic point for oxy- and deoxyHb lies close to the peak absorption of each species, as well as to the absorbance of methemoglobin (not shown). In addition, background absorbance at 700 nm can be subtracted to obtain more reproducible net absorbance readings (ΔAbs = 570 nm minus 700 nm).

Minor hemolysis during blood collection and RBC isolation process is nearly inevitable. To control for hemolysis in our experiments, we calculated a relative increase in ΔAbs com- pared with the average hemolysis measurements of the untreated control in an experiment, and we excluded all experiments where we found more than 0.05 increase in ΔAbs as compared with baseline hemolysis. This ΔAbs reflects a lysis of roughly 0.05% hct, a modest percentage but one that can have a significant effect on the ATP levels observed.

In summary, assessment of ATP release from RBCs in suspension is deceptively challenging due to serious and often inevitable methodological pitfalls such as hemolysis. Moreover, since RBCs lack a nucleus, classical loss-of-function and rescue-of-function experiments are only feasible by using pharmacological inhibitors and activators (which lack specificity) or in gene-targeted mouse models. Although detection of cytoplasmic proteins in RBCs is technically demanding because of the presence of high concentrations of Hb,[102] proof of the presence of a certain protein in RBCs needs to be presented by Western blot analysis or other proteomic approaches, not only on the basis of the effects

of pharmacological inhibitors/stimulators (e.g., the participation of proteins like PKA[162] in ATP release has been proposed without being proven at the protein level). Therefore, additional investigation is needed to understand the physiological role of regulated ATP release, and the mechanisms underpinning its regulation, especially using genetic animal models.

Novelty of Findings

Recent discussion of hemolysis-derived ATP release from RBCs[210] left lingering questions about the study of ATP release from RBCs. The data presented here resolve multiple details that until now remained contentious or unproven. Whereas Sikora *et al.*[210] showed ATP release to be indistinguishable from hemolysis following treatment with cAMP agonists (a source of resultant debate[223, 224]), our results show that cAMP agonists fail to induce any ATP release, offering paired mass spectrometry measurements to confirm elevation of intracellular cAMP following treatment. This finding refutes the published consensus pathway,[33] providing much-needed correction to the previously untested assumption that Panx1 activation occurs downstream of cAMP activation in RBCs. Our study also specifically examines the highly cited and now-canonical RBC Panx1 stimulation condition of hypotonic, high-potassium buffer,[207] showing that the resulting ATP release is driven by hemolysis. Finally, we now provide physiologic data from Panx1$^{-/-}$ mice, showing that genetic deletion of Panx1 has no effect on endurance exercise capacity. These findings provide key details to facilitate further refinement of existing models of ATP release from RBCs.

Conclusion: Challenges and Perspectives on Regulated ATP Release from RBCs

The data presented here exclude the role of cAMP in Panx1-dependent ATP release induced by pharmacologic activation of AC, but not necessarily of Panx1 in the effects of hypoxia and shear stress.[210, 223, 224] We found that stimulation of the pathway via endogenous or exogenous cAMP failed to induce ATP release from WT or Panx1$^{-/-}$ RBCs. As no direct evidence has been presented of a role for PKA, nor has the previously reported role of CFTR[164] been conclusively proven to connect cAMP to Panx1 activation, it now appears unlikely that RBC deformation and hypoxia stimulate the same signaling pathway in RBCs.[33] While we are confident that Panx1 is expressed in RBCs, we argue that the previously proposed cAMP-dependent pathway as the central hub for controlled ATP release cannot fully explain all the effects of the different stimuli reported to activate ATP release from RBCs. We also find no effect on endurance capacity as a result of genetic deletion of Panx1 from mice, calling into question the physiologic importance of Panx1 in this pathway's support of muscle function. A few key questions remain: is RBC deformability in fact a prerequisite for hypoxic ATP release? Are other laboratories able to reproduce stimulation of non- hemolytic ATP release downstream of cAMP stimulation, and if so, is the mechanism PKA and Panx1-dependent? Finally, is CFTR directly involved in cAMP-dependent or Panx1-dependent ATP release from RBCs, and if so, how? Further experimentation with Panx1$^{-/-}$ RBCs exposed to hypoxic conditions or shear stress would be helpful to confirm or deny the role of Panx1 in hypoxic or mechanotransduction-dependent pathways. Future in vitro and in vivo work will need to tease out more details

to identify the true connectivity of this reported pathway, as well as confirm its physiological relevance in supply of oxygen to skeletal muscle.

Acknowledgements: Lukas Diederich, Christina Panknin, Miriam Cortese-Krott, and Edwin Kerry Jackson contributed human RBC experiments and mass spectrometry data. Joshua Drake and Zhen Yan provided technical support for exercise capacity tests. Robyn Sherman assisted on immunolabeling protocols. Leon DeLalio performed DAB staining on kidney slice images. Silvia Penuela and Dale Laird provided Panx1 antibodies. Brant Isakson assisted with data analysis and manuscript preparation.

CHAPTER 4. ENDOTHELIAL HEMOGLOBIN ALPHA IS A SIGNIFICANT REGULATOR OF EXERCISE FITNESS IN MICE

4.1 Abstract

Hemoglobin alpha (Hbα) is redundantly encoded by the genes *Hba1* and *Hba2*, and our laboratory has demonstrated that it is expressed in the ECs of resistance arteries. We have previously shown that siRNA knockdown of endothelial *Hba1* decreases protein expression of Hbα and increases NO signaling in the vascular wall. Additionally, pharmacologic inhibition of the interaction between endothelial Hbα and endothelial nitric oxide synthase reduces blood pressure. To further study the role of endothelial Hbα, we have produced a novel genetically modified mouse in which the second and third exons of the *Hba1* gene are flanked by loxP sites ($Hba1^{fl/fl}$). We crossed this $Hba1^{fl/fl}$ mouse with a Cdh5-Cre/ERT2 mouse line to produce a tamoxifen-inducible genetic model of endothelial *Hba1* deletion (EC $Hba1^{\Delta/\Delta}$). We compared EC $Hba1^{\Delta/\Delta}$ with $Hba1^{-/-}$ (global deletion of *Hba1*) mice and found that both models exhibit reduced expression of Hbα protein in the ECs of skeletal muscle arteries and arterioles. However, while $Hba1^{-/-}$ mice show significant decreases in RBC parameters such as hct and mean cell volume, EC $Hba1^{\Delta/\Delta}$ RBC parameters are unaffected. To examine the role of endothelial Hbα in hypoxic blood flow control, we measured acute endurance capacity via a treadmill running test. EC $Hba1^{\Delta/\Delta}$ mice exhibited a significant reduction in exercise capacity, reflecting the exercise phenotype shown in $Hba1^{-/-}$ mice. Preliminary data suggests that EC $Hba1^{\Delta/\Delta}$ mice display impaired dilation to hypoxia, pointing to a central role for EC Hbα in exercise hyperemia. We conclude that endothelial *Hba1* is an important regulator of vascular function and skeletal muscle performance.

4.2 Introduction

Hb has received significant attention since the early 2000s for its function as a nitrite reductase.[118, 119, 122, 225] In contrast to oxygenated heme, which rapidly oxidizes NO to nitrate,[113, 114] deoxygenated heme is also capable of reducing nitrite to produce NO.[117] The physiologic relevance of this mechanism is underscored by the identification by Gladwin *et al*. of a significant plasma nitrite A/V gradient, demonstrating consumption of nitrite from plasma during transit from the arterial to venous circulation.[120] The magnitude of this A/V gradient increased during exercise, suggesting a dilatory mechanism in response to increased blood O_2 extraction by metabolically active skeletal muscle. The narrative of nitrite reduction to NO as a mechanism of exercise hyperemia has been supported by subsequent human studies demonstrating its independence from enzymatic NO production,[117] as well as dose-dependence on nitrite and hypoxic conditions.[121]

Previous research in the field has understandably been performed with an assumed focus on the Hb carried in circulating RBCs; however, concerns exist about the limitations on NO release from partially deoxygenated RBCs in a dense environment of both oxyHb and deoxyHb, where potent NO scavenging imposes a severe limitation on its transit to the vascular wall. The magnitude of NO escape flux from RBCs to the ECs in this context has been estimated to be orders of magnitude lower than that resulting from enzymatic NO production in the endothelium.[119] Thus, while the Hb nitrite reductase mechanism is supported by compelling evidence, RBC-bound Hb appears unlikely to supply the majority of its effect.

The more recent discovery by the Isakson laboratory that Hbα is expressed in the ECs of resistance arteries[38] provides a potential alternative, with a novel pool of Hb optimally located to produce bioavailable NO when deoxygenated. Indeed, the localization of Hbα to the MEJ of resistance arteries, intrinsic to its ability to scavenge eNOS-derived NO in normoxic conditions,[39] demonstrates the preferential localization of eNOS and Hbα for NO production as a vasodilatory signal to adjacent SMCs. Therefore, we hypothesized that Hbα in resistance arterial ECs functions as a nitrite reductase during hypoxic conditions such as exercise to produce NO and stimulate vasodilation.

4.3 Results and Discussion

Creation of an Hba1$^{fl/fl}$ mouse model

In order to target endothelial Hbα specifically via cre/lox technology, we created an Hba1$^{fl/fl}$ mouse in which the second and third exons of the Hba1 gene are flanked by loxP sites. Working in conjunction with Ingenious Targeting Laboratory, targeted iTL BF1 (C57Bl/6 FLP) embryonic stem cells were microinjected into Balb/c blastocysts. A schematic of the modified *Hba1* gene with neomycin cassette, FRT sites, and LoxP sites inserted is shown in Fig. 7A. Resulting chimeras with predominantly black coats, indicating proportionally high genetic contribution of targeted stem cells, were bred with C57Bl/6 mice to generate offspring with germline neomycin cassette deletion (Fig. 7B). Deletion of the neomycin cassette (Fig. 7C) and retention of the distal LoxP sequence (Fig. 7D) were confirmed by PCR. The Hba1$^{fl/fl}$ line may be crossed with a wide variety of

mouse lines expressing cell-type-specific cre recombinase in order to genetically delete *Hba1* with locational precision.

FIGURE 7. CREATION OF AN HBA1$^{FL/FL}$ MOUSE MODEL

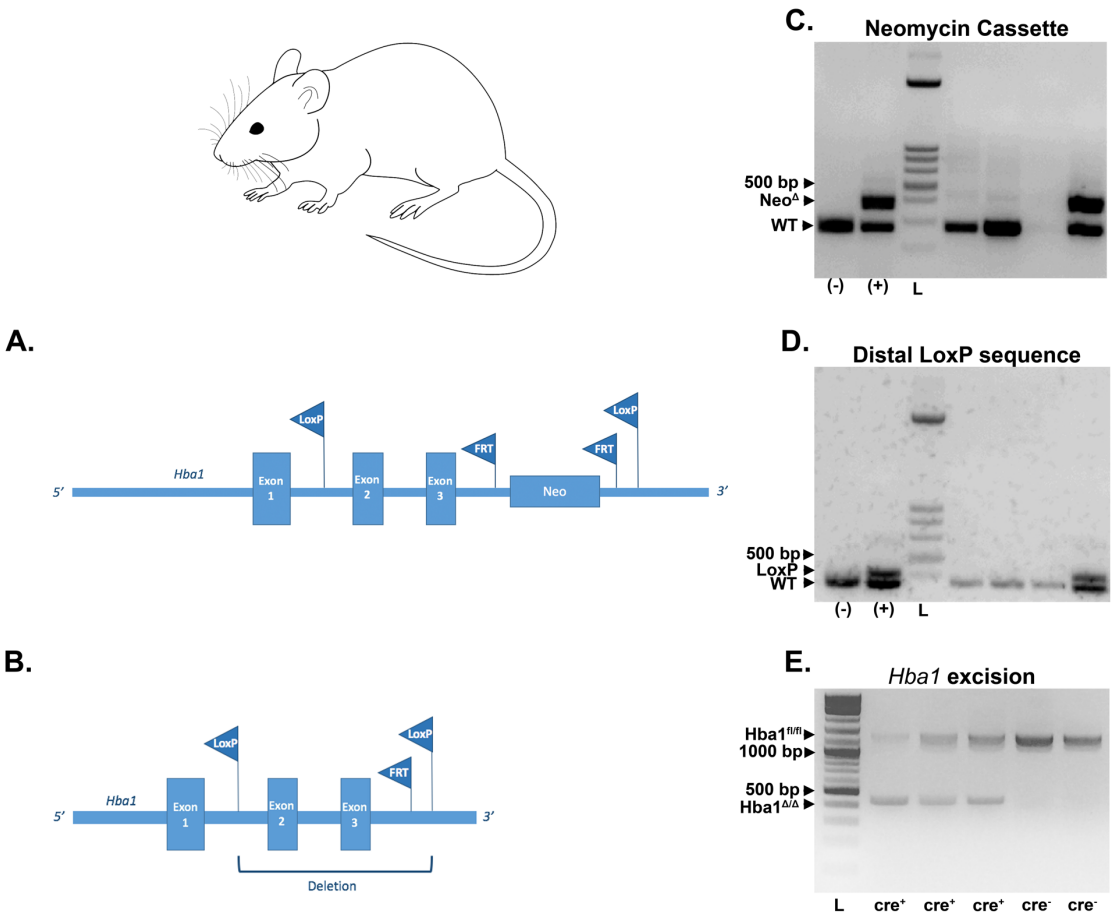

Figure 7. Creation of an Hba1$^{fl/fl}$ mouse model.

A: Schematic of modified *Hba1* gene with neomycin cassette, FRT sites, and LoxP sites inserted. **B:** Following FLP-FRT site-directed recombination, LoxP sites flank exons 2 and 3, engineered for deletion of this region in the presence of cre recombinase enzyme. **C:** A second band (Neo$^{\Delta}$) above the band for the WT sequence (WT) indicates deletion of the neomycin cassette. **D:** A second band (LoxP) above the band for the WT sequence (WT) indicates retention of the distal LoxP sequence. **E:** Confirmation of *Hba1* deletion in muscle tissue. A second band at 450 BP below the 1300 BP band for the full-length sequence indicates deletion of the Hba1 gene in cre^{+}, but not cre^{-}, mice. Ladder (L) intervals are 100 BP. Negative (-) and positive (+) controls as marked.

Endothelial-specific deletion of Hba1

To target endothelial Hbα, we bred $Hba1^{fl/fl}$ mice with Cdh5-cre/ERT2 mice, which carry a tamoxifen-inducible, EC-specific cre gene on a C57Bl/6 background, to yield $Hba1^{fl/fl}$ Cdh5-cre/ERT2 ("EC $Hba1^{\Delta/\Delta}$") mice, a model of tamoxifen-inducible, EC-specific *Hba1* deletion. In EC $Hba1^{\Delta/\Delta}$ mice, *Hba1* deletion was confirmed via PCR in hindlimb muscle tissue of cre^- and cre^+ animals (Fig. 7E), indicated by a second band of 450 base pairs below the 1300 base pair band of the full-length *Hba1* sequence. To verify loss of Hbα protein expression in the endothelium of EC $Hba1^{\Delta/\Delta}$ mice, we excised TDAs from EC $Hba1^{\Delta/\Delta}$ mice and $Hba1^{fl/fl}$ controls, and labeled transverse sections of the TDA with immunofluorescence for Hbα expression. Confocal microscopic imaging demonstrates Hbα expression in the ECs, but not SMCs, of $Hba1^{fl/fl}$ TDAs. However, in comparison to $Hba1^{fl/fl}$ littermate controls (Fig. 8A), EC $Hba1^{\Delta/\Delta}$ TDAs show dramatically reduced expression of endothelial Hbα protein (Fig. 8B). IgG and secondary antibody controls demonstrate specificity of our immunofluorescent labeling protocol (Fig. 8C-D). Low levels of residual Hbα expression may derive from the *Hba2* gene, which produces structurally indistinguishable Hbα protein to that from *Hba1*. However, loss of the overwhelming majority of Hbα expression provides protein-level evidence of successful deletion of the *Hba1* gene, corroborating the $Hba1^{fl/fl}$ data shown in Fig. 7.

Because O_2 binding and NO reactions are common features of numerous globins that bind heme, we used immunofluorescence confocal microscopy to examine the expression of Hbα, Hbβ, Cytoglobin, Myoglobin, and Neuroglobin in the TDA of both EC $Hba1^{fl/fl}$ control mice and EC $Hba1^{\Delta/\Delta}$ mice. This approach allowed us not only to understand

broader globin expression in our model system, but also to check for signs of compensation in the expression levels of other globins in the TDA following genetic deletion of *Hba1*. In $Hba1^{fl/fl}$ TDAs, we observed robust endothelial expression of Hbα (Fig. 9A), as well as low levels of cytoglobin in the endothelium (Fig. 9C) and adventitial staining for cytoglobin (Fig. 9C) and neuroglobin (Fig 9E). As reported by our laboratory previously,[38] no Hbβ expression was observed (Fig. 9B). Notably, since myoglobin has been prominently discussed in the context of hypoxic nitrite reductase activity,[115] we observed no myoglobin expression in the TDA (Fig. 9D). In EC $Hba1^{\Delta/\Delta}$ TDAs, while we observed almost complete loss of Hbα expression in the endothelium (Fig. 9F), we saw similar expression (or lack thereof) of the other globins compared to $Hba1^{fl/fl}$ controls (Fig. 9F-J). IgG staining showed no off-target fluorescence (Fig. 9K-O).

FIGURE 8. EC HBA1$^{\Delta/\Delta}$ MICE EXHIBIT REDUCED ENDOTHELIAL HBα EXPRESSION

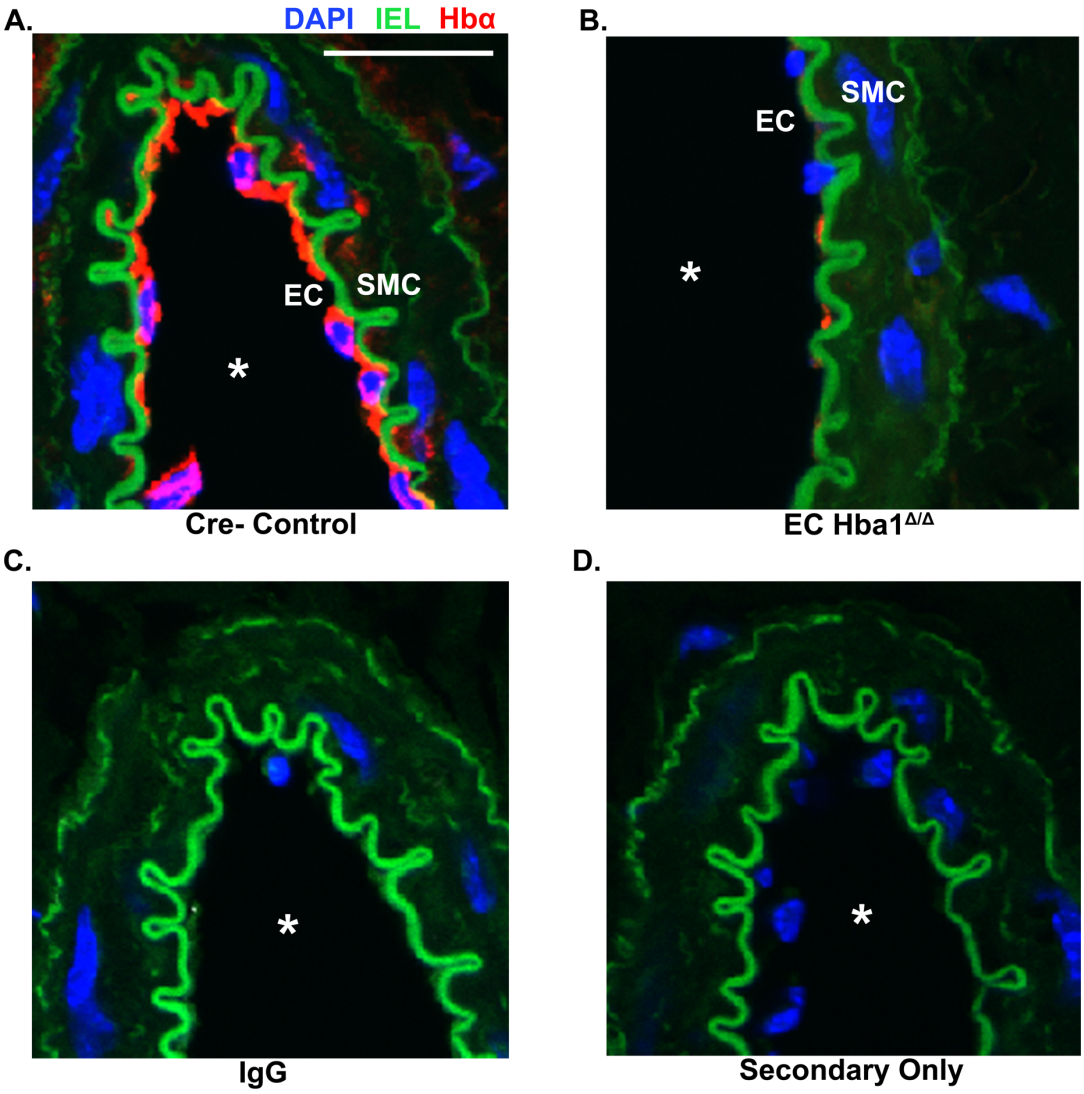

Figure 8. EC Hba1$^{\Delta/\Delta}$ mice exhibit reduced endothelial Hbα expression.

A: Immunofluorescence imaging of Hbα expression (red) in the TDA of an Hba1$^{fl/fl}$ mouse. Internal elastic lamina (IEL) marked by autofluorescence (green), cell nuclei marked by DAPI (blue). **B:** TDA of an Hba1$^{fl/fl}$Cdh5-Cre/ERT2^{+} (EC Hba1$^{\Delta/\Delta}$) mouse. **C and D:** IgG isotype control and secondary-only control images of the artery in **A.** * = vessel lumen, EC = endothelial cells, SMC = smooth muscle cells. Scale bar = 20 μm.

FIGURE 9. EXPRESSION OF GLOBINS IN HBA1$^{FL/FL}$ AND EC HBA1$^{\Delta/\Delta}$ TDAs

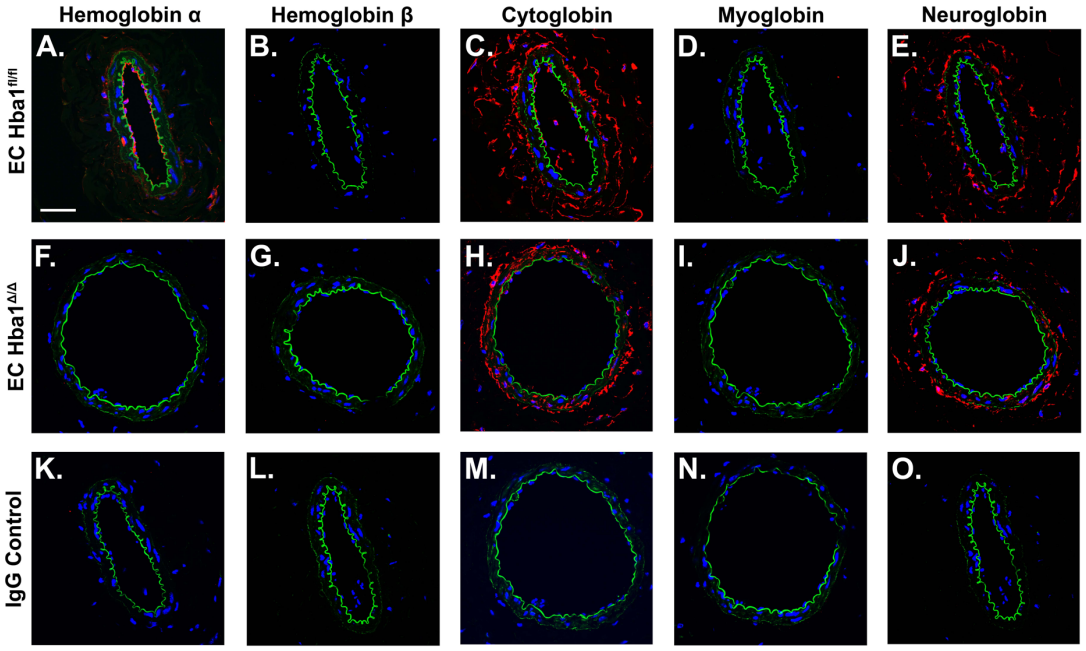

Figure 9. Expression of globins in Hba1$^{fl/fl}$ and EC Hba1$^{\Delta/\Delta}$ TDAs

A-E: Staining for globin expression in the Hba1$^{fl/fl}$ TDA: Hbα (**A**), Hbβ (**B**), Cytoglobin (**C**), Myoglobin (**D**), Neuroglobin (**E**). **F-J:** Staining for globin expression in the EC Hba1$^{\Delta/\Delta}$ TDA: Hbα (**F**), Hbβ (**G**), Cytoglobin (**H**), Myoglobin (**I**), Neuroglobin (**J**). **K-O:** IgG control staining performed alongside the staining in panels **A-J**. Scale bar in A = 50 μm.

Creation of an Hba1$^{\Delta 36\text{-}39/wt}$ Mouse Model

Since endothelial Hbα expression in resistance arteries was originally identified in the context of scavenging enzymatic NO production,[38, 39] loss of this function is an important variable to consider in pursuing its genetic deletion. While NO produced by nitrite reduction is believed to play a particularly elevated role in hypoxic vasodilation,[117, 121, 122] experimental modulation of enzymatic NO production is nevertheless an important confounding variable. Since expression of endothelial Hbα may potentially affect both enzymatic and non-enzymatic NO production, distinguishing between the two is critical to the correct interpretation of results that stem from altered NO signaling. Our laboratory has demonstrated that the NO scavenging activity of endothelial Hbα is dependent on its ability to bind eNOS, and that disruption of this interaction leads to increased NO bioavailability and vasodilation.[226] Therefore, we created an additional mouse model with the intent of eliminating this function while preserving the other structural and functional roles of the Hbα protein.

To specifically disrupt the ability of Hbα to bind to eNOS, we used CRISPR/Cas9 technology to specifically delete four amino acids from the conserved region of *Hba1*-derived Hbα that binds to eNOS[39] (Fig. 10A). Immunofluorescence confocal microscopic imaging demonstrates that, in comparison to Hba1$^{wt/wt}$ littermate controls (Fig. 10B), expression of endothelial Hbα protein is unaffected in Hba1$^{\Delta 36\text{-}39/wt}$ TDAs (Fig. 10C). We then used a proximity ligation assay (PLA) to study the extent of close interaction between Hbα and eNOS in these mice. While both Hbα (Fig. 11A, D) and eNOS (Fig. 11B, E) are expressed at similar levels in Hba1$^{wt/wt}$ and Hba1$^{\Delta 36\text{-}39/wt}$ mice, the majority of PLA signal

is lost in Hba1$^{\Delta 36\text{-}39/wt}$ mice as compared to Hba1$^{wt/wt}$ mice (Fig. 11C, F; quantified in Fig. 11J). These results demonstrate the successful impairment of Hbα-eNOS binding while preserving the expression levels of both proteins. Notably, when breeding this mosue line we found non-Mendelian ratios resulting from (Hba1$^{\Delta 36\text{-}39/wt}$ x Hba1$^{\Delta 36\text{-}39/wt}$) litters, with over-representation of heterozygous and WT pups but no Hba1$^{\Delta 36\text{-}39/\Delta 36\text{-}39}$ pups. Embryonic lethality of the Hba1$^{\Delta 36\text{-}39/\Delta 36\text{-}39}$ genotype points to the physiological importance of the Hbα-eNOS interaction, perhaps particularly so in early stages of development. This finding also underscores the importance of our inducible cre-lox approach to creation of EC Hba1$^{\Delta/\Delta}$ mice, as induction of cre recombinase deletion of *Hba1* at 6-7 weeks of age precludes concern of developmental effects and reduces the likelihood and timeframe of any compensatory changes resulting from *Hba1* deletion.

FIGURE 10. CREATION OF AN HBA1 $^{\Delta 36\text{-}39/WT}$ MOUSE MODEL

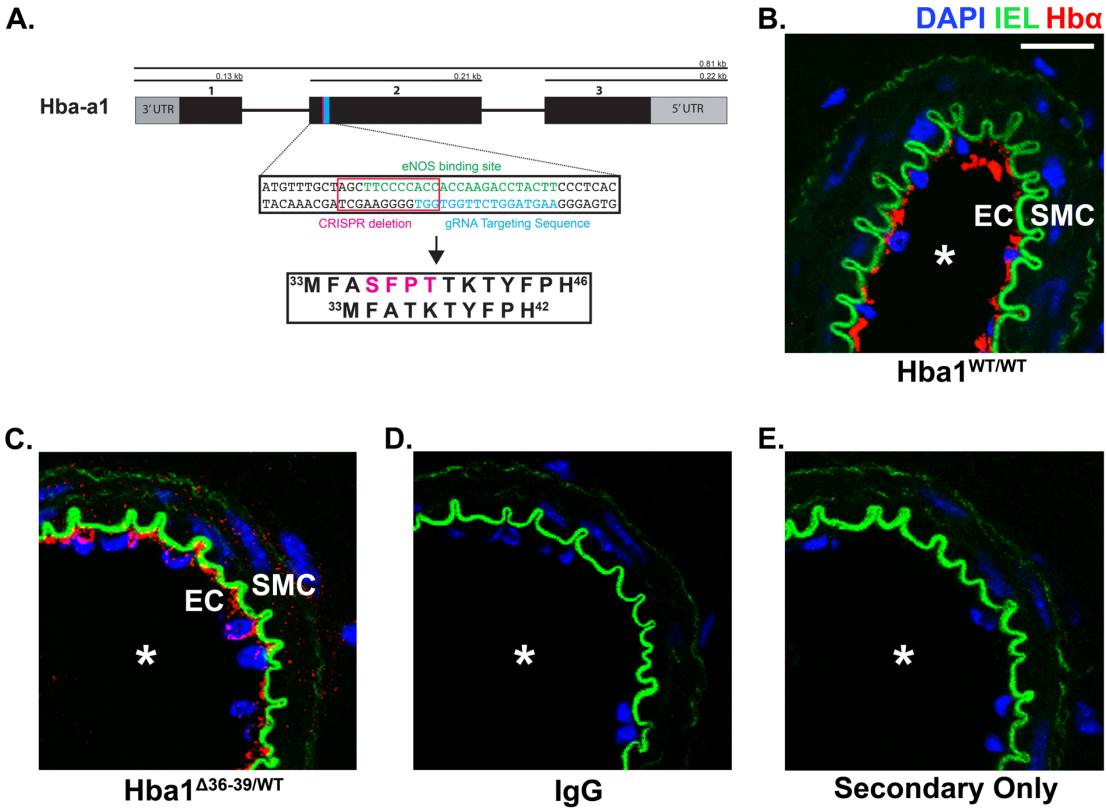

Figure 10. Creation of an Hba1$^{\Delta 36\text{-}39/wt}$ mouse model.

A: Schematic of modified *Hba1* gene with four-amino-acid CRISPR deletion in eNOS binding site. **B:** Imunofluorescence imaging of Hbα expression (red) in the TDA of an Hba1$^{wt/wt}$ mouse. IEL marked by autofluorescence (green), cell nuclei marked by DAPI (blue). **C:** TDA of an Hba1$^{\Delta 36\text{-}39/wt}$ mouse. **D and E:** IgG isotype control and secondary-only control images of the artery in **C**. ***** = vessel lumen, EC = endothelial cells, SMC = smooth muscle cells. Scale bar = 20μm.

FIGURE 11. HBA1$^{\Delta 36\text{-}39/WT}$ MICE EXPRESS HBα WITH IMPAIRED ABILITY TO BIND TO ENOS

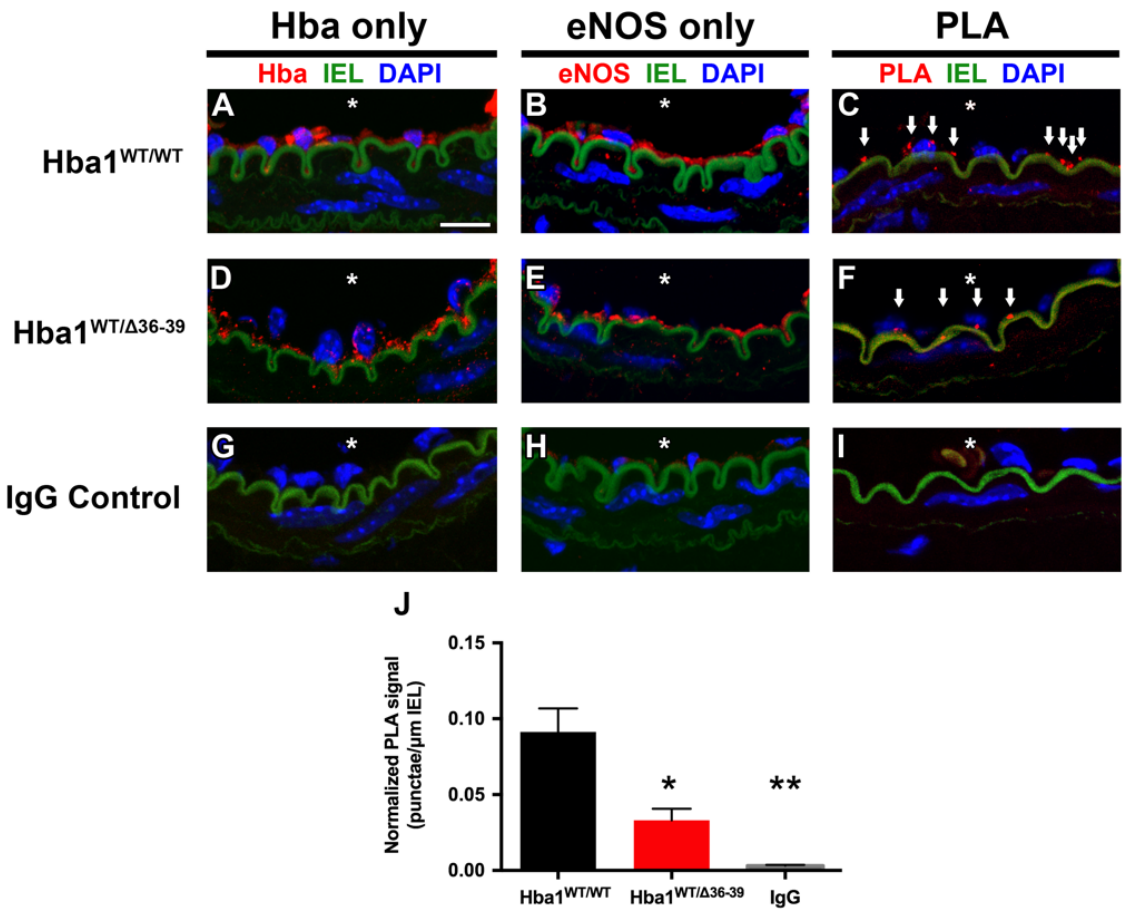

Figure 11. Hba1$^{\Delta 36\text{-}39/wt}$ mice express Hbα with impaired ability to bind to eNOS.

A: Hbα protein expression (red) in the ECs of an Hba1$^{wt/wt}$ control TDA. IEL marked by autofluorescence (green), cell nuclei marked by DAPI (blue). **B:** eNOS expression (red) in the ECs of an Hba1$^{wt/wt}$ control TDA. **C:** Proximity ligation assay (PLA) signal (red) marks locations of close apposition between Hbα and eNOS in an Hba1$^{wt/wt}$ TDA. **D, E,** and **F:** Hbα expression **(D)**, eNOS expression **(E)**, and PLA signal **(F)** in an Hba1$^{\Delta 36\text{-}39/wt}$ TDA. **G, H,** and **I:** IgG isotype controls. **J:** Quantification of PLA signal in **C, F,** and **I**, normalized to length of IEL. * = $p<0.05$ vs. Hba1$^{wt/wt}$ control; ** = $p<0.005$. Scale bar = 10μm.

Cell-type specificity of Hbα effects

A critical detail in our creation of an EC Hba1$^{\Delta/\Delta}$ model is the cell type specificity of Hbα genetic deletion. As the overwhelming majority of cardiovascular Hbα expression is found in the erythroid lineage of cells responsible for the creation of RBC Hb, we drew blood from each of our mouse lines to collect complete blood counts and assess the presence or absence of anemia in our models. As a positive control for alpha thalassemic anemia, we tested Hba1$^{-/-}$ mice that our laboratory has described previously.[198] Hba1$^{-/-}$ mice displayed significant decreases in Hb, hct, and mean RBC volume (Fig. 12A, D, G), including a 25% reduction in hct, as compared to Hba1$^{+/+}$ littermates. Notably, these changes occurred in the absence of any reduction in RBC count (data not shown), indicating an inability for RBC progenitors to produce sufficient Hb protein, as opposed to alternate explanations such as defects in cell differentiation or elevated RBC removal. In contrast to Hba1$^{-/-}$ mice, however, EC Hba1$^{\Delta/\Delta}$ and Hba1$^{\Delta 36\text{-}39/wt}$ mice showed no difference from their controls in Hb (Fig. 12B, C), hct (Fig. 12E, F), or mean RBC volume (Fig 12H, I). Unchanged Hbα expression in RBCs demonstrates specificity of our Hba1$^{\Delta/\Delta}$ model to the endothelium with regards to RBCs, the primary alternative source of vascular Hbα protein. This specificity is important to the study of endothelial Hbα, given the overwhelming abundance of tetrameric Hb in RBCs. Furthermore, unaltered complete blood count (CBC) profiles in Hba1$^{\Delta 36\text{-}39/wt}$ mice provide some evidence of normal heme coordination and oxygen binding capability in Hbα$^{\Delta 36\text{-}39}$, as dysfunctional Hbα protein might be expected to result in erythropoietic compensation for dramatically reduced O_2 carrying capacity.[227] Therefore, these results corroborate both the endothelial specificity of

the Hba1$^{\Delta/\Delta}$ model, and the functional specificity of the Hba1$^{\Delta 36\text{-}39/wt}$ model to eNOS binding.

FIGURE 12. HBA1$^{-/-}$ MICE ARE ANEMIC, BUT NOT EC HBA1$^{\Delta/\Delta}$ OR HBA1$^{\Delta 36\text{-}39/WT}$ MICE

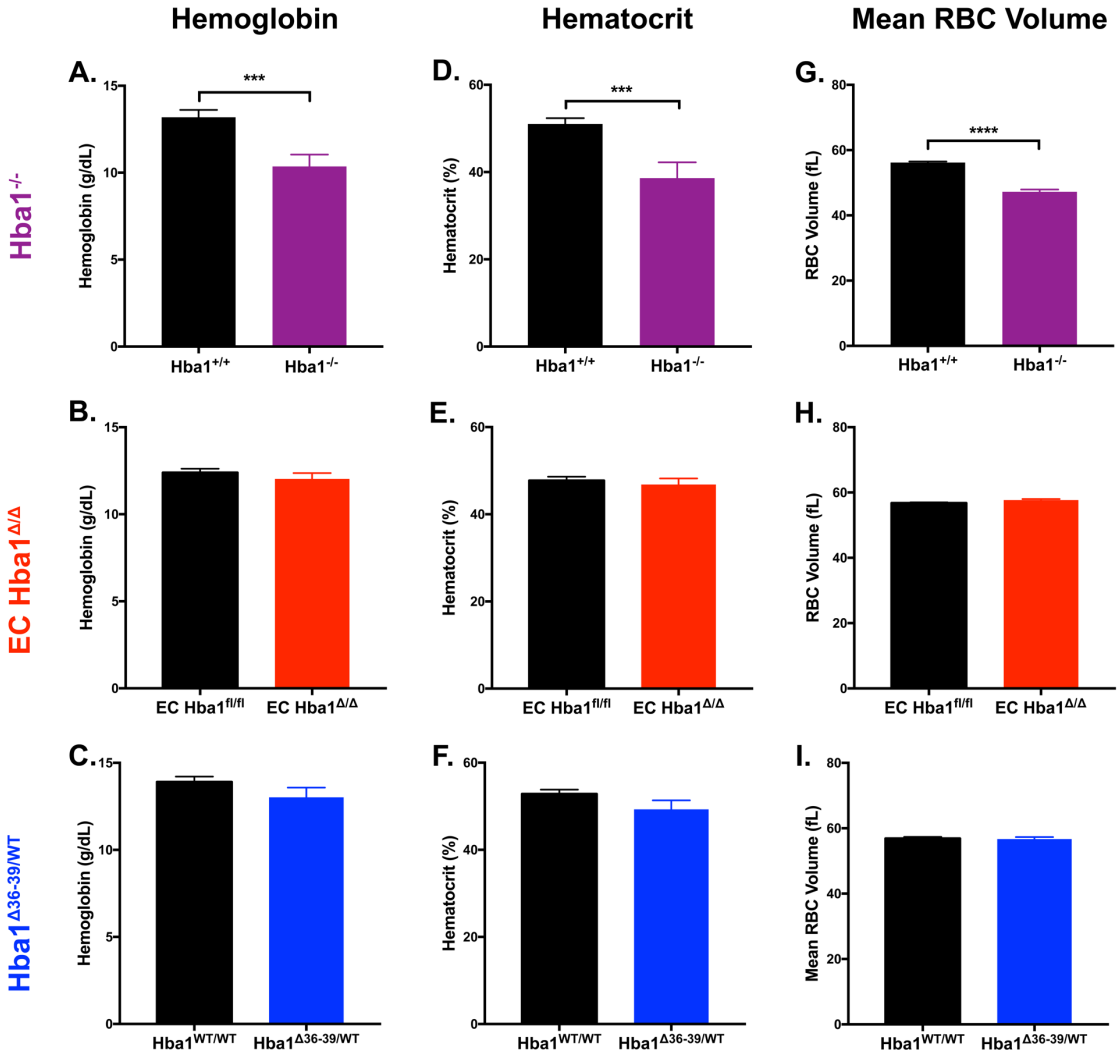

Figure 12. Hba1$^{-/-}$ mice are anemic, but not EC Hba1$^{\Delta/\Delta}$ or Hba1$^{\Delta 36\text{-}39/wt}$ mice.

Comparison of blood parameters from Hba1$^{-/-}$ mice (**A, D, G**) to those of EC Hba1$^{\Delta/\Delta}$ mice (**B, E, H**), and Hba1$^{\Delta 36\text{-}39/wt}$ mice (**C, F, I**). **A:** Blood Hb content is significantly decreased in Hba1$^{-/-}$ mice versus littermate Hba1$^{+/+}$ controls. **B:** Blood Hb content is unchanged in EC Hba1$^{\Delta/\Delta}$ mice versus littermate Hba1$^{fl/fl}$ controls. **C:** Blood Hb content is unchanged in Hba1$^{\Delta 36\text{-}39/wt}$ mice versus littermate Hba1$^{wt/wt}$ controls. **D:** Hct is significantly decreased in Hba1$^{-/-}$ mice. **E:** Hct is unchanged in EC Hba1$^{\Delta/\Delta}$ mice. **F:** Hct is unchanged in Hba1$^{\Delta 36\text{-}39/wt}$ mice. **G:** Mean RBC volume is significantly decreased in Hba1$^{-/-}$ mice. **H:** Mean RBC volume is unchanged in EC Hba1$^{\Delta/\Delta}$ mice. **I:** Mean RBC volume is unchanged in Hba1$^{\Delta 36\text{-}39/wt}$ mice. N = 7-15 (Hba1$^{-/-}$), N = 17-20 (EC Hba1$^{\Delta/\Delta}$), N = 5-6 (Hba1$^{\Delta 36\text{-}39/wt}$).

Endothelial Hbα contributes to exercise fitness

To assess the broad cardiovascular impact of *Hba1* deletion on exercise, we subjected the mouse models described above to a graded treadmill test of acute endurance capacity. As a global model of alpha thalassemia, $Hba1^{-/-}$ mice are not limited to endothelial Hbα effects, but display a broadly anemic phenotype (Fig. 4); therefore, we hypothesized that they would display severely impaired endurance capacity. As expected, $Hba1^{-/-}$ mice showed a 40% decrease in acute endurance capacity versus $Hba1^{+/+}$ controls (Fig. 13A), measured by total distance run before failure. Because EC $Hba1^{\Delta/\Delta}$ mice exhibit *Hba1* deletion in ECs but express normal Hbα levels in RBCs, we hypothesized that they would underperform in an endurance test to a lesser extent than the global $Hba1^{-/-}$ mice. Indeed, EC $Hba1^{\Delta/\Delta}$ mice displayed reduced endurance capacity, with a decrease relative to controls of half the extent of that observed in $Hba1^{-/-}$ mice. EC $Hba1^{\Delta/\Delta}$ mice underperformed $Hba1^{fl/fl}$ controls by roughly 20% in distance ran (Fig. 13B). Finally, we tested $Hba1^{\Delta 36\text{-}39/wt}$ mice to rule out the Hbα-eNOS interaction as a cause of our findings in the EC $Hba1^{\Delta/\Delta}$ line. Whereas both $Hba1^{\Delta 36\text{-}39/wt}$ and $Hba1^{wt/wt}$ mice underperformed other mouse lines in our endurance test, we observed no decrease in performance in $Hba1^{\Delta 36\text{-}39/wt}$ mice as compared to $Hba1^{wt/wt}$ controls (Fig. 13C). This result suggests that the decreased endurance capacity observed in global $Hba1^{-/-}$ and EC $Hbal^{\Delta/\Delta}$ mice is not due to a deficiency in the ability of EC Hbα to scavenge eNOS-derived NO, but is the result of an independent mechanism.

As a control measurement for demonstrated effort, we measured blood lactate concentration in all mice before and after exercise. We observed an increase in blood

lactate (Δ Lactate) across every group (Fig. 13D-F), demonstrating that exertion exceeded lactate threshold before failure in the acute endurance capacity test. While all groups displayed an overall increase in blood lactate as a result of the exercise protocol, we noted a trend towards lower Δ Lactate in EC $Hba1^{fl/fl}$ mice versus controls, and a trend towards higher Δ Lactate in $Hba1^{-/-}$ mice versus controls, although neither difference was significant. However, there was no correlation between the distance mice ran and their Δ Lactate (data not shown), suggesting that mice typically exceeded lactate threshold prior to failure and subsequently experienced an elevation of blood lactate unrelated to the distance covered prior to that point.

FIGURE 13. HBA1$^{-/-}$ AND EC HBA1$^{\Delta/\Delta}$ MICE EXHIBIT IMPAIRED ENDURANCE CAPACITY, BUT HBA1$^{\Delta 36\text{-}39/WT}$ MICE ARE UNAFFECTED

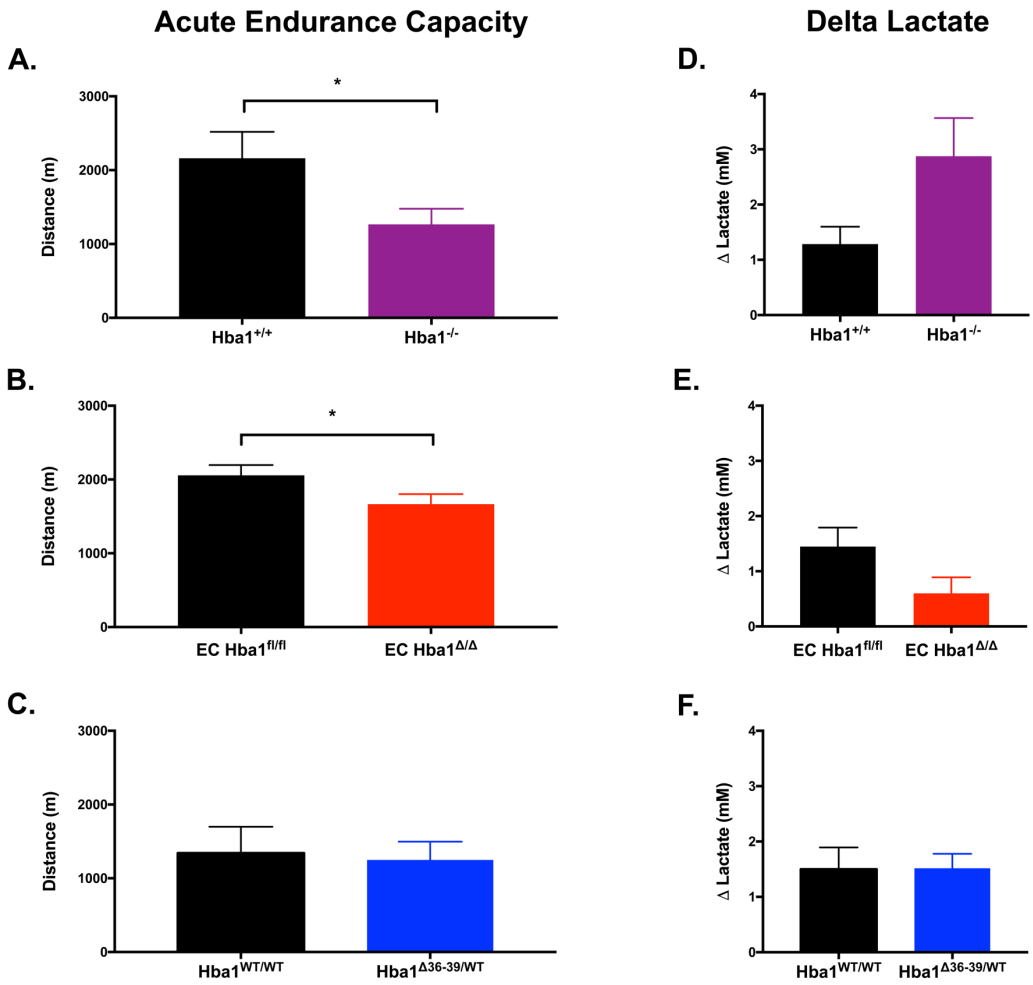

Figure 13. Hba1$^{-/-}$ and EC Hba1$^{\Delta/\Delta}$ mice exhibit impaired endurance capacity, but Hba1$^{\Delta 36\text{-}39/wt}$ mice are unaffected.

A: Acute endurance capacity was assessed via a graded treadmill test, measuring total distance traveled until failure. **A:** Hba1$^{-/-}$ mice showed a 40% decrease in acute endurance capacity versus littermate Hba1$^{+/+}$ controls. **B:** EC Hba1$^{\Delta/\Delta}$ mice showed a 20% decrease in acute endurance capacity versus littermate Hba1$^{fl/fl}$ controls. **C:** Hba1$^{\Delta 36\text{-}39/wt}$ mice showed no change in acute endurance capacity versus littermate Hba1$^{wt/wt}$ controls. **D, E,** and **F:** Change in blood lactate during the exercise test was measured to further confirm fatigue. N = 4-7 (Hba1$^{-/-}$), N = 23-25 (EC Hba1$^{\Delta/\Delta}$), N=6 (Hba1$^{\Delta 36\text{-}39/wt}$).

EC Hba1$^{\Delta/\Delta}$ mice exhibit normal capillary density

In addition to the dilatory state of upstream arteries, capillary density is another important determinant of skeletal muscle perfusion.[228] To rule out these structural changes as an influence on skeletal muscle perfusion and exercise performance, we measured capillary density in both the fast-twitch plantaris muscle and the slow-twitch soleus muscle of the mouse hindlimb. In preliminary data (EC Hba1$^{\Delta/\Delta}$ N = 6-8, Hba1$^{\Delta 36\text{-}39/wt}$ N = 3-5), we observed no change in capillary density in either the soleus (Fig. 14A) or plantaris (Fig. 14B) muscles of EC Hba1$^{\Delta/\Delta}$ mice, compared to Hba1$^{fl/fl}$ controls. However, we saw a significant increase in capillary density in the slow-twitch soleus muscle of Hba1$^{\Delta 36\text{-}39/wt}$ mice compared to Hba1$^{wt/wt}$ controls (Fig. 14C). Capillary density in the fast-twitch plantaris muscle of Hba1$^{\Delta 36\text{-}39/wt}$ mice was not significantly different from Hba1$^{wt/wt}$ controls (Fig. 14D), although it trended upwards in preliminary data.

This result is indicative of angiogenesis in Hba1$^{\Delta 36\text{-}39/wt}$ mice, perhaps as a result of unrestrained NO signaling in the vascular wall throughout development. Increased capillary density in the soleus muscle to a greater extent than that observed in the plantaris muscle is understandable given the greater reliance of slow-twitch muscles on oxidative metabolism, and therefore on blood supply of O_2, than that of fast-twitch muscles. Notably, induction of cre recombinase activity in EC Hba1$^{\Delta/\Delta}$ mice does not take place until the mice receive tamoxifen injections starting at 6 weeks of age, highlighting developmental effects as a possible cause of the different capillary density effects observed between the EC Hba1$^{\Delta/\Delta}$ and Hba1$^{\Delta 36\text{-}39/wt}$ strains.

FIGURE 14. EC HBA1$^{\Delta/\Delta}$ MICE EXHIBIT NORMAL CAPILLARY DENSITY IN HINDLIMB MUSCLES, BUT HBA1$^{\Delta 36\text{-}39/WT}$ MICE EXHIBIT INCREASED CAPILLARY DENSITY.

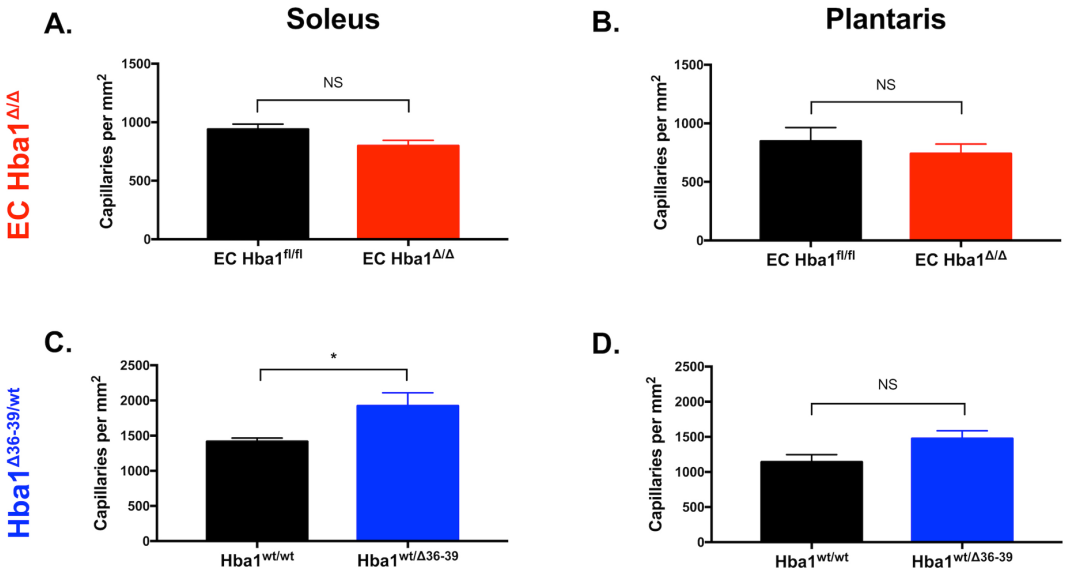

Figure 14. EC Hba1$^{\Delta/\Delta}$ mice exhibit normal capillary density in hindlimb muscles, but Hba1$^{\Delta 36\text{-}39/wt}$ mice exhibit increased capillary density.

A: Capillary density was measured in cross-sections of the slow-twitch soleus hindlimb muscles of EC Hba1$^{\Delta/\Delta}$ mice and compared to that of littermate Hba1$^{fl/fl}$ controls. **B:** Capillary density comparison between fast-twitch plantaris muscles of EC Hba1$^{\Delta/\Delta}$ mice and Hba1$^{fl/fl}$ controls. **C:** Capillary density comparison between slow-twitch soleus muscles of Hba1$^{\Delta 36\text{-}39/wt}$ mice and Hba1$^{wt/wt}$ controls. **D:** Capillary density comparison between fast-twitch plantaris muscles of Hba1$^{\Delta 36\text{-}39/wt}$ mice and Hba1$^{wt/wt}$ controls. N = 6-8 (EC Hba1$^{\Delta/\Delta}$), N = 3-5 (Hba1$^{\Delta 36\text{-}39/wt}$).

Myography

In comparison with arteries taken from control mice, $Hba1^{-/-}$ TDAs show reduced constriction to α-adrenergic stimulation with PE.[198] Preliminary data suggests a similar phenotype in EC $Hba1^{\Delta/\Delta}$ mice, which constrict less strongly to PE than $Hba1^{fl/fl}$ controls (Fig. 15A). To study the effect of endothelial *Hba1* deletion on skeletal muscle artery dilation in response to hypoxia, we developed a hypoxic treatment condition using sodium dithionite (NaS_2O_4), which has been used previously as an oxygen scavenger to study Hb O_2 release kinetics[229] and the nitrite reductase activity of Hb,[230] as well as in arteries to study other mechanisms of hypoxic vasodilation.[231] Endothelial function of each vessel was tested prior to experimentation via dilatory response to 1μM NS309 following PE preconstriction, after which the bath was replaced with new buffer and the vessel was allowed to re-equilibrate.

Based on previous studies using NaS_2O_4 with RBCs and Hb in the literature and seeking excess for a positive control, we selected 5mM NaS_2O_4 as a stimulation condition to induce dilation of TDAs following preconstriction with 1μM PE. When applied at 5mM, we found that NaS_2O_4 caused rapid, total dilation of TDAs taken from WT C57Bl/6 mice (data not shown). Following this result, we tested lower concentrations of NaS_2O_4 to identify a more dynamic range for treatment, identifying 1mM as a stimulation concentration that caused 100% dilation of a C57Bl/6 TDA over a roughly 10-minute timeframe (Fig. 15C). When an EC $Hba1^{\Delta/\Delta}$ TDA was preconstricted with 1μM PE and stimulated it with 1mM NaS_2O_4, however, we observed less than 40% dilation, a much weaker response than what we observed in WT arteries (Fig. 15B). In consideration of the

reduced response of EC Hba1$^{\Delta/\Delta}$ arteries to a PE dose-response curve (Fig. 15A), we also tested a higher dose of 10μM PE as a preconstriction condition for EC Hba1$^{\Delta/\Delta}$ TDAs, but following this greater preconstriction, treatment with 1mM NaS_2O_4 yielded a similar dilation of less than 40% (Fig. 15D). However, following incomplete dilation to 1mM NaS_2O_4, EC Hba1$^{\Delta/\Delta}$ TDAs still dilated rapidly and completely to a subsequent higher dose of 5mM NaS_2O_4 (Fig. 15D).

These preliminary results suggest that EC Hba1$^{\Delta/\Delta}$ mice may exhibit decreased vasodilation in response to hypoxia, although interpretation is limited both by low n-value and a lack of data from littermate Hba1$^{fl/fl}$ controls. Robust dilation to 5mM NaS_2O_4 in EC Hba1$^{\Delta/\Delta}$ vessels (Fig. 15D) is also intriguing, as it indicates that excess NaS_2O_4 treatment (which may be considered full anoxia) still elicits a forceful dilatory response. While not the only possible explanation, this observation could be a result of a redundant nitrite reductase mechanism activated at the lower pO_2 levels that result in the deoxygenation of other globins (e.g. cytoglobin, neuroglobin) we detected in the mouse TDA (Fig. 9C, E), as a strong "burst" of nitrite reductase activity has been similarly identified in the presence of deoxygenated myoglobin.[118]

FIGURE 15. EC HBA1$^{\Delta/\Delta}$ MICE DISPLAY IMPAIRED VASODILATION IN RESPONSE TO HYPOXIA

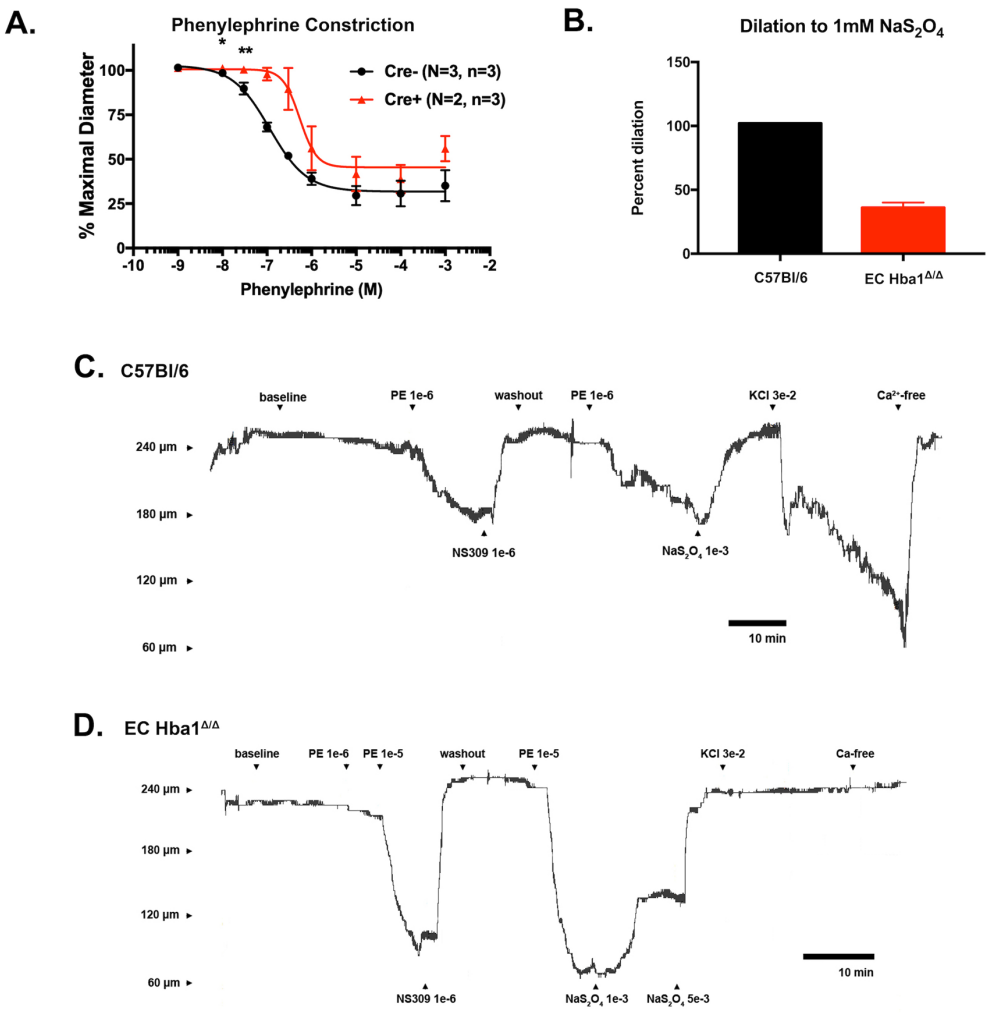

Figure 15. EC Hba1$^{\Delta/\Delta}$ mice display impaired vasodilation in response to hypoxia.

A: Cannulated, pressurized TDAs from EC Hba1$^{\Delta/\Delta}$ mice and Hba1$^{fl/fl}$ controls were treated with escalating doses of PE, measuring the resulting constriction of the vessel. N = 2-3. **B:** Preliminary comparison between C57Bl/6 TDA (N = 1) and EC Hba1 TDAs (N = 2) of dilation to 1mM NaS_2O_4 following PE preconstriction. **C** and **D:** Representative traces of the pressure myography experiments compared in **B.** Application of drugs and other conditions occurred at timepoints indicated by black arrows. Time scale bar = 10 minutes.

Acknowledgements: Angela Best assisted in the creation of $Hba1^{fl/fl}$ and $Hba1^{\Delta 36\text{-}39/wt}$ mouse lines. Sara Murphy assisted with confirmation of *Hba1* excision (Fig. 7E). Aditi Islam assisted in the staining and confocal imaging of EC $Hba1^{\Delta/\Delta}$ TDAs (Fig. 8 and 9) and hindlimb muscle sections for capillary density (Fig. 14). TC Steven Keller IV contributed the confocal imaging and PLA experiments characterizing the $Hba1^{\Delta 36\text{-}39/wt}$ model in Fig. 10 and Fig. 11. Henry Askew Page contributed PE dose-response curves in Fig. 15A.

CHAPTER 5. GENERAL DISCUSSION AND FUTURE DIRECTIONS

Control of blood flow to active skeletal muscle is a complex physiological process with numerous regulatory inputs. Mechanisms of arterial dilation in response to downstream metabolic demand are of great interest because they allow a general increase in blood flow during exercise to be directed specifically to the tissues with elevated metabolic demand. Numerous pathways have been presented as candidates to explain this response, and a modern consensus is that a highly integrated set of initial signals and downstream messengers mediate the temporal and locational variables with built-in redundancy.[3, 7-9] The literature points to NO as an important signaling axis in the vasodilatory response to hypoxic exercise[31, 117] with multiple mechanisms of NO production proposed as a result of different upstream processes.[33, 122] The research presented in this dissertation focuses on two proposed pathways of NO generation as a vasodilatory response to exercise-induced hypoxia.

5.1 Panx1-dependent ATP release from RBCs in hypoxia

First, we examined the pathway by which RBCs are proposed to release ATP into the vascular lumen in response to hypoxic stimulation via elevation of cAMP and activation of Panx1 channels.[33] Luminal ATP in turn activates P2Y receptors on the endothelium to initiate downstream vasodilatory signaling pathways including eNOS activation and NO release.[154] The interest and expertise of our laboratory in studying Panx1 channels led us to examine the mechanism of Panx1 activation in RBCs during hypoxia.

According to a previously proposed pathway,[33] RBC deoxygenation leads to AC activation and cAMP production, causing Panx1 activation and ATP release. We sought to understand the mechanism by which elevated cAMP caused Panx1 activation in this setting; however, we found that neither treatment of RBCs with a cAMP analog (Fig. 5), nor upstream pharmacologic stimulations that resulted in elevation of intracellular cAMP (Fig. 6), caused ATP release. Furthermore, stimulation of RBCs with a cAMP analog yielded similar results in both WT and $Panx1^{-/-}$ RBCs, as well as in the presence or absence of the Panx1 inhibitor CBX (Fig. 5). Based on these results, we were unable to verify claims in the literature that cAMP lies upstream of Panx1 in a pathway of ATP release from RBCs.

Seeking additional methods of Panx1 stimulation in RBCs, we discovered methodological concerns with another Panx1 stimulation condition reported in the literature, as the ATP release we observed from RBCs in response to hypotonic, high-K^+ stimulation was strongly correlated with RBC lysis (Fig. 4). These findings of irreproducibility led us to question the methods used in assessing Panx1 activity and ATP release from RBCs, including both experimental treatment of ATP (Fig. 3A-D) and spectroscopic measurement of hemolysis (Fig. 3E). In particular, we highlighted the need for hemolysis data to be reported alongside ATP release from individual samples. To eliminate the variable of oxygenation (important in a field where hypoxia is a key stimulation condition) and minimize variability in hemolysis measurements, we also recommended a best practice of measuring cell-free Hb absorbance not at the absorbance peaks of oxyHb or deoxyHb, but rather at the isosbestic wavelengths where absorbance is equal between the two species.

Finally, to assess the overarching importance of Panx1 to regulation of blood flow in exercise, we compared the performance of $Panx1^{-/-}$ mice and $Panx1^{fl/fl}$ controls in an incremental treadmill test of acute endurance capacity. Finding no difference in exercise performance between the two groups (Fig. 2A), we drew a two-part conclusion: either Panx1 does not play an essential role in hypoxic ATP release from RBCs, or if it does, this pathway does not make a significant contribution to muscular performance during exercise. Future directions in this area should focus first at the level of blood flow, measuring the effects of Panx1 deletion on perfusion of exercising skeletal muscle. This test would provide additional detail to distinguish between the two possible conclusions resulting from our exercise test findings. At the cellular mechanistic level, the possibility remains that Panx1-dependent ATP release may be activated by mechanical stimulation,[205, 206] or by hypoxia via a different mechanism of activation. Alternate stimulation conditions should be tested with caution to control for the methodological concerns discussed above.

5.2 Endothelial Hbα as a nitrite reductase in hypoxia

Lacking evidence to support further exploration of ATP release from RBCs in hypoxia, we turned our focus to a different reported mechanism of vasodilation in exercise hyperemia. The nitrite reductase activity of deoxyHb has been well documented,[117, 121] as well as a significant A/V gradient for plasma nitrite[232] that increases in magnitude during exercise. Previous study of this mechanism has focused on Hb in RBCs, but concerns have been raised regarding the ability of RBC Hb to provide sufficient NO flux to vascular smooth muscle to achieve hypoxic vasodilation.[119] However, our laboratory is uniquely

positioned to consider this mechanism of NO production from a novel angle, having discovered Hbα expression in the endothelium of skeletal muscle resistance arteries.[38, 39] Given its optimal location in relation to SMCs, we hypothesized that endothelial Hbα is an important contributor of NO to SMCs as a mechanism of exercise hyperemia.

To study this question, we developed a novel $Hba1^{fl/fl}$ mouse model (Fig. 7), which we bred with a line featuring inducible, endothelial-specific cre recombinase. The resulting EC $Hba1^{\Delta/\Delta}$ mouse line features genetic deletion of the *Hba1* gene in ECs, resulting in severely reduced expression of Hbα protein in the endothelium of the TDA (Fig. 8), while having no effect on the expression of other globins in the TDA wall (Fig. 9). Importantly, EC $Hba1^{\Delta/\Delta}$ mice had no changes to Hb levels in the blood, in contrast to $Hba1^{-/-}$ mice, a global model of *Hba1* deletion, which display an anemic phenotype (Fig. 12). In order to separate the hypothesized nitrite reductase role for EC Hbα from the Isakson laboratory's previous finding that EC Hbα functionally couples with eNOS to scavenge enzymatically produced NO, we used CRISPR-Cas9 technology to disrupt the eNOS binding region of Hbα with a four amino acid deletion in *Hba1*. In $Hba1^{\Delta 36\text{-}39/wt}$ mice, Hbα expression is unaffected in the vascular wall of the TDA (Fig. 10) and in RBCs (Fig. 12), but $Hb\alpha^{\Delta 36\text{-}39}$ displays impaired ability to associate to eNOS. Thus, we are equipped with three mouse models targeting Hbα: global deletion ($Hba1^{-/-}$), endothelial-specific inducible deletion (EC $Hba1^{\Delta/\Delta}$), and disruption of Hbα-eNOS binding ($Hba1^{\Delta 36\text{-}39/wt}$).

Due to the possibility of physiological compensation for a lack of blood flow and O_2 delivery to tissue in our knockout mouse models, we examined both capillary density and mitochondrial content in the hindlimb muscles. In preliminary data from EC $Hba1^{\Delta/\Delta}$

mice and $Hba1^{fl/fl}$ controls, we saw no difference in capillary density of either fast-twitch, less oxidative plantaris muscles or slow-twitch, highly oxidative soleus muscles; however, in $Hba1^{\Delta 36\text{-}39/wt}$ mice, we observed a statistically significant increase in capillary density in the soleus muscle versus $Hba1^{wt/wt}$ controls (Fig. 14). This result is indicative of angiogenic compensation in $Hba1^{\Delta 36\text{-}39/wt}$ mice, particularly in the slow-twitch soleus muscle, which is heavily reliant on oxidative metabolism. In contrast, we saw no change in mitochondria content (as measured by voltage dependent anion channel (VDAC) expression normalized to total protein) in the soleus, plantaris, or the mixed fiber type gastrocnemius hindlimb muscles of $Hba1^{\Delta 36\text{-}39/wt}$ mice relative to controls (Fig. 16). These findings are useful to rule out loss or gain of cellular energy production capacity as a contributing factor to changes in exercise capacity. We plan to perform the same assessment of mitochondrial content in the EC $Hba1^{\Delta/\Delta}$ mice as soon as feasible.

FIGURE 16. MITOCHONDRIA CONTENT IN HBA1$^{\Delta 36\text{-}39/WT}$ MICE HINDLIMB MUSCLES IS UNCHANGED

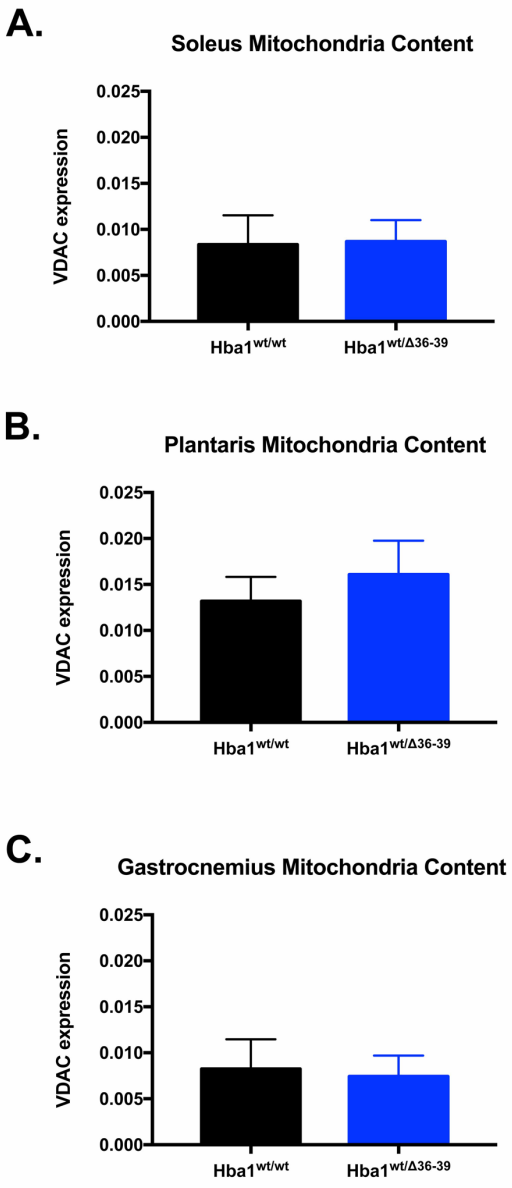

Figure 16. Mitochondria content in Hba1$^{\Delta 36\text{-}39/wt}$ mouse hindlimb muscles is unchanged

A: VDAC expression in the soleus muscles of Hba1$^{\Delta 36\text{-}39/wt}$ mice and Hba1$^{wt/wt}$ controls, quantified from Western blot. **B:** VDAC expression in the plantaris muscles of Hba1$^{\Delta 36\text{-}39/wt}$ mice and Hba1$^{wt/wt}$ controls. **C:** VDAC expression in the soleus muscles of Hba1$^{\Delta 36\text{-}39/wt}$ mice and Hba1$^{wt/wt}$ controls. Expression of individual proteins was normalized to total protein detected per lane. N = 3-5 per group.

To study the overall impact of these genetic deletions on broad exercise performance, we subjected each of these three Hbα-targeted mouse strains to a test of acute endurance capacity. As previously with Panx1$^{-/-}$ mice, we hypothesized that if EC Hbα plays an important role as a nitrite reductase to support exercise hyperemia, both Hba1$^{-/-}$ and EC Hba1$^{\Delta/\Delta}$ mice would exhibit impaired exercise capacity compared to controls, and we observed exactly this result (Fig. 13). Our finding that Hba1$^{\Delta 36\text{-}39/wt}$ mice performed similarly to their controls (Fig. 13) suggested that the results of Hba1$^{-/-}$ and EC Hba1$^{\Delta/\Delta}$ mice were not due to removal of the Hbα-eNOS function, allowing us to rule out Hbα scavenging of enzymatically produced NO (and resulting systemic dilation) as a cause of these results.

After establishing an exercise phenotype for EC Hba1$^{\Delta/\Delta}$ mice, we sought to demonstrate the mechanistic basis for these results. We hypothesized that loss of *Hba1* would prevent TDAs from dilating properly in response to hypoxia, which would explain reduced exercise performance on the basis of a lack of ability to increase local blood flow and supply needed levels of O_2 to highly aerobic skeletal muscle. To test this response, we are developing a pressure myography protocol in which preconstriction to PE serves as a sympathomimetic to approximate the broad sympathetic constriction signaling observed during exercise.[12] Following PE preconstriction, addition of a moderate dose of the oxygen scavenger NaS_2O_4 induces hypoxia and steady, complete dilation in the WT TDA (Fig. 15 B,C). Preliminary data shows impaired dilation in EC Hba1$^{\Delta/\Delta}$ TDAs (Fig. 15 B,D), indicating that endothelial Hbα plays a critical role in hypoxic dilation. Notably, a higher dose of NaS_2O_4 causes rapid, complete dilation in both WT (data not shown) and EC

$Hba1^{\Delta/\Delta}$ mice (Fig. 15D), implying a redundant system activated in more severely hypoxic conditions, perhaps indicative of one or more of the other globins with oxygen affinities of an order of magnitude greater than Hb. To understand the effects of this experimental setup more precisely, we plan to use an oxygen sensing probe to measure the hypoxia generated by the addition of different concentrations of NaS_2O_4 to the bath that perfuses the vessel in these experiments. This measurement will provide better insight into the precise levels of hypoxia achieved in different stimulation conditions, to allow for more complete analysis of their experimental effects.

Future experiments based on PE preconstriction followed by NaS_2O_4 stimulation should standardize PE preconstriction conditions to permit more precise comparison of EC $Hba1^{\Delta/\Delta}$ and $Hba1^{fl/fl}$ arteries. This may be achieved by preconstricting arteries to the same level of constriction, varying PE dose as necessary. To calculate the needed stimulation concentrations of PE, we intend to increase the n-value of our PE dose-response curves on EC $Hba1^{\Delta/\Delta}$ vessels (Fig. 15A) and determine more precisely the loss of responsiveness to PE following *Hba1* deletion. Additionally, we are preparing an experiment that will repeat our existing myography protocol following pretreatment of vessels with CO, which competitively displaces other gases in the heme binding sites of Hb. In doing so, we hypothesize that the dilatory response of TDAs (from all groups) to NaS_2O_4 will be lost, providing additional evidence that Hbα is central to the mechanism of dilation.

Additional future experiments could allow us to understand multiple facets of endothelial Hbα nitrite reductase function in greater detail. To rule out eNOS-derived NO as a source of dilation in these experiments, pretreatment of vessels with the l-arginine

derivative L-NAME, a NOS inhibitor, would isolate the hypothesized mechanism of NO production in the absence of NOS-derived NO. We hypothesize that dilation to NaS_2O_4 would be unaffected by L-NAME pretreatment, and the only effect would be to render EC $Hba1^{\Delta/\Delta}$ vessels equally responsive to PE preconstriction as $Hba1^{fl/fl}$ controls. To study the secondary, powerful dilation at high NaS_2O_4 concentrations, EC $Hba1^{\Delta/\Delta}$ mice could be bred with mice lacking expression of the other globins whose expression we measured in the TDA (Fig. 9). We hypothesize that a dual knockout of either cytoglobin or neuroglobin alongside endothelial Hbα deletion would result in loss of this stronger anoxic dilation.

Finally, the specific mechanism of NO production by deoxygenated Hbα may be demonstrated by measurement of NO release in response to hypoxia, preparing vessels *en face*, loading them with the fluorescent NO sensor DAF-FM, and measuring fluorescence following hypoxic stimulation as a direct output for NO release. We hypothesize that this experiment would show decreased fluorescence from EC $Hba1^{\Delta/\Delta}$ mice compared to $Hba1^{fl/fl}$ controls.

In conclusion, NO signaling plays an important role in arterial dilation to facilitate the hyperemic response to skeletal muscle activity during exercise. We examined two mechanisms proposed to facilitate hypoxic NO production. We determined that ATP release from RBCs via Panx1 is unlikely to play a significant role in this response, in contrast to a hypothesized pathway reported in the literature, and have highlighted methodological considerations for others performing research in this area. Subsequently, we have identified the nitrite reductase activity of endothelial Hbα as a novel potential regulator of arterial dilation in response to hypoxia and described the future experiments

needed to further confirm this mechanism. Endothelial Hbα may represent a novel target for nitrite-based therapies to improve blood flow regulation.

CHAPTER 6: REFERENCES

1. Segal SS, Duling BR. Communication between feed arteries and microvessels in hamster striated muscle: Segmental vascular responses are functionally coordinated. *Circ Res*. 1986;59:283-290
2. Sutera SP, Skalak R. The history of poiseuille's law. *Annual Review of Fluid Mechanics*. 1993;25:1-20
3. Segal SS. Regulation of blood flow in the microcirculation. *Microcirculation*. United States; 2005:33-45.
4. Joyner MJ, Casey DP. Regulation of increased blood flow (hyperemia) to muscles during exercise: A hierarchy of competing physiological needs. *Physiological Reviews*. 2015;95:549-601
5. Andersen P, Saltin B. Maximal perfusion of skeletal muscle in man. *The Journal of physiology*. 1985;366:233-249
6. Boushel R, Langberg H, Green S, Skovgaard D, Bülow J, Kjær M. Blood flow and oxygenation in peritendinous tissue and calf muscle during dynamic exercise in humans. *The Journal of Physiology*. 2000;524:305-313
7. Delp MD. Control of skeletal muscle perfusion at the onset of dynamic exercise. *Med Sci Sports Exerc*. 1999;31:1011-1018
8. Joyner MJ, Proctor DN. Muscle blood flow during exercise: The limits of reductionism. *Med Sci Sports Exerc*. 1999;31:1036-1040
9. Sarelius I, Pohl U. Control of muscle blood flow during exercise: Local factors and integrative mechanisms. *Acta physiologica (Oxford, England)*. 2010;199:349-365

10. Corcondilas A, Koroxenidis GT, Shepherd JT. Effect of a brief contraction of forearm muscles on forearm blood flow. *Journal of Applied Physiology*. 1964;19:142-146

11. Donald DE, Rowlands DJ, Ferguson DA. Similarity of blood flow in the normal and the sympathectomized dog hind limb during graded exercise. *Circ Res*. 1970;26:185-199

12. Secher NH, Clausen JP, Klausen K, Noer I, Trap-Jensen J. Central and regional circulatory effects of adding arm exercise to leg exercise. *Acta Physiol Scand*. 1977;100:288-297

13. Marshall RJ, Schirger A, Shepherd JT. Blood pressure during supine exercise in idiopathic orthostatic hypotension. *Circulation*. 1961;24:76-81

14. Tschakovsky ME, Rogers AM, Pyke KE, Saunders NR, Glenn N, Lee SJ, Weissgerber T, Dwyer EM. Immediate exercise hyperemia in humans is contraction intensity dependent: Evidence for rapid vasodilation. *J appl physiol (1985)*. United States; 2004:639-644.

15. Joyner MJ, Halliwill JR. Neurogenic vasodilation in human skeletal muscle: Possible role in contraction-induced hyperaemia. *Acta physiol scand*. England; 2000:481-488.

16. VanTeeffelen JW, Segal SS. Rapid dilation of arterioles with single contraction of hamster skeletal muscle. *Am j physiol heart circ physiol*. United States; 2006:H119-127.

17. Moore AW, Bearden SE, Segal SS. Regional activation of rapid onset vasodilatation in mouse skeletal muscle: Regulation through alpha-adrenoreceptors. *J Physiol*. 2010;588:3321-3331

18. Sheriff DD, Rowell LB, Scher AM. Is rapid rise in vascular conductance at onset of dynamic exercise due to muscle pump? *Am J Physiol*. 1993;265:H1227-1234

19. Tschakovsky ME, Shoemaker JK, Hughson RL. Vasodilation and muscle pump contribution to immediate exercise hyperemia. *Am J Physiol*. 1996;271:H1697-1701

20. Shoemaker JK, Tschakovsky ME, Hughson RL. Vasodilation contributes to the rapid hyperemia with rhythmic contractions in humans. *Can J Physiol Pharmacol*. 1998;76:418-427

21. Tschakovsky ME, Sheriff DD. Immediate exercise hyperemia: Contributions of the muscle pump vs. Rapid vasodilation. *J appl physiol (1985)*. United States; 2004:739-747.

22. Dyke CK, Dietz NM, Lennon RL, Warner DO, Joyner MJ. Forearm blood flow responses to handgripping after local neuromuscular blockade. *J Appl Physiol (1985)*. 1998;84:754-758

23. Scott JB, Rudko M, Radawski D, Haddy FJ. Role of osmolarity, k+, h+, mg++, and o2 in local blood flow regulation. *Am J Physiol*. 1970;218:338-345

24. Mohrman DE, Sparks HV. Role of potassium ions in the vascular response to a brief tetanus. *Circ Res*. 1974;35:384-390

25. Armstrong ML, Dua AK, Murrant CL. Potassium initiates vasodilatation induced by a single skeletal muscle contraction in hamster cremaster muscle. *J Physiol*. 2007;581:841-852

26. Mohrman DE. Lack of influence of potassium or osmolality on steady-state exercise hyperemia. *Am J Physiol*. 1982;242:H949-954

27. Lash JM, Bohlen HG. Perivascular and tissue po2 in contracting rat spinotrapezius muscle. *Am J Physiol*. 1987;252:H1192-1202

28. Black JE, Roddie IC. The mechanism of the changes in forearm vascular resistance during hypoxia. *J Physiol*. 1958;143:226-235

29. Duling BR, Berne RM. Longitudinal gradients in periarteriolar oxygen tension. A possible mechanism for the participation of oxygen in local regulation of blood flow. *Circ Res*. 1970;27:669-678

30. Joyner MJ, Casey DP. Muscle blood flow, hypoxia, and hypoperfusion. *J Appl Physiol (1985)*. 2014;116:852-857

31. Casey DP, Madery BD, Curry TB, Eisenach JH, Wilkins BW, Joyner MJ. Nitric oxide contributes to the augmented vasodilatation during hypoxic exercise. *J Physiol*. 2010;588:373-385

32. Ellsworth ML, Forrester T, Ellis CG, Dietrich HH. The erythrocyte as a regulator of vascular tone. *American Journal of Physiology - Heart and Circulatory Physiology*. 1995;269:H2155-H2161

33. Sprague RS, Ellsworth ML. Erythrocyte-derived atp and perfusion distribution: Role of intracellular and intercellular communication. *Microcirculation*. 2012;19:430-439

34. Billaud M, Lohman AW, Straub AC, Looft-Wilson R, Johnstone SR, Araj CA, Best AK, Chekeni FB, Ravichandran KS, Penuela S, Laird DW, Isakson BE. Pannexin1 regulates alpha1-adrenergic receptor- mediated vasoconstriction. *Circ Res*. 2011;109:80-85

35. Billaud M, Sandilos JK, Isakson BE. Pannexin 1 in the regulation of vascular tone. *Trends Cardiovasc Med*. 2012;22:68-72

36. Lohman AW, Billaud M, Isakson BE. Mechanisms of atp release and signalling in the blood vessel wall. *Cardiovasc Res*. 2012;95:269-280

37. Lohman AW, Isakson BE. Differentiating connexin hemichannels and pannexin channels in cellular atp release. *FEBS Lett*. 2014;588:1379-1388

38. Straub AC, Lohman AW, Billaud M, Johnstone SR, Dwyer ST, Lee MY, Bortz PS, Best AK, Columbus L, Gaston B, Isakson BE. Endothelial cell expression of haemoglobin alpha regulates nitric oxide signalling. *Nature*. 2012;491:473-477

39. Straub AC, Butcher JT, Billaud M, Mutchler SM, Artamonov MV, Nguyen AT, Johnson T, Best AK, Miller MP, Palmer LA, Columbus L, Somlyo AV, Le TH, Isakson BE. Hemoglobin alpha/enos coupling at myoendothelial junctions is required for nitric oxide scavenging during vasoconstriction. *Arterioscler Thromb Vasc Biol*. 2014;34:2594-2600

40. Butcher JT, Johnson T, Beers J, Columbus L, Isakson BE. Hemoglobin α in the blood vessel wall. *Free Radical Biology and Medicine*. 2014;73:136-142

41. Biwer LA, Taddeo EP, Kenwood BM, Hoehn KL, Straub AC, Isakson BE. Two functionally distinct pools of enos in endothelium are facilitated by myoendothelial junction lipid composition. *Biochim Biophys Acta*. 2016;1861:671-679

42. SoRelle R. Nobel prize awarded to scientists for nitric oxide discoveries. *Circulation*. 1998;98:2365-2366

43. Furchgott RF, Zawadzki JV. The obligatory role of endothelial cells in the relaxation of arterial smooth muscle by acetylcholine. *Nature*. 1980;288:373-376

44. Rapoport RM, Murad F. Agonist-induced endothelium-dependent relaxation in rat thoracic aorta may be mediated through cgmp. *Circ Res*. 1983;52:352-357

45. Rapoport RM, Draznin MB, Murad F. Endothelium-dependent relaxation in rat aorta may be mediated through cyclic gmp-dependent protein phosphorylation. *Nature*. 1983;306:174

46. Ignarro LJ, Buga GM, Wood KS, Byrns RE, Chaudhuri G. Endothelium-derived relaxing factor produced and released from artery and vein is nitric oxide. *Proc Natl Acad Sci U S A*. 1987;84:9265-9269

47. Wang GR, Zhu Y, Halushka PV, Lincoln TM, Mendelsohn ME. Mechanism of platelet inhibition by nitric oxide: In vivo phosphorylation of thromboxane receptor by cyclic gmp-dependent protein kinase. *Proceedings of the National Academy of Sciences of the United States of America*. 1998;95:4888-4893

48. Riddell DR, Owen JS. Nitric oxide and platelet aggregation. *Vitam Horm*. 1999;57:25-48

49. Rastaldo R, Pagliaro P, Cappello S, Penna C, Mancardi D, Westerhof N, Losano G. Nitric oxide and cardiac function. *Life sci*. Netherlands; 2007:779-793.

50. Garg UC, Hassid A. Nitric oxide-generating vasodilators and 8-bromo-cyclic guanosine monophosphate inhibit mitogenesis and proliferation of cultured rat vascular smooth muscle cells. *The Journal of clinical investigation*. 1989;83:1774-1777

51. Nakaki T, Nakayama M, Kato R. Inhibition by nitric oxide and nitric oxide-producing vasodilators of dna synthesis in vascular smooth muscle cells. *Eur J Pharmacol*. 1990;189:347-353

52. Lima B, Forrester MT, Hess DT, Stamler JS. S-nitrosylation in cardiovascular signaling. *Circulation research*. 2010;106:633-646

53. Sarti P, Forte E, Mastronicola D, Giuffre A, Arese M. Cytochrome c oxidase and nitric oxide in action: Molecular mechanisms and pathophysiological implications. *Biochim biophys acta*. Netherlands: A 2011 Elsevier B.V; 2012:610-619.

54. Chen K, Pittman RN, Popel AS. Nitric oxide in the vasculature: Where does it come from and where does it go? A quantitative perspective. *Antioxidants & redox signaling*. 2008;10:1185-1198

55. Stasch J-P, Pacher P, Evgenov OV. Soluble guanylate cyclase as an emerging therapeutic target in cardiopulmonary disease. *Circulation*. 2011;123:2263-2273

56. Stamler JS, Loh E, Roddy MA, Currie KE, Creager MA. Nitric oxide regulates basal systemic and pulmonary vascular resistance in healthy humans. *Circulation*. 1994;89:2035-2040

57. Ignarro LJ, Harbison RG, Wood KS, Kadowitz PJ. Activation of purified soluble guanylate cyclase by endothelium-derived relaxing factor from intrapulmonary artery and vein: Stimulation by acetylcholine, bradykinin and arachidonic acid. *J Pharmacol Exp Ther*. 1986;237:893-900

58. Carvajal JA, Germain AM, Huidobro-Toro JP, Weiner CP. Molecular mechanism of cgmp-mediated smooth muscle relaxation. *J cell physiol*. United States: 2000 Wiley-Liss, Inc.; 2000:409-420.

59. Collins P, Griffith TM, Henderson AH, Lewis MJ. Endothelium-derived relaxing factor alters calcium fluxes in rabbit aorta: A cyclic guanosine monophosphate-mediated effect. *J Physiol*. 1986;381:427-437

60. Lincoln TM, Komalavilas P, Cornwell TL. Pleiotropic regulation of vascular smooth muscle tone by cyclic gmp-dependent protein kinase. *Hypertension*. 1994;23:1141-1147

61. Gao N, Huang J, He W, Zhu M, Kamm KE, Stull JT. Signaling through myosin light chain kinase in smooth muscles. *J Biol Chem*. 2013;288:7596-7605

62. Sandoo A, van Zanten JJCSV, Metsios GS, Carroll D, Kitas GD. The endothelium and its role in regulating vascular tone. *The open cardiovascular medicine journal*. 2010;4:302-312

63. Förstermann U, Sessa WC. Nitric oxide synthases: Regulation and function. *European heart journal*. 2012;33:829-837d

64. Toda N, Ayajiki K, Okamura T. Control of systemic and pulmonary blood pressure by nitric oxide formed through neuronal nitric oxide synthase. *J Hypertens*. 2009;27:1929-1940

65. Nathan CF, Hibbs JB, Jr. Role of nitric oxide synthesis in macrophage antimicrobial activity. *Curr opin immunol*. England; 1991:65-70.

66. Gunnett CA, Lund DD, McDowell AK, Faraci FM, Heistad DD. Mechanisms of inducible nitric oxide synthase-mediated vascular dysfunction. *Arterioscler thromb vasc biol*. United States; 2005:1617-1622.

67. Feron O, Dessy C, Opel DJ, Arstall MA, Kelly RA, Michel T. Modulation of the endothelial nitric-oxide synthase-caveolin interaction in cardiac myocytes. Implications for the autonomic regulation of heart rate. *J Biol Chem*. 1998;273:30249-30254

68. Forstermann U, Closs EI, Pollock JS, Nakane M, Schwarz P, Gath I, Kleinert H. Nitric oxide synthase isozymes. Characterization, purification, molecular cloning, and functions. *Hypertension*. 1994;23:1121-1131

69. Huang PL, Huang Z, Mashimo H, Bloch KD, Moskowitz MA, Bevan JA, Fishman MC. Hypertension in mice lacking the gene for endothelial nitric oxide synthase. *Nature*. 1995;377:239-242

70. Shesely EG, Maeda N, Kim HS, Desai KM, Krege JH, Laubach VE, Sherman PA, Sessa WC, Smithies O. Elevated blood pressures in mice lacking endothelial nitric oxide synthase. *Proc Natl Acad Sci U S A*. 1996;93:13176-13181

71. Ando H, Kubin T, Schaper W, Schaper J. Cardiac microvascular endothelial cells express alpha-smooth muscle actin and show low nos iii activity. *Am J Physiol*. 1999;276:H1755-1768

72. Laughlin MH, Turk JR, Schrage WG, Woodman CR, Price EM. Influence of coronary artery diameter on enos protein content. *Am j physiol heart circ physiol*. United States; 2003:H1307-1312.

73. Shimokawa H, Yasutake H, Fujii K, Owada MK, Nakaike R, Fukumoto Y, Takayanagi T, Nagao T, Egashira K, Fujishima M, Takeshita A. The importance of the hyperpolarizing mechanism increases as the vessel size decreases in endothelium-dependent relaxations in rat mesenteric circulation. *J Cardiovasc Pharmacol*. 1996;28:703-711

74. Urakami-Harasawa L, Shimokawa H, Nakashima M, Egashira K, Takeshita A. Importance of endothelium-derived hyperpolarizing factor in human arteries. *J Clin Invest*. 1997;100:2793-2799

75. Ju H, Zou R, Venema VJ, Venema RC. Direct interaction of endothelial nitric-oxide synthase and caveolin-1 inhibits synthase activity. *J Biol Chem*. 1997;272:18522-18525

76. Figueroa XF, González DR, Martínez AD, Durán WN, Boric MP. Ach-induced endothelial no synthase translocation, no release and vasodilatation in the hamster microcirculation in vivo. *The Journal of physiology*. 2002;544:883-896

77. Harris MB, Ju H, Venema VJ, Liang H, Zou R, Michell BJ, Chen ZP, Kemp BE, Venema RC. Reciprocal phosphorylation and regulation of endothelial nitric-oxide synthase in response to bradykinin stimulation. *J biol chem*. United States; 2001:16587-16591.

78. Heiss EH, Dirsch VM. Regulation of enos enzyme activity by posttranslational modification. *Current pharmaceutical design*. 2014;20:3503-3513

79. Fleming I, Fisslthaler B, Dimmeler S, Kemp BE, Busse R. Phosphorylation of thr(495) regulates ca(2+)/calmodulin-dependent endothelial nitric oxide synthase activity. *Circ Res*. 2001;88:E68-75

80. Loot AE, Schreiber JG, Fisslthaler B, Fleming I. Angiotensin ii impairs endothelial function via tyrosine phosphorylation of the endothelial nitric oxide synthase. *J Exp Med*. 2009;206:2889-2896

81. Schrage WG, Joyner MJ, Dinenno FA. Local inhibition of nitric oxide and prostaglandins independently reduces forearm exercise hyperaemia in humans. *The Journal of physiology*. 2004;557:599-611

82. Paniagua OA, Bryant MB, Panza JA. Role of endothelial nitric oxide in shear stress-induced vasodilation of human microvasculature: Diminished activity in hypertensive and hypercholesterolemic patients. *Circulation*. 2001;103:1752-1758

83. Lu D, Kassab GS. Role of shear stress and stretch in vascular mechanobiology. *Journal of the Royal Society, Interface*. 2011;8:1379-1385

84. Sriram K, Laughlin JG, Rangamani P, Tartakovsky DM. Shear-induced nitric oxide production by endothelial cells. *Biophysical journal*. 2016;111:208-221

85. Niebauer J, Cooke JP. Cardiovascular effects of exercise: Role of endothelial shear stress. *Journal of the American College of Cardiology*. 1996;28:1652-1660

86. Tschakovsky ME, Joyner MJ. Nitric oxide and muscle blood flow in exercise. *Applied Physiology, Nutrition, and Metabolism*. 2007;33:151-160

87. Blitzer ML, Loh E, Roddy MA, Stamler JS, Creager MA. Endothelium-derived nitric oxide regulates systemic and pulmonary vascular resistance during acute hypoxia in humans. *J am coll cardiol*. United States; 1996:591-596.

88. Weisbrod CJ, Minson CT, Joyner MJ, Halliwill JR. Effects of regional phentolamine on hypoxic vasodilatation in healthy humans. *J Physiol*. 2001;537:613-621

89. Liu X, Miller MJ, Joshi MS, Sadowska-Krowicka H, Clark DA, Lancaster JR, Jr. Diffusion-limited reaction of free nitric oxide with erythrocytes. *J Biol Chem*. 1998;273:18709-18713

90. Butler AR, Megson IL, Wright PG. Diffusion of nitric oxide and scavenging by blood in the vasculature. *Biochimica et Biophysica Acta (BBA) - General Subjects*. 1998;1425:168-176

91. Liao JC, W. Hein T, Vaughn MW, Huang K-T, Kuo L. Intravascular flow decreases erythrocyte consumption of nitric oxide. *PNAS*. 1999;96:8757-8761

92. Azarov I, Huang KT, Basu S, Gladwin MT, Hogg N, Kim-Shapiro DB. Nitric oxide scavenging by red blood cells as a function of hematocrit and oxygenation. *J biol chem*. United States; 2005:39024-39032.

93. Kleinbongard P, Schulz R, Rassaf T, Lauer T, Dejam A, Jax T, Kumara I, Gharini P, Kabanova S, Ozuyaman B, Schnurch HG, Godecke A, Weber AA, Robenek M, Robenek H, Bloch W, Rosen P, Kelm M. Red blood cells express a functional endothelial nitric oxide synthase. *Blood*. United States; 2006:2943-2951.

94. Vaughn MW, Huang KT, Kuo L, Liao JC. Erythrocytes possess an intrinsic barrier to nitric oxide consumption. *J Biol Chem*. 2000;275:2342-2348

95. Helms C, Kim-Shapiro DB. Hemoglobin-mediated nitric oxide signaling. *Free Radical Biology and Medicine*. 2013;61:464-472

96. Jubelin BC, Gierman JL. Erythrocytes may synthesize their own nitric oxide. *Am j hypertens*. United States; 1996:1214-1219.

97. Kang ES, Ford K, Grokulsky G, Wang YB, Chiang TM, Acchiardo SR. Normal circulating adult human red blood cells contain inactive nos proteins. *J lab clin med*. United States; 2000:444-451.

98. Cortese-Krott MM, Rodriguez-Mateos A, Sansone R, Kuhnle GG, Thasian-Sivarajah S, Krenz T, Horn P, Krisp C, Wolters D, Heiss C, Kroncke KD, Hogg N, Feelisch M, Kelm M. Human red blood cells at work: Identification and visualization of erythrocytic enos activity in health and disease. *Blood*. United States; 2012:4229-4237.

99. Wood KC, Cortese-Krott MM, Kovacic JC, Noguchi A, Liu VB, Wang X, Raghavachari N, Boehm M, Kato GJ, Kelm M, Gladwin MT. Circulating blood endothelial nitric oxide synthase contributes to the regulation of systemic blood pressure and nitrite homeostasis. *Arterioscler Thromb Vasc Biol*. 2013;33:1861-1871

100. Ulker P, Sati L, Celik-Ozenci C, Meiselman HJ, Baskurt OK. Mechanical stimulation of nitric oxide synthesizing mechanisms in erythrocytes. *Biorheology*. 2009;46:121-132

101. Bor-Kucukatay M, Wenby RB, Meiselman HJ, Baskurt OK. Effects of nitric oxide on red blood cell deformability. *Am j physiol heart circ physiol*. United States; 2003:H1577-1584.

102. Cortese-Krott MM, Kelm M. Endothelial nitric oxide synthase in red blood cells: Key to a new erythrocrine function? *Redox Biology*. 2014;2:251-258

103. Shu X, Keller TCS, Begandt D, Butcher JT, Biwer L, Keller AS, Columbus L, Isakson BE. Endothelial nitric oxide synthase in the microcirculation. *Cellular and Molecular Life Sciences*. 2015;72:4561-4575

104. Bryk AH, Wisniewski JR. Quantitative analysis of human red blood cell proteome. *J Proteome Res*. 2017;16:2752-2761

105. Olafson BD, Goddard WA. Molecular description of dioxygen bonding in hemoglobin. *Proceedings of the National Academy of Sciences*. 1977;74:1315

106. Barcroft J, Roberts F. The dissociation curve of hæmoglobin. *The Journal of Physiology*. 1909;39:143-148

107. Hsia CCW. Respiratory function of hemoglobin. *New England Journal of Medicine*. 1998;338:239-248

108. Perrella M, Bresciani D, Rossi-Bernardi L. The binding of co2 to human hemoglobin. *Journal of Biological Chemistry*. 1975;250:5413-5418

109. Blumenthal I. Carbon monoxide poisoning. *J R Soc Med*. 2001;94:270-272

110. Han TH, Hyduke DR, Vaughn MW, Fukuto JM, Liao JC. Nitric oxide reaction with red blood cells and hemoglobin under heterogeneous conditions. *Proc Natl Acad Sci U S A*. 2002;99:7763-7768

111. Heberlein KR, Straub AC, Isakson BE. The myoendothelial junction: Breaking through the matrix? *Microcirculation*. 2009;16:307-322

112. Straub AC, Zeigler AC, Isakson BE. The myoendothelial junction: Connections that deliver the message. *Physiology (Bethesda)*. 2014;29:242-249

113. Eich RF, Li T, Lemon DD, Doherty DH, Curry SR, Aitken JF, Mathews AJ, Johnson KA, Smith RD, Phillips GN, Jr., Olson JS. Mechanism of no-induced oxidation of myoglobin and hemoglobin. *Biochemistry*. United States; 1996:6976-6983.

114. Tejero J, Gladwin MT. The globin superfamily: Functions in nitric oxide formation and decay. *Biol Chem*. 2014;395:631-639

115. Totzeck M, Hendgen-Cotta UB, Luedike P, Berenbrink M, Klare JP, Steinhoff H-J, Semmler D, Shiva S, Williams D, Kipar A, Gladwin MT, Schrader J, Kelm M, Cossins AR, Rassaf T. Nitrite regulates hypoxic vasodilation via myoglobin–dependent nitric oxide generation. *Circulation*. 2012;126:325-334

116. Tejero J, Sparacino-Watkins CE, Ragireddy V, Frizzell S, Gladwin MT. Exploring the mechanisms of the reductase activity of neuroglobin by site-directed mutagenesis of the heme distal pocket. *Biochemistry*. 2015;54:722-733

117. Cosby K, Partovi KS, Crawford JH, Patel RP, Reiter CD, Martyr S, Yang BK, Waclawiw MA, Zalos G, Xu X, Huang KT, Shields H, Kim-Shapiro DB, Schechter AN, Cannon RO, 3rd, Gladwin MT. Nitrite reduction to nitric oxide by deoxyhemoglobin vasodilates the human circulation. *Nat med*. United States; 2003:1498-1505.

118. Huang Z, Shiva S, Kim-Shapiro DB, Patel RP, Ringwood LA, Irby CE, Huang KT, Ho C, Hogg N, Schechter AN, Gladwin MT. Enzymatic function of hemoglobin as a nitrite reductase that produces no under allosteric control. *J Clin Invest*. 2005;115:2099-2107

119. Robinson JM, Lancaster JR, Jr. Hemoglobin-mediated, hypoxia-induced vasodilation via nitric oxide: Mechanism(s) and physiologic versus pathophysiologic relevance. *Am j respir cell mol biol*. United States; 2005:257-261.

120. Gladwin MT, Shelhamer JH, Schechter AN, Pease-Fye ME, Waclawiw MA, Panza JA, Ognibene FP, Cannon RO. Role of circulating nitrite and s-nitrosohemoglobin in the regulation of regional blood flow in humans. *Proceedings of the National Academy of Sciences*. 2000;97:11482-11487

121. Maher AR, Milsom AB, Gunaruwan P, Abozguia K, Ahmed I, Weaver RA, Thomas P, Ashrafian H, Born GV, James PE, Frenneaux MP. Hypoxic modulation

of exogenous nitrite-induced vasodilation in humans. *Circulation*. United States; 2008:670-677.

122. Gladwin Mark T. Evidence mounts that nitrite contributes to hypoxic vasodilation in the human circulation. *Circulation*. 2008;117:594-597

123. Lundberg JO, Weitzberg E, Gladwin MT. The nitrate-nitrite-nitric oxide pathway in physiology and therapeutics. *Nat rev drug discov*. England; 2008:156-167.

124. Lundberg JO, Weitzberg E. No generation from nitrite and its role in vascular control. *Arterioscler thromb vasc biol*. United States; 2005:915-922.

125. Doel JJ, Benjamin N, Hector MP, Rogers M, Allaker RP. Evaluation of bacterial nitrate reduction in the human oral cavity. *Eur j oral sci*. England; 2005:14-19.

126. Tiso M, Schechter AN. Nitrate reduction to nitrite, nitric oxide and ammonia by gut bacteria under physiological conditions. *PLOS ONE*. 2015;10:e0119712

127. Lundberg JO, Weitzberg E, Cole JA, Benjamin N. Nitrate, bacteria and human health. *Nature Reviews Microbiology*. 2004;2:593

128. Drury AN, Szent-Györgyi A. The physiological activity of adenine compounds with especial reference to their action upon the mammalian heart1. *The Journal of Physiology*. 1929;68:213-237

129. Belardinelli L, Linden J, Berne RM. The cardiac effects of adenosine. *Progress in Cardiovascular Diseases*. 1989;32:73-97

130. Berne Robert M, Rubio R, Curnish Richard R. Release of adenosine from ischemic brain. *Circulation Research*. 1974;35:262-271

131. Winn HR, Rubio GR, Berne RM. The role of adenosine in the regulation of cerebral blood flow. *Journal of Cerebral Blood Flow & Metabolism*. 1981;1:239-244

132. Burnstock G, Ralevic V. Purinergic signaling and blood vessels in health and disease. *Pharmacol rev*. United States; 2014:102-192.

133. Lohman AW, Weaver JL, Billaud M, Sandilos JK, Griffiths R, Straub AC, Penuela S, Leitinger N, Laird DW, Bayliss DA, Isakson BE. S-nitrosylation inhibits pannexin 1 channel function. *J Biol Chem*. 2012;287:39602-39612

134. Billaud M, Chiu YH, Lohman AW, Parpaite T, Butcher JT, Mutchler SM, DeLalio LJ, Artamonov MV, Sandilos JK, Best AK, Somlyo AV, Thompson RJ, Le TH, Ravichandran KS, Bayliss DA, Isakson BE. A molecular signature in the pannexin1 intracellular loop confers channel activation by the alpha1 adrenoreceptor in smooth muscle cells. *Sci Signal*. 2015;8:ra17

135. Good Miranda E, Chiu Y-H, Poon Ivan KH, Medina Christopher B, Butcher Joshua T, Mendu Suresh K, DeLalio Leon J, Lohman Alexander W, Leitinger N, Barrett E, Lorenz Ulrike M, Desai Bimal N, Jaffe Iris Z, Bayliss Douglas A, Isakson Brant E, Ravichandran Kodi S. Pannexin 1 channels as an unexpected new target of the anti-hypertensive drug spironolactone. *Circulation Research*. 2018;122:606-615

136. Good ME, Eucker SA, Li J, Bacon HM, Lang SM, Butcher JT, Johnson TJ, Gaykema RP, Patel MK, Zuo Z, Isakson BE. Endothelial cell pannexin1 modulates severity of ischemic stroke by regulating cerebral inflammation and myogenic tone. *JCI Insight*. 2018;3

137. DeLalio LJ, Keller AS, Chen J, Boyce AKJ, Artamonov MV, Askew-Page HR, Keller TCSt, Johnstone SR, Weaver RB, Good ME, Murphy SA, Best AK, Mintz EL, Penuela S, Greenwood IA, Machado RF, Somlyo AV, Swayne LA, Minshall RD, Isakson BE. Interaction between pannexin 1 and caveolin-1 in smooth muscle can regulate blood pressure. *Arterioscler Thromb Vasc Biol*. 2018;38:2065-2078

138. Gordan R, Gwathmey JK, Xie L-H. Autonomic and endocrine control of cardiovascular function. *World journal of cardiology*. 2015;7:204-214

139. Kennedy C, Saville VL, Burnstock G. The contributions of noradrenaline and atp to the responses of the rabbit central ear artery to sympathetic nerve stimulation depend on the parameters of stimulation. *European Journal of Pharmacology*. 1986;122:291-300

140. Ralevic V, Burnstock G. Postjunctional synergism of noradrenaline and adenosine 5'-triphosphate in the mesenteric arterial bed of the rat. *Eur j pharmacol*. Netherlands; 1990:291-299.

141. Vial C, Evans RJ. P2x(1) receptor-deficient mice establish the native p2x receptor and a p2y6-like receptor in arteries. *Mol Pharmacol*. 2002;62:1438-1445

142. Muir TC, Wardle KA. The electrical and mechanical basis of co-transmission in some vascular and non-vascular smooth muscles. *Journal of Autonomic Pharmacology*. 1988;8:203-218

143. Evans RJ, Cunnane TC. Relative contributions of atp and noradrenaline to the nerve evoked contraction of the rabbit jejunal artery. *Naunyn-Schmiedeberg's Archives of Pharmacology*. 1992;345:424-430

144. Gitterman DP, Evans RJ. Nerve evoked p2x receptor contractions of rat mesenteric arteries; dependence on vessel size and lack of role of l-type calcium channels and calcium induced calcium release. *British journal of pharmacology*. 2001;132:1201-1208

145. Ralevic V. Purines as neurotransmitters and neuromodulators in blood vessels. *Curr Vasc Pharmacol*. 2009;7:3-14

146. Van Coevorden A, Boeynaems JM. Physiological concentrations of adp stimulate the release of prostacyclin from bovine aortic endothelial cells. *Prostaglandins*. United States; 1984:615-626.

147. Luckhoff A, Busse R. Increased free calcium in endothelial cells under stimulation with adenine nucleotides. *J Cell Physiol*. 1986;126:414-420

148. Deussen A, Strauer BE, Schrader J, Kelm M, Feelisch M. Release of endothelium derived nitric oxide in relation to pressure and flow. *Cardiovascular Research*. 1991;25:831-836

149. Bodin P, Bailey D, Burnstock G. Increased flow-induced atp release from isolated vascular endothelial cells but not smooth muscle cells. *Br J Pharmacol*. 1991;103:1203-1205

150. John K, Barakat AI. Modulation of atp/adp concentration at the endothelial surface by shear stress: Effect of flow-induced atp release. *Annals of Biomedical Engineering*. 2001;29:740-751

151. Qin KR, Xiang C, Xu Z, Cao LL, Ge SS, Jiang ZL. Dynamic modeling for shear stress induced atp release from vascular endothelial cells. *Biomechanics and Modeling in Mechanobiology*. 2008;7:345-353

152. Yamamoto K, Imamura H, Ando J. Shear stress augments mitochondrial atp generation that triggers atp release and ca2+ signaling in vascular endothelial cells. *American Journal of Physiology-Heart and Circulatory Physiology*. 2018;315:H1477-H1485

153. Bodin P, Burnstock G. Evidence that release of adenosine triphosphate from endothelial cells during increased shear stress is vesicular. *J Cardiovasc Pharmacol*. 2001;38:900-908

154. Motte S, Communi D, Pirotton S, Boeynaems JM. Involvement of multiple receptors in the actions of extracellular atp: The example of vascular endothelial cells. *Int j biochem cell biol*. Netherlands; 1995:1-7.

155. Harrington LS, Mitchell JA. Novel role for p2x receptor activation in endothelium-dependent vasodilation. *British journal of pharmacology*. 2004;143:611-617

156. Bodin P, Burnstock G. Atp-stimulated release of atp by human endothelial cells. *J Cardiovasc Pharmacol*. 1996;27:872-875

157. Bergfeld GR, Forrester T. Release of atp from human erythrocytes in response to a brief period of hypoxia and hypercapnia. *Cardiovasc Res*. 1992;26:40-47

158. Dietrich HH, Ellsworth ML, Sprague RS, Dacey RG, Jr. Red blood cell regulation of microvascular tone through adenosine triphosphate. *Am J Physiol Heart Circ Physiol*. 2000;278:H1294-1298

159. Olearczyk JJ, Stephenson AH, Lonigro AJ, Sprague RS. Heterotrimeric g protein gi is involved in a signal transduction pathway for atp release from erythrocytes. *Am j physiol heart circ physiol*. United States; 2004:H940-945.

160. Sprague RS, Bowles EA, Hanson MS, DuFaux EA, Sridharan M, Adderley S, Ellsworth ML, Stephenson AH. Prostacyclin analogs stimulate receptor-mediated camp synthesis and atp release from rabbit and human erythrocytes. *Microcirculation*. 2008;15:461-471

161. Sprague RS, Bowles EA, Olearczyk JJ, Stephenson AH, Lonigro AJ. The role of g protein beta subunits in the release of atp from human erythrocytes. *J Physiol Pharmacol*. 2002;53:667-674

162. Sprague RS, Ellsworth ML, Stephenson AH, Lonigro AJ. Participation of camp in a signal-transduction pathway relating erythrocyte deformation to atp release. *Am J Physiol Cell Physiol*. 2001;281:C1158-1164

163. Sridharan M, Adderley SP, Bowles EA, Egan TM, Stephenson AH, Ellsworth ML, Sprague RS. Pannexin 1 is the conduit for low oxygen tension-induced atp release from human erythrocytes. *Am J Physiol Heart Circ Physiol*. 2010;299:H1146-1152

164. Sprague RS, Ellsworth ML, Stephenson AH, Kleinhenz ME, Lonigro AJ. Deformation-induced atp release from red blood cells requires cftr activity. *Am J Physiol*. 1998;275:H1726-1732

165. Sridharan M, Sprague RS, Adderley SP, Bowles EA, Ellsworth ML, Stephenson AH. Diamide decreases deformability of rabbit erythrocytes and attenuates low

oxygen tension-induced atp release. *Exp Biol Med (Maywood)*. 2010;235:1142-1148

166. Locovei S, Bao L, Dahl G. Pannexin 1 in erythrocytes: Function without a gap. *Proc Natl Acad Sci U S A*. 2006;103:7655-7659

167. Panchin Y, Kelmanson I, Matz M, Lukyanov K, Usman N, Lukyanov S. A ubiquitous family of putative gap junction molecules. *Curr biol*. England; 2000:R473-474.

168. Bruzzone R, Hormuzdi SG, Barbe MT, Herb A, Monyer H. Pannexins, a family of gap junction proteins expressed in brain. *Proc Natl Acad Sci U S A*. 2003;100:13644-13649

169. Bond SR, Naus CC. The pannexins: Past and present. *Front Physiol*. 2014;5:58

170. Lohman AW, Billaud M, Straub AC, Johnstone SR, Best AK, Lee M, Barr K, Penuela S, Laird DW, Isakson BE. Expression of pannexin isoforms in the systemic murine arterial network. *J Vasc Res*. 2012;49:405-416

171. Begandt D, Good ME, Keller AS, DeLalio LJ, Rowley C, Isakson BE, Figueroa XF. Pannexin channel and connexin hemichannel expression in vascular function and inflammation. *BMC Cell Biol*. 2017;18:2

172. Bao L, Locovei S, Dahl G. Pannexin membrane channels are mechanosensitive conduits for atp. *FEBS Lett*. 2004;572:65-68

173. Lohman AW, Leskov IL, Butcher JT, Johnstone SR, Stokes TA, Begandt D, DeLalio LJ, Best AK, Penuela S, Leitinger N, Ravichandran KS, Stokes KY,

Isakson BE. Pannexin 1 channels regulate leukocyte emigration through the venous endothelium during acute inflammation. *Nat Commun*. 2015;6:7965

174. Qiu F, Dahl G. A permeant regulating its permeation pore: Inhibition of pannexin 1 channels by atp. *Am J Physiol Cell Physiol*. 2009;296:C250-255

175. Sandilos JK, Bayliss DA. Physiological mechanisms for the modulation of pannexin 1 channel activity. *J Physiol*. 2012;590:6257-6266

176. Iglesias R, Spray DC, Scemes E. Mefloquine blockade of pannexin1 currents: Resolution of a conflict. *Cell communication & adhesion*. 2009;16:131-137

177. Chiu YH, Ravichandran KS, Bayliss DA. Intrinsic properties and regulation of pannexin 1 channel. *Channels (Austin)*. 2014;8:103-109

178. Ma W, Compan V, Zheng W, Martin E, North RA, Verkhratsky A, Surprenant A. Pannexin 1 forms an anion-selective channel. *Pflugers Arch*. 2012;463:585-592

179. Romanov RA, Bystrova MF, Rogachevskaya OA, Sadovnikov VB, Shestopalov VI, Kolesnikov SS. The atp permeability of pannexin 1 channels in a heterologous system and in mammalian taste cells is dispensable. *J Cell Sci*. 2012;125:5514-5523

180. Ambrosi C, Gassmann O, Pranskevich JN, Boassa D, Smock A, Wang J, Dahl G, Steinem C, Sosinsky GE. Pannexin1 and pannexin2 channels show quaternary similarities to connexons and different oligomerization numbers from each other. *J Biol Chem*. 2010;285:24420-24431

181. Good ME, Begandt D, DeLalio LJ, Keller AS, Billaud M, Isakson BE. Emerging concepts regarding pannexin 1 in the vasculature. *Biochem soc trans*. England; 2015:495-501.

182. Sandilos JK, Chiu YH, Chekeni FB, Armstrong AJ, Walk SF, Ravichandran KS, Bayliss DA. Pannexin 1, an atp release channel, is activated by caspase cleavage of its pore-associated c-terminal autoinhibitory region. *J Biol Chem*. 2012;287:11303-11311

183. Dourado M, Wong E, Hackos DH. Pannexin-1 is blocked by its c-terminus through a delocalized non-specific interaction surface. *PLOS ONE*. 2014;9:e99596

184. Chekeni FB, Elliott MR, Sandilos JK, Walk SF, Kinchen JM, Lazarowski ER, Armstrong AJ, Penuela S, Laird DW, Salvesen GS, Isakson BE, Bayliss DA, Ravichandran KS. Pannexin 1 channels mediate 'find-me' signal release and membrane permeability during apoptosis. *Nature*. 2010;467:863-867

185. Locovei S, Wang J, Dahl G. Activation of pannexin 1 channels by atp through p2y receptors and by cytoplasmic calcium. *FEBS Lett*. 2006;580:239-244

186. Pelegrin P, Surprenant A. Pannexin-1 mediates large pore formation and interleukin-1beta release by the atp-gated p2x7 receptor. *EMBO J*. 2006;25:5071-5082

187. Locovei S, Scemes E, Qiu F, Spray DC, Dahl G. Pannexin1 is part of the pore forming unit of the p2x7 receptor death complex *FEBS Letters*. 2007;581:483-488

188. Negoro H, Urban-Maldonado M, Liou LS, Spray DC, Thi MM, Suadicani SO. Pannexin 1 channels play essential roles in urothelial mechanotransduction and intercellular signaling. *PLoS One*. 2014;9:e106269

189. Wang J, Dahl G. Scam analysis of panx1 suggests a peculiar pore structure. *J Gen Physiol*. 2010;136:515-527

190. Qiu F, Wang J, Dahl G. Alanine substitution scanning of pannexin1 reveals amino acid residues mediating atp sensitivity. *Purinergic Signalling*. 2012;8:81-90

191. Beckel JM, Argall AJ, Lim JC, Xia J, Lu W, Coffey EE, Macarak EJ, Shahidullah M, Delamere NA, Zode GS, Sheffield VC, Shestopalov VI, Laties AM, Mitchell CH. Mechanosensitive release of adenosine 5'-triphosphate through pannexin channels and mechanosensitive upregulation of pannexin channels in optic nerve head astrocytes: A mechanism for purinergic involvement in chronic strain. *Glia*. 2014;62:1486-1501

192. Zhang M, Piskuric NA, Vollmer C, Nurse CA. P2y2 receptor activation opens pannexin-1 channels in rat carotid body type ii cells: Potential role in amplifying the neurotransmitter atp. *J Physiol*. 2012;590:4335-4350

193. Bruzzone R, Barbe MT, Jakob NJ, Monyer H. Pharmacological properties of homomeric and heteromeric pannexin hemichannels expressed in xenopus oocytes. *J neurochem*. England; 2005:1033-1043.

194. Huang YA, Roper SD. Intracellular ca(2+) and trpm5-mediated membrane depolarization produce atp secretion from taste receptor cells. *J Physiol*. 2010;588:2343-2350

195. Silverman WR, de Rivero Vaccari JP, Locovei S, Qiu F, Carlsson SK, Scemes E, Keane RW, Dahl G. The pannexin 1 channel activates the inflammasome in neurons and astrocytes. *J Biol Chem*. 2009;284:18143-18151

196. Retamal MA. Connexin and pannexin hemichannels are regulated by redox potential. *Front Physiol*. 2014;5:80

197. Keller AS, Diederich L, Panknin C, DeLalio LJ, Drake JC, Sherman R, Jackson EK, Yan Z, Kelm M, Cortese-Krott MM, Isakson BE. Possible roles for atp release from rbcs exclude the camp-mediated panx1 pathway. *Am J Physiol Cell Physiol*. 2017;313:C593-C603

198. Lechauve C, Butcher JT, Freiwan A, Biwer LA, Keith JM, Good ME, Ackerman H, Tillman HS, Kiger L, Isakson BE, Weiss MJ. Endothelial cell α-globin and its molecular chaperone α-hemoglobin–stabilizing protein regulate arteriolar contractility. *The Journal of Clinical Investigation*. 2018;128:5073-5082

199. Laker RC, Drake JC, Wilson RJ, Lira VA, Lewellen BM, Ryall KA, Fisher CC, Zhang M, Saucerman JJ, Goodyear LJ, Kundu M, Yan Z. Ampk phosphorylation of ulk1 is required for targeting of mitochondria to lysosomes in exercise-induced mitophagy. *Nat Commun*. 2017;8:548

200. Berne RM. Cardiac nucleotides in hypoxia: Possible role in regulation of coronary blood flow. *Am J Physiol*. 1963;204:317-322

201. Wolf MM, Berne RM. Coronary vasodilator properties of purine and pyrimidine derivatives. *Circulation Research*. 1956;4:343

202. Ellsworth ML. Red blood cell-derived atp as a regulator of skeletal muscle perfusion. *Med sci sports exerc*. United States; 2004:35-41.

203. Sprague RS, Ellsworth ML, Stephenson AH, Lonigro AJ. Atp: The red blood cell link to no and local control of the pulmonary circulation. *Am J Physiol*. 1996;271:H2717-2722

204. Erkens R, Suvorava T, Kramer CM, Diederich L, Kelm M, Cortese-Krott MM. Modulation of local and systemic heterocellular communication by mechanical forces: A role of enos. *Antioxid Redox Signal*. 2016

205. Wan J, Forsyth AM, Stone HA. Red blood cell dynamics: From cell deformation to atp release. *Integr Biol (Camb)*. 2011;3:972-981

206. Wan J, Ristenpart WD, Stone HA. Dynamics of shear-induced atp release from red blood cells. *Proc Natl Acad Sci U S A*. 2008;105:16432-16437

207. Qiu F, Wang J, Spray DC, Scemes E, Dahl G. Two non-vesicular atp release pathways in the mouse erythrocyte membrane. *FEBS Lett*. 2011;585:3430-3435

208. Cinar E, Zhou S, DeCourcey J, Wang Y, Waugh RE, Wan J. Piezo1 regulates mechanotransductive release of atp from human rbcs. *Proc Natl Acad Sci U S A*. 2015;112:11783-11788

209. Melhorn MI, Brodsky AS, Estanislau J, Khoory JA, Illigens B, Hamachi I, Kurishita Y, Fraser AD, Nicholson-Weller A, Dolmatova E, Duffy HS, Ghiran IC. Cr1-mediated atp release by human red blood cells promotes cr1 clustering and modulates the immune transfer process. *J Biol Chem*. 2013;288:31139-31153

210. Sikora J, Orlov SN, Furuya K, Grygorczyk R. Hemolysis is a primary atp-release mechanism in human erythrocytes. *Blood*. 2014;124:2150-2157

211. Montalbetti N, Leal Denis MF, Pignataro OP, Kobatake E, Lazarowski ER, Schwarzbaum PJ. Homeostasis of extracellular atp in human erythrocytes. *J Biol Chem*. 2011;286:38397-38407

212. Cotterrell D, Whittam R. The influence of the chloride gradient across red cell membranes on sodium and potassium movements. *J Physiol*. 1971;214:509-536

213. Jennings ML. Proton fluxes associated with erythrocyte membrane anion exchange. *J Membr Biol*. 1976;28:187-205

214. Gunn RB, Dalmark M, Tosteson DC, Wieth JO. Characteristics of chloride transport in human red blood cells. *J Gen Physiol*. 1973;61:185-206

215. Vitvitsky VM, Frolova EV, Martinov MV, Komarova SV, Ataullakhanov FI. Anion permeability and erythrocyte swelling. *Bioelectrochemistry*. Netherlands; 2000:169-177.

216. Goldman D, Fraser GM, Ellis CG, Sprague RS, Ellsworth ML, Stephenson AH. Toward a multiscale description of microvascular flow regulation: O(2)-dependent release of atp from human erythrocytes and the distribution of atp in capillary networks. *Frontiers in Physiology*. 2012;3:246

217. Balderas E, Ateaga-Tlecuitl R, Rivera M, Gomora JC, Darszon A. Niflumic acid blocks native and recombinant t-type channels. *J Cell Physiol*. 2012;227:2542-2555

218. Ripoll C, Lederer WJ, Nichols CG. On the mechanism of inhibition of katp channels by glibenclamide in rat ventricular myocytes. *J Cardiovasc Electrophysiol*. 1993;4:38-47

219. Schultz BD, DeRoos AD, Venglarik CJ, Singh AK, Frizzell RA, Bridges RJ. Glibenclamide blockade of cftr chloride channels. *Am J Physiol*. 1996;271:L192-200

220. Scott-Ward TS, Li H, Schmidt A, Cai Z, Sheppard DN. Direct block of the cystic fibrosis transmembrane conductance regulator cl(-) channel by niflumic acid. *Mol membr biol*. England; 2004:27-38.

221. Sharonova IN, Dvorzhak AY. Blockade of gabaa receptor channels by niflumic acid prevents agonist dissociation. *Biochemistry (Moscow) Supplement Series A: Membrane and Cell Biology*. 2013;7:37-44

222. McCullough WT, Collins DM, Ellsworth ML. Arteriolar responses to extracellular atp in striated muscle. *Am J Physiol*. 1997;272:H1886-1891

223. Kirby BS, Schwarzbaum PJ, Lazarowski ER, Dinenno FA, McMahon TJ. Liberation of atp secondary to hemolysis is not mutually exclusive of regulated export. *Blood*. 2015;125:1844-1845

224. Sikora J, Orlov SN, Furuya K, Grygorczyk R. Response: Hemolysis is a primary and physiologically relevant atp release mechanism in human erythrocytes. *Blood*. 2015;125:1845-1846

225. Gladwin MT, Kim-Shapiro DB. The functional nitrite reductase activity of the heme-globins. *Blood*. 2008;112:2636-2647

226. Keller TCt, Butcher JT, Broseghini-Filho GB, Marziano C, DeLalio LJ, Rogers S, Ning B, Martin JN, Chechova S, Cabot M, Shu X, Best AK, Good ME, Simao Padilha A, Purdy M, Yeager M, Peirce SM, Hu S, Doctor A, Barrett E, Le TH, Columbus L, Isakson BE. Modulating vascular hemodynamics with an alpha globin mimetic peptide (hbalphax). *Hypertension*. 2016;68:1494-1503

227. Gabrilove J. Overview: Erythropoiesis, anemia, and the impact of erythropoietin. *Semin hematol*. United States; 2000:1-3.

228. Reis DJ, Wooten GF. The relationship of blood flow to myoglobin, capillary density, and twitch characteristics in red and white skeletal muscle in cat. *The Journal of physiology*. 1970;210:121-135

229. Vandegriff KD, Olson JS. The kinetics of o2 release by human red blood cells in the presence of external sodium dithionite. *J Biol Chem*. 1984;259:12609-12618

230. Grubina R, Basu S, Tiso M, Kim-Shapiro DB, Gladwin MT. Nitrite reductase activity of hemoglobin s (sickle) provides insight into contributions of heme redox potential versus ligand affinity. *J biol chem*. United States; 2008:3628-3638.

231. Quayle JM, Turner MR, Burrell HE, Kamishima T. Effects of hypoxia, anoxia, and metabolic inhibitors on katp channels in rat femoral artery myocytes. *Am j physiol heart circ physiol*. United States; 2006:H71-80.

232. Gladwin MT, Shelhamer JH, Schechter AN, Pease-Fye ME, Waclawiw MA, Panza JA, Ognibene FP, Cannon RO, 3rd. Role of circulating nitrite and s-nitrosohemoglobin in the regulation of regional blood flow in humans. *Proc Natl Acad Sci U S A*. 2000;97:11482-11487